

**ANAEROBIC REACTOR DEVELOPMENT  
FOR COMPLEX ORGANIC WASTEWATER**

*A Thesis*

*Submitted by*

**AJIT HARIDAS**

*For the award of the degree  
of*

***DOCTOR OF PHILOSOPHY***

*Under*

*The Faculty of Engineering*

**SCHOOL OF ENGINEERING  
COCHIN UNIVERSITY OF SCIENCE AND TECHNOLOGY  
KOCHI-682 022**

**2010**

## Certificate

Certified that this thesis entitled “**Anaerobic Reactor Development for Complex Organic Wastewater**”, submitted to the Cochin University of Science and Technology, Kochi for the award of Ph.D Degree, under the Faculty of Engineering is the record of bonafide research carried out by **Ajit Haridas**, under my supervision and guidance. This work did not form part of any dissertation submitted for the award of any degree, diploma, associateship, fellowship or other similar title or recognition from this or any other institution.

Kochi –22,  
31-07-2010.

**Prof. (Dr.) Babu. T. Jose**  
Supervising Guide,  
Faculty of Engineering.  
Cochin University of Science and Technology

## Declaration

I, Ajit Haridas, hereby declare that the work presented in the thesis entitled "**Anaerobic reactor development for complex organic wastewater**", being submitted to Cochin University of Science and Technology for award of Ph.D degree under the Faculty of Engineering, is the outcome of original work done by me under the supervision of **Dr. Babu T. Jose**, Emeritus Professor, School of Engineering, Cochin University of Science and Technology, Kochi. This work did not form part of any dissertation submitted for the award of any degree, diploma, associateship, fellowship or other similar title or recognition from this or any other institution.

Kochi -22,  
31-07-2010.

**Ajit Haridas**

## Acknowledgment

I am deeply indebted to my guide Prof. Babu T. Jose, for persuading me to do this thesis, repeatedly stressing the importance of having a PhD, and bringing me back on track on occasions when I slacked and the morale sagged. I express my heartfelt gratitude to him.

Dr. Renu Pawels, CUSAT spent so much time and effort to help me through all the formalities of the university. Without her help, I would have failed at the bureaucratic gauntlets and no amount of thanks will suffice.

In making this thesis, I have drawn nourishment from various streams. The most important branch is 24 years of research into anaerobic treatment and biological treatment at NIIST, (formerly RRL Thiruvanthapuram). It is only right that I thank first of all, CSIR for all the research support it has provided. CSIR provided a project for scale-up studies on the BFBR. I thank the Director, NIIST for permitting me to register for PhD.

This is the right place to trace my journey in anaerobic technology and remember with gratitude the co-workers, assistants, project staff and students who shared in the successes and failures. My first brush with anaerobic digestion started 30 years ago, as a B.Tech student of Chemical Engineering at IIT Madras, with a few bottle experiments on water hyacinth digestion, with little experimental capability and on shaky theoretical foundations. I resumed the journey after I joined the then RRL Thiruvananthapuram in 1986. My first UASB reactor was built with a borrowed 4 inch dia. 1 m long QVF glass column and metering pumps salvaged from junk. It took years before broken tubing and sludge all over the floor became a rare sight when returning to the laboratory in the morning. Around 1992, I got my first research money came from MOEF for developing a treatment system for centrifuge latex effluent. We could finally buy peristaltic pumps. But, unknowingly we stumbled into the problem of sulphide inhibition of anaerobic treatment. It gave us our first innovation in anaerobic technology, - a process for sulphide inhibition control of anaerobic reactors – still today, the most cost-effective technique available. Dr.P.C Sabumon, now at Vellore Institute of Technology, and Shyam K P, now employed by Singapore University, spent days and nights to run the anaerobic reactor and its sulphide inhibition control system.

Confident, after developing the UASB and granular sludge on centrifuge latex effluent, we tried to run the reactor on palm oil mill effluent. It was a dramatic failure and we learnt what would happen if we run a UASB on a solids and lipid rich wastewater. Since then, the unsolved issue of complex wastewater has been at the back of my mind.

My next project was on sulphide oxidation, and its new concept RFLR reactor. It could not have been done without the efforts of S.Majundar, and Dr.B.Krishnakumar. It was my first experience in developing new reactor concepts. The next major development work was the BFBR. S.Suresh worked literally 24x7 to operate and perfect this reactor. Dr. Manilal, who has been with me since after the first lab UASB, reported seeing protozoa in the BFBR sludge. I said that would be unlikely because protozoa would not get enough energy to run around and grow in an anaerobic reactor. Later it was confirmed, and set me thinking what protozoa were doing

in the BFBR. Sheela Ravikumar spent so much time to identify and count painstakingly the every day variation in numbers. Priya M. and Nimi Narayanan started their PhD on anaerobic protozoa, guided by Manilal. Krishnakumar set up a microscope that allowed us to see methanogens directly under fluorescence and characterise these using FISH methods. Simi worked on the BFBR filtration studies. Smt. Soosan Pannikar set up and operated modified versions of BFBR with mechanical agitation and sludge settler before the buoyant filter, specifically for the treatment of sewage. She will hopefully write it out for her PhD, after having stood up to the most trying circumstances imaginable in an institute. Abdul Jaleel ran comparative studies on BFBR using two different filter media and came up with intriguing results. KR Chitra developed the protocols and analysed the LCFAs in the BFBR liquor, with unmatched care and precision. Meanwhile I started another stream of anaerobic technology with the leach bed reactor for solids, but that is another story. Everything in the laboratory was made possible by the efforts of my technical assistants, Karunasankar Roat and Shaji Kumar.

In 1995, the World Bank financed our modern Wastewater Technology Laboratory at RRL. I got a chance to spend 3 months at the Wageningen Agricultural University and met Prof Gatzte Lettinga and Dr. Look Hulshoff-Pol. Till I saw the lab UASBs at Wageningen, I had never seen one other than my own. I saw a full scale UASB at Eerbeek. What more can an anaerobic technologist ask than seeing the UASB in the place of its origin? It gave me the courage to design full-scale UASBs for industrial effluent treatment and later develop the BFBR. Several clients (Bhavani Distilleries, Amitron Pune, KRMC Ltd, EPA Chennai) have put their faith and money in my reactor designs. Each time was a learning process. Sree Sakthi Paper Mills is putting up a variant of the BFBR reactor and I am waiting for the day it will be commissioned. All the design drawings were made possible by the efforts put in by Vijayaprasad. Wageningen confirmed my belief that there are no high-rate reactors for complex wastewaters.

Another stream of knowledge that has gone into this thesis is mathematical modelling. Even while an undergraduate in 1980, we attempted a mathematical model referring to the single publication then available to us (Graef SP, Andrews JF, AIChE Sym. Series, 1973). Those days we punched cards, wrote Fortran, and used the IMSL library subroutines, on IITM's IBM 370, which was the dream machine in this part of the country. My thesis in graduate school at University of Delaware, USA, had been in then fashionable mathematical modelling, spending months at the text-only CRT terminals of a DEC10 mainframe. Modelling sharpened analysis but I felt it produced no new knowledge and so, at RRL, I worked mainly as an experimenter on biological process development. After doing the anaerobic process model for the BFBR, I am able to see modelling as a tool that can provide insight into complex processes. The BFBR model was based on lectures delivered by Prof. Mark von Loosdrecht (TU Delft) at CUSAT on the ASM model. I thank Prof. Mohandas, former Dean of CUSAT for inviting me to workshops on Environmental Technology conducted at CUSAT by some of the most eminent professors from The Netherlands.

All my colleagues, staff and students have stood by me and helped me in so many ways. I name, in particular, J. Ansari, Dr. Rugmini Sukumaran and Dr. Ramaswamy.

Finally, I would like to dedicate this thesis to the ethics, culture and spirit of science, in its struggle to survive within the country's scientific establishment.

# Anaerobic reactor development for complex organic wastewater

## Synopsis

Anaerobic treatment is applied extensively for removal of organic pollutants (COD) from wastewater. It is more competitive than aerobic treatment in applications where the quantity of COD to be removed is large. The major fraction of COD is converted to useful methane gas, and only a small fraction becomes waste sludge. The COD loading rate of anaerobic reactors is higher than that of aerobic reactors and hence small reactors are sufficient for the treatment of same quantity of COD.

Chapter 2 surveys anaerobic technology and identifies directions for improving reactor technology.

High-rate anaerobic reactors have reduced the cost of anaerobic treatment plants. High-rate reactors routinely achieve organic loading rates 8 to 10 kg COD/ m<sup>3</sup> reactor / d and hydraulic retention times of the order of a few hours. High-rate reactor designs can be broadly classified as fixed film (eg. fixed film, fluidized bed) and suspended growth reactors (eg. UASB, EGSB). The fixed film reactors provide an inert carrier media for growth of anaerobic consortia as a biofilm. Biomass is retained as settleable flocs or granules in suspended growth reactors. The UASB is the most common reactor in use. The CSTR is a suspended growth reactor but is not a high-rate reactor since there is no mechanism to separate and retain biomass.

High-rate reactors have been successfully applied for the treatment of a wide range of industrial and domestic wastewater. However, wastewaters containing degradable COD in mostly particulate form, is not treatable at high-rate in these reactors. Such effluents are termed 'complex organic wastewater' in this thesis. Examples of such wastewaters include dairy effluent, slaughterhouse effluent and palm oil mill effluent. Municipal sewage can also be considered as complex organic wastewater. The development of a high-rate anaerobic reactor capable of treatment of complex wastewater is necessary.

This thesis concerns the development of a new high-rate anaerobic reactor called the 'Buoyant Filter Bioreactor – BFBR' for the high-rate treatment of complex organic wastewater. Current high-rate anaerobic reactors are based on the principle of decoupling biomass retention times from the hydraulic retention times. This works only when the rate limiting step in the reactor is a microbial growth process – typically acetoclastic

methanogenesis. In the treatment of complex wastewater, the rate limiting step is extracellular enzymatic hydrolysis. The central hypothesis in the development of the BFBR is that high-rate treatment of complex wastewater requires the decoupling of *particulate-COD* retention time from the hydraulic retention time. Particulate COD, if retained sufficiently long in the reactor should undergo complete conversion. The BFBR is designed to retain particulates with the reactor using a deep-bed filter system.

Chapter 4 describes the development of BFBR. The BFBR has an upper chamber and a lower chamber. Between the two chamber is a buoyant filter bed that filters the reactor liquor. The filter media is made from expanded polystyrene beads. The feed wastewater is pumped into the lower chamber which contains methanogenic sludge. Gas produced accumulates in the lower chamber, while the liquor filters through the buoyant filter bed into the upper chamber from where it can overflow. The gas accumulated in the lower chamber is released periodically. During gas release, filtered liquor from the upper chamber flow back through the filter bed into the lower chamber, fluidizing the filter bed in the downward direction. The solids captured in the filter bed are backwashed into the lower chamber. The periodic gas release is achieved automatically using a gas siphon system.

Chapter 5 gives the materials and methods used to study the performance of the BFBR. The fabrication of the BFBR and the methods of testing and monitoring performance are described.

The BFBR was operated with complex wastewater prepared from full fat milk. All nutrients were provided in sufficient quantity. Another effluent was prepared with oleate emulsion as the sole carbon source.

Chapter 6 gives results of the experiments.

Prior to reactor operation, the buoyant filter was characterised by filtration tests on bulking anaerobic digester sludge. At filtration velocity 1 m/h, it was found that filter efficiencies were in the range of 70 % for 1 to 2 mm filter media, and 90% for 0.5 to 1 mm filter media. The pressure drop build up was linearly related to filtration velocity. At filtration velocity up to 1 m/h, the pressure drop for 1 to 2 mm filter media reached 10 cm H<sub>2</sub>O in about 15 minutes for 1 to 2 mm media, and in 5 minutes for 0.5 to 1mm media. Operating the filter at higher pressure deforms the EPS bead media and causes non-linear increase in pressure drop.

The fluidization velocity for backwash was determined and found to follow the Richardson-Zaki formula quite well. The filter bed is effectively cleaned by backwashing. But if the filter is operated at high pressure, sludge and filter media bond to form aggregates that are not broken up during backwash.

The BFBR was operated for more than 400 d with milk effluent. COD loads up to 8 kg/m<sup>2</sup>/d were applied. There was no choking of the filter bed in long term operation. The filter backwash by fluidization was applied at 15 to 20 minute intervals automatically. The filter pressure drop during operation never exceeded 15 cm H<sub>2</sub>O.

The COD removal efficiency at steady state was above 85% at all the OLRs applied. The maximum organic loading rate applied during the period reported is 10 kg COD/(m<sup>3</sup>.day). COD removal efficiency during steady state at this loading was 90%. Through out the operation of the BFBR, effluent COD was less than 450 mg/l. During pseudo-steady state at all loading rates, the effluent COD was less than 250 mg/l. On prolonged steady operation, effluent quality improved and very low COD was obtained even at high organic loading rates. Towards the end of the reported period, with feed COD was in the range of 3200 to 3500 mg/l, the effluent total COD was only 120 mg/l total of which soluble COD was 80 mg/l.

Unexpectedly, the BFBR sludge started showing good settleability, with irregular shaped dense flocs. Microscopic examination showed the presence of protozoa in the sludge. These are anaerobic protozoa and are capable of ingesting particulates. The protozoa contain endosymbiotic methanogens that presumably convert hydrogen and acetate to methane. The population of protozoa in the BFBR shows a succession from small rounds to amoeboids to flagellates to ciliates. The residual COD in the BFBR effluent is negatively correlated to ciliate numbers in the sludge. The ciliate rich BFBR treated effluent is very clear, reminiscent of activated sludge treatment.

Chapter 7 develops a simulation model for the BFBR in order to get more insight into the process dynamics of the system. The idealized BFBR is represented as a CSTR with a zero volume filter that has specified efficiency for retention of each particulate component. The reactor model is combined with an anaerobic process model, similar to ADM1. The rate processes are taken as microbial growth, decay, enzymatic hydrolysis and gas transfer. The process model has 8 soluble components, 14 particulate components, 4 soluble inorganic components and 3 gas components. The number of processes considered is 25. The model is implemented in MATLAB and has been designed

to insert new components and processes without reprogramming. The model has careful accounting of COD, total carbon, nitrogen, sulphur and charge balances. pH is estimated from by solving algebraic charge balance equation at each time step.

The model was used to simulate the performance of BFBR with sewage and with milk effluent. The expected performance is obtained by adjusting the filtration efficiency parameters. It is seen that retention efficiency for microbial biomass exceeds the filtration efficiency measured during filtration study with bulking sludge. This implies that mechanisms that improve filterability, such as biologically induced flocculation or granulation are responsible for the retention of the required mass of bacteria. On the other hand, particulate substrates are retained by physical filtration mechanism. Therefore, we conclude that although growth rate of microorganisms such as acetoclastic methanogens is slower than hydrolysis of particulates, the microbial substrate uptake rates in a reactor are higher than particulate hydrolysis rates because *organisms accumulate, while particulates get washed out*. Hence active methods of retaining particulates inside the reactor, as in the BFBR, increase the overall reactor COD loading and conversion rate.

The model reproduces the behaviour of BFBR with a initial build up in concentration of particulates in the reactor followed by degradation during start-up. The model also shows that BFBR is suitable for sewage treatment.

Chapter 8 discusses aspects of scale-up of BFBR for field application. The aspects discussed are:

- constraints on the reactor vessel because of the arrangement of filter, gas accumulator and filtered effluent storage are brought out.
- The gas-solids-separators optimization for BFBR.
- Selection of mixing system
- Design of automatic gas release system

The final chapter gives the conclusions and a comparison of BFBR with other anaerobic reactors and a discussion of aspects of scale-up for future development of the BFBR. A summary of the operating parameters of the BFBR is given below:

The recommended process design parameters for the BFBR are summarised below:

- a. Organic loading rate for complex organic wastewater  
COD loading rate: 6 to 8 kg COD /m<sup>3</sup>/d.
- b. Filter specifications:  
Filter media size: 1 to 1.5 mm

Filter depth: 10 to 15 cm  
Filtration velocity: 1 to 2 m/h  
Filter pressure drop: < 20 cm w.c.  
Filter backwash velocity: 130 m/h  
Bed expansion: 30%  
Filter backwash interval: 15 to 30 minutes  
Filter backwash volume: > 100% of filter volume

#### References:

1. US 6,592,751 dated July 15, 2003. Device for treatment of wastewater. Inventor: Ajit Haridas; Assignee. Council of Scientific and Industrial Research, New Delhi.
2. Ajit Haridas, S. Suresh, K.R. Chitra, V.B. Manilal. 2005. The Buoyant Filter Bioreactor: a high-rate anaerobic reactor for complex wastewater—process dynamics with dairy effluent. *Water Research* 39 993–1004
3. Priya M, Haridas A, Manilal VB. 2007. Involvement of protozoa in anaerobic wastewater treatment process. *Water Res.* 41,20, 4639-4645.  
Panicker, S.J., Philipose, M.C., Haridas, A. 2008. Buoyant Filter Bio-Reactor (BFBR)-a novel anaerobi

---

*Anaerobic reactor development  
for complex organic wastewater*

---

## Contents

---

<b>1.</b>	<b>Introduction</b> .....	<b>1</b>
1.1.	The role of anaerobic waste treatment in environmental management .....	1
1.2.	Advantages of anaerobic treatment .....	1
1.3.	Limitations of anaerobic treatment .....	2
<b>2.</b>	<b>Literature Survey</b> .....	<b>3</b>
2.1.	Science of anaerobic degradation .....	3
2.1.1.	biogeochemical view of the microbial carbon mineralization .....	3
2.1.2.	Thermodynamics of microbial metabolism.....	4
2.1.3.	Anaerobic mineralization of organic compounds .....	5
2.1.4.	Solubilisation and hydrolysis .....	5
2.1.5.	proteins .....	5
2.1.6.	carbohydrates.....	6
2.1.7.	Lipids.....	6
2.1.8.	Acidification.....	7
2.1.9.	Acetogenesis.....	8
2.1.10.	Methanogenesis.....	8
2.2.	Anaerobic reactor technology.....	10
2.2.1.	Wastewater treatment.....	11
2.2.2.	Fixed film systems .....	12
2.2.3.	Suspended growth systems.....	13
2.2.4.	Sludge digestion .....	14
2.2.5.	Solids digestion.....	14
2.3.	Limitations of anaerobic technology .....	15
2.3.1.	Inhibition due to toxic compounds .....	15
2.4.	Mass transfer limitations.....	18
2.4.1.	Efficiency limitations .....	18
2.4.2.	Limitations for treatment of complex wastewater .....	19
2.5.	Complex wastewaters and examples .....	20

2.6.	Anaerobic treatment of sewage.....	21
2.7.	UASB reactors for the treatment of sewage .....	22
2.8.	Removal of suspended solids in UASB reactors .....	26
2.9.	Anaerobic sludge digestion .....	26
2.10.	Reactor design for anaerobic degradation of complex wastewater .....	27
2.11.	Hypothesis.....	28
2.12.	The BFBR concept.....	28
<b>3.</b>	<b>Scope of work .....</b>	<b>30</b>
<b>4.</b>	<b>Development of new reactor BFBR .....</b>	<b>32</b>
4.1.	Principles .....	32
4.2.	Design of equipment .....	33
4.3.	Hydraulic testing.....	34
<b>5.</b>	<b>Materials and Methods .....</b>	<b>35</b>
5.1.	BFBR arrangement.....	35
5.2.	Filter design .....	39
5.3.	Filter media preparation.....	40
5.4.	filter backwash .....	40
5.4.1.	Operation of automatic backwash system.....	40
5.5.	Reactor mixing.....	41
5.6.	Reactor pH control .....	41
5.7.	Model complex wastewaters for experimentation.....	42
5.8.	Feed system.....	43
5.9.	Analytical methods .....	43
<b>6.</b>	<b>Results : BFBR operation and performance .....</b>	<b>46</b>
6.1.	Feed system and pumping: .....	46
6.2.	Filtration .....	46
6.3.	Fluidized filter bed backwash .....	52
6.3.1.	Backwash volume .....	54
6.4.	Reactor mixing.....	55
6.4.1.	milk effluent .....	56
6.4.2.	LCFA effluent .....	56
6.5.	Milk effluent: Discussion of experimental results .....	61
6.5.1.	pH and alkalinity.....	61
6.5.2.	COD removal.....	61
6.5.3.	Methane yield and biogas production .....	62
6.5.4.	Scum accumulation and degradation.....	62
6.6.	LCFA effluent: microbiological aspects.....	66

6.6.1. Discussion of microbiological characteristics of LCFA fed BFBR .....	72
<b>7. Development of a mathematical model of BFBR .....</b>	<b>75</b>
7.1. Model concept.....	76
7.2. Model equations and matrix representation .....	78
7.3. Rate expression .....	82
7.3.1. Microbial growth .....	83
7.3.2. Microbial decay .....	87
7.3.3. Enzymatic reactions.....	87
7.3.4. Gas mass transfer rate processes.....	88
7.4. Equilibrium processes.....	90
7.4.1. Acid base reactions.....	90
7.4.2. Precipitation reactions .....	92
7.5. Parameter values.....	94
7.5.1. Rate expressions and kinetic constants .....	99
7.6. Model implementation.....	102
7.6.1. MATLAB programming language.....	102
7.6.2. Data input interface .....	104
7.6.3. pH calculation.....	106
7.6.4. Output data presentation .....	107
7.7. Simulations .....	108
7.7.1. Simulation of sewage treatment.....	109
7.7.2. Case 7. Simulation of milk effluent treatment in laboratory BFBR .....	131
7.8. Discussion of BFBR based on simulation results .....	133
7.9. Source code description .....	135
<b>8. Aspects of scale-up of BFBR.....</b>	<b>137</b>
8.1. Process design specifications .....	137
8.2. Reactor vessel shape and L/D ratio. ....	138
8.3. Mixing system.....	138
8.4. Backwash.....	138
8.5. Filter arrangement.....	139
8.6. Filter media manufacture .....	139
8.7. Design of automatic filter backwash control system .....	139
8.8. Start-up and shut down issues .....	140
8.9. Remarks on costs.....	140
<b>9. Conclusions .....</b>	<b>141</b>
9.1. Key findings .....	142
9.2. Comparison of BFBR and existing reactors .....	144

9.3. Future developments in BFBR technology. ....	144
9.4. Further study of the science of anaerobic degradation of complex waste...	145
<b>10. References .....</b>	<b>146</b>
<b>Appendix (Source code Case 6 ).....</b>	<b>149</b>

## **1. Introduction**

---

The small amount of oxygen that dissolves in water supports the existence of higher aquatic life-forms. Dissolved oxygen is quickly depleted by the discharge of sewage and industrial effluents. It is common to see the symptoms of oxygen depletion - the dead, dark and foul-smelling rivers and canals in urban areas of developing countries. When a developing country can afford to spend on pollution control, wastewater treatment is usually the first item on the environmental agenda. Most wastewater treatment plants are based on biological treatment processes.

### **1.1. The role of anaerobic waste treatment in environmental management**

---

Biological treatment is used extensively for the removal of organic contaminants from municipal and industrial wastewaters. Chemical oxygen demand (COD) is the measure of organic contaminants in wastewater relevant to design and evaluation of biological treatment processes. The two most important biological processes applied for COD removal are the aerobic and the anaerobic processes. Aerobic processes oxidize COD and are most useful when COD concentrations in the wastewater are low and when high quality treatment is desired. Anaerobic processes are used in the treatment wastewaters with higher COD concentration and also in the treatment of sludge. Anaerobic treatment is usually used as a pre-treatment before aerobic treatment.

### **1.2. Advantages of anaerobic treatment**

---

Anaerobic treatment is more competitive than aerobic treatment in applications where the quantity of COD to be removed is large. Since anaerobic treatment does not require oxygen supply, the power needed for operating aeration machinery is avoided. Anaerobic treatment recovers major part of the COD in the wastewater as methane gas which is a valuable fuel. Anaerobic

treatment plants usually produce more energy than is consumed. Anaerobic treatment produces less waste sludge than aerobic treatment. The COD loading rate of anaerobic reactors is higher than that of aerobic reactors and hence small reactors are sufficient for the treatment of same quantity of COD. The specific activity of anaerobic sludge is higher than that of aerobic sludge and hence the lower amount of biomass is sufficient to achieve a required rate of COD removal.

### 1.3. Limitations of anaerobic treatment

---

Anaerobic treatment cannot be used to remove nutrients - nitrogen or phosphorous from wastewater. Poorly designed anaerobic treatment systems are prone to instabilities, because anaerobic mineralisation is a complex process requiring the co-operative action of several types of microorganisms. Upsets caused by acidification is a common problem and pH control is an important factor in stable operation. The cost of alkali required for pH control can negate all cost advantages of anaerobic treatment. Anaerobic treatment is not able to achieve quality standards (deep removal of COD) of aerobic treatment. In municipal sewage treatment, anaerobic treatment is not able to reduce pathogens concentrations sufficiently. Industrial wastewaters that contain sulphates and sulphides are not amenable to anaerobic treatment because of the production of toxic hydrogen sulphide. Anaerobic reactors take long time for start-up and, therefore, seeding with quality sludge becomes important. Complex wastewaters containing insoluble COD such as colloidal fat are difficult to treat in anaerobic reactors.

## 2. Literature Survey

---

Anaerobic digestion is said to have been used for producing biogas for heating bath water in Assyria in 10<sup>th</sup> century BC<sup>1</sup>. Volta concluded in 1776 that the amount of gas produced is correlated to the amount of decaying matter. 'In 1808, Sir Humphry Davy determined that methane was present in the gases produced by cattle manure. The first anaerobic digester was built at a leper colony in Bombay, India in 1859. In 1895, anaerobic digestion technology was developed in Exeter, England, where a septic tank was used to generate gas for the sewer gas destructor lamp, a type of gas lighting. Also in England, in 1904, the first dual purpose tank for both sedimentation and sludge treatment was installed in Hampton'.<sup>2</sup> In 1861, Pasteur discovered anaerobic microorganisms but the microbial nature of anaerobic degradation was scientifically recognized and studied only from the 1930s.

### 2.1. Science of anaerobic degradation

---

#### 2.1.1. biogeochemical view of the microbial carbon mineralization

---

The mineralization of organic carbon is an integral part of the biogeochemical carbon cycle. Microbial processes achieve the mineralization of organic matter by aerobic oxidation in the presence of oxygen. Oxygen has poor solubility in aqueous medium and penetration of oxygen into organic matter is usually limited to micron sized layers in contact with air. Hence anaerobic conditions are found in environments such as swamps, bottom sediments under water, deep within soils, inside large waste heaps and inside the gut of animals. In these environments, anaerobic organisms mineralize organic matter forming its most reduced form, methane and its the most oxidized form, carbon dioxide. Methane generated during the mineralization either escapes into the atmosphere or is oxidized to carbon dioxide in upper soil layers and aerobic

water columns by methanotrophic bacteria. Methane is a very potent greenhouse gas because of its high retention time in the atmosphere. The global warming potential of methane is estimated at 20 times that of carbon dioxide on mole basis. A major anthropogenic source of methane is intensive farming of animals such as cattle, pigs and poultry and rice cultivation in flooded paddy fields. The atmospheric methane concentration increase in last 150 years is closely correlated to human population increase. Therefore, the capture and utilization of methane in anaerobic reactors and prevention of fugitive emission of methane from anaerobic treatment systems is important from the global environment perspective.

Micro-organisms obtain energy for growth through the degradation of organic materials. Anaerobic degradation is mediated by anaerobic bacteria, archae and possibly other organisms like fungi. The strict anaerobic environment does not harbour higher organisms like multi-cellular animals. Anaerobic mineralization reactions yield very low free energy per mole of organic substrate (food) when compared with the oxidation of the same substrate with oxygen to carbon dioxide and water. The aerobic environment is characterized by the presence of up to 10 trophic layers, i.e., layers of a food chain which feed on lower organisms. The anaerobic environment is almost devoid of trophic layers. In the field of anaerobic wastewater treatment, there is no mention of a trophic layer that feeds on bacteria. The reason why there are few organisms in upper trophic layers is the poor energy yield of anaerobic conversions and corresponding poor biomass yield. It is obvious that the biomass in the trophic layer above will be very small. It also implies that organisms in the upper trophic layer have to feed voraciously to sustain metabolic activity and growth.

### 2.1.2. Thermodynamics of microbial metabolism

The complex biochemical reactions of microbial metabolism can be understood more easily by categorising into energy generating process (catabolism) and biomass synthesis (anabolism). Despite the tremendous diversity of microbial life, the composition of biomass and the anabolic processes within all micro-organisms are remarkably similar. The energy generating process used to generate the free energy needed to drive biomass synthesis is extremely diverse. Free energy is captured in high energy molecules

such as ATP and NADP. These molecules are used as reactants to drive forward synthesis reactions. The processes used to generate energy are redox reactions. Electrons, or equivalently, hydrogen is transferred from a energy substrate molecule to a electron acceptor. When the electron acceptor is a separate compound, taken in by the cell for this express purpose, the process is called respiration. When a compound is split and electrons transferred from one part to the other, it is called fermentation. Both respiration and fermentation are important in anaerobic processes. The reduction of  $\text{CO}_2$  with  $\text{H}_2$ , forming  $\text{CH}_4$  is an example of respiratory process found among a large class of methanogenic bacteria in the anaerobic system, while the cleavage of acetic acid to  $\text{CH}_4$  and  $\text{CO}_2$  is an example of fermentation.

#### 2.1.2.1. Fermentation

In the fermentative processes, a substrate is broken up into parts which are oxidized with respect to the substrate and reduced with respect to the substrate. The most important steps in the anaerobic breakdown of organic matter are fermentative processes. These are mainly the acidogenic processes involving production of fatty acids from complex organic molecules. The net result of anaerobic digestion can also be considered a fermentation with organic matter measured as COD broken into reduced  $\text{CH}_4$  and oxidized  $\text{CO}_2$ .

#### 2.1.3. Anaerobic mineralization of organic compounds

Anaerobic mineralization occurs through the combined action of a wide range of microorganisms. The main reaction stages in the generally accepted anaerobic digestion model can be classified as a) solubilization and hydrolysis b) acidogenesis c) acetogenesis d) methanogenesis.

#### 2.1.4. Solubilisation and hydrolysis

#### 2.1.5. proteins

Proteins are polymers of amino acids, joined together by peptide bonds. Many proteins in their active state are soluble but are easily coagulated to insoluble forms by heat, acids and tannins. Proteins are hydrolysed by the action of enzymes known as proteases. The amino acids that result from the degradation of proteins are easily converted to methane. Another product of the mineralization of amino acids is ammonia, which is toxic at high concentrations (>1000 mg/l). The unionized form of ammonia is the toxic

species and hence inhibition is more at higher pH ranges. It is very likely that solids digesters that treat manure, fish and meat waste operate under ammonia inhibition.

#### 2.1.6. carbohydrates

---

Complex carbohydrates are polysaccharides – chains of glucose and other sugars linked together by mainly 2 types of bonds. They are hydrolysed by the action of several enzymes specific to each carbohydrate. Among the polysaccharides, there are polymers such as lignin and cellulose, (formed by glucose linked by beta1-4 glucosidic bonds) which are highly resistant to hydrolysis. Bacteria and fungi produce cellulase enzymes for the hydrolysis of celluloses. Lignin is very poorly hydrolysed in the anaerobic environment, and its degradation for all practical purposes is zero.

#### 2.1.7. Lipids

---

Lipid (or fats) are polymers of long chain fatty acids (LCFA) linked to a glycerol molecule. In usual fats, three identical fatty acids molecules are linked to one glycerol molecule and hence termed triglyceride. The main fats of interest are triglycerides of LCFAs containing 16, 18 or more carbons. When fats undergo hydrolysis, it produces glycerol and LCFA.

The hydrolysis of fats is carried out by lipase enzymes. The hydrolysis of soluble fats is quite rapid, but the solubility of fats is generally poor at neutral and acidic pH. Solubility improves slightly with pH~8.0. In anaerobic reactors, fats are poorly degraded. The formation of “scum” is a phenomenon well known in anaerobic reactors treating wastewaters containing fats. A scum layer forms in septic tanks which is a low rate anaerobic reactor treating a complex fat containing wastewater – sewage. Fats are known to cause catastrophic failure by sludge washout in dairy effluent treatment anaerobic reactors, because the buoyancy of microbial sludge is reduced by accumulated fats. Fatty materials have a greater tendency to capture gas bubbles as compared to UASB anaerobic sludge. The degradation of fats is a key issue to be addressed in the development of a high rate reactor for the treatment of complex wastewater.

Fats are unusual in another important aspect. The hydrolysis product, LCFA is poorly soluble. LCFA has to be degraded to a substantial extent before all the substrate is solubilised. The scum noticed in anaerobic reactors treating fat

containing wastewater contains considerable quantity of insoluble LCFA. The anaerobic degradation of LCFA is not considered to be an exocellular enzymatic process. It is known to take place via a process termed  $\beta$ -oxidation, whereby an acetate is removed from the end of the LCFA chain, along with the production of  $H_2$  molecule.  $\beta$ -oxidation generates energy and certain classes of micro-organisms make a living carrying out this process. This process is continued till all the LCFA is converted to acetate and  $H_2$ . On COD basis, 66% of the COD flow from LCFA degradation (other than biomass synthesis) is converted to acetate and 33% to  $H_2$ .  $\beta$ -oxidation is thermodynamically feasible only when end product concentrations are fairly low. Hence other classes of micro-organisms that remove  $H_2$  and acetate (mainly through methanogenesis) are always required in the anaerobic consortium for complete removal of LCFA. The degradation of LCFA is often the rate-limiting step in the anaerobic mineralization process.

LCFAs are known to cause toxicity and inhibition of anaerobic wastewater treatment reactors. Some studies report irreversible inhibition. On the other hand, fats are considered good substrates for methanogenesis in the anaerobic treatment of solids wastes, giving improved yield of methane. The conflicting views on anaerobic degradation of fat expressed by anaerobic process technologists from wastewater and solid waste sides have not attracted sufficient comment in scientific papers.

#### 2.1.8. Acidification

---

The process of formation of volatile fatty acids (VFA) from various compounds is termed acidification. Acetic acid, propionic acid and butyric acid are VFA found in millimolar concentration in most anaerobic reactors. These acids are in almost fully ionized form at the pH range of importance in anaerobic reactors with active methanogenesis. There is no single class of bacteria responsible for acidification, rather VFA are the product of many of the fermentative processes involved in the breakdown of soluble sugars, amino acids, and LCFA. Some fermentative processes produce lactate and ethanol rather than VFA.

### 2.1.9. Acetogenesis

---

Acetogenesis is the penultimate step in the anaerobic mineralization process. Acetogenesis produces acetate from substrates such as butyrate, propionate, lactate and ethanol. Acetate can also be synthesized from CO<sub>2</sub> and H<sub>2</sub>. The formation of acetate from carbon monoxide is also reported in anaerobic reactors fed with syngas as substrate. The formation of acetate from fatty acids higher than butyrate is fairly fast and therefore such VFAs not found in substantial quantity in anaerobic reactors. H<sub>2</sub> is a by-product of acetogenesis. As the VFA size reduces, the free energy of acetogenesis become less favourable and the reaction is increasing difficult. Acetate formation from propionate is the most difficult. Propionate degradation is thermodynamically feasible only under very low hydrogen partial pressure, less than 5 Pa. Such low partial pressures are maintained by close associated growth (syntrophic growth) of propionate degrading organism with hydrogen consuming organism. Acetogenesis from propionate degradation is can become rate-limiting in the treatment of soluble wastewaters.

### 2.1.10. Methanogenesis

---

Methanogenesis is final stage of anaerobic mineralization. Methane is formed by two different routes – by the dissociation of acetate and by the reduction of carbon dioxide with hydrogen. Methane can also be produced from simple one carbon compounds such as methanol, formate and methylamine by direct fermentation.

Methane formation reactions provide energy for the growth of methanogenic microorganisms. Methanogenic microorganisms are not classified not as bacteria but as a different kingdom called archae-bacteria, because of major differences in structure of cell membrane from eubacteria. There is also great internal diversity within methanogens. Archaea share some characteristics with higher organisms classified in the kingdom Eukaryae, and therefore evolutionary theories place the divergence of Archaea from Eukaryae later than that of Archaea from Eubacteriaaea.

#### 2.1.10.1. *Acetoclastic methanogenesis*

---

Most of the methane (above 60%) in anaerobic reactors is formed by acetoclastic methanogenic bacteria from the dissociation of acetate.

Acetoclastic methanogens form a distinct class of methanogenic bacteria. Some of these organisms can also utilize other substrates such as hydrogen, while others are specialized in using acetate as the sole energy source (also electron donor). In particular, there are two groups of acetoclastic methanogens, whose competition for acetate is of particular importance in anaerobic reactors – the Methanooseta and Methanosarcina. The Methanosarcina are versatile and utilize acetate, hydrogen, formate, methylamines and methanol as energy sources forming methane in the process. The Methanooseta are specialized acetate utilisers in the form of long rods or filaments, and are able to grow faster than Methanosarcina under low acetate concentration. The filamentous morphology is generally observed in microbial ecology to be favoured at substrate limited conditions, and is a typical example of the competition between  $\mu_m$  strategists and  $K_s$  strategist organisms. In our experience, at start-up, anaerobic reactors are initially exposed to high VFA concentrations. When methanogenic conditions set in, the VFA concentration are lowered and the reactors operate under a seeming steady state with VFA concentration in the range of 12-20 mM. When these steady conditions are maintained for periods ranging from 20 to 60 days, a sudden change can be observed with a washout of large quantities of biomass, without reduction of methanogenesis and a new steady state with less than 5 mM acetate is reached. This phenomenon is attributable to new microbial flora dominated by Methanooseta type methanogens, and a steady state where Methanosarcina type is unable to obtain energy substrates. In practical applications, reactors with Methanooseta type organisms achieve low COD in the effluent and the methanogenic activity of the biomass is high. However, it is subject to catastrophic failure if VFA overloading occurs. The phenomenon of methanogenic population change is closely linked with the formation of granular sludge in UASB reactors.

For the purpose of modelling studies, the following values of growth constants are used.

	$\mu_{max}$ (d <sup>-1</sup> )	$K_s$ (g-acetate-COD/l)
Slow growing acetoclastic methanogens	0.35	0.04
Fast growing acetoclastic methanogens	0.7	0.3

### *2.1.10.2. Hydrogenotrophic methanogenesis*

---

The generation of methane by the reduction of CO<sub>2</sub> with hydrogen is termed hydrogenotrophic methanogenesis. H<sub>2</sub> is the simplest energy substrate available and the biochemical process for hydrogenotrophic methanogenesis is quite primitive. Nearly all methanogens are capable of reducing carbon dioxide.

## *2.2. Anaerobic reactor technology*

---

The earliest anaerobic reactors were septic tanks (1880) and anaerobic filters for sewage treatment. After the development of activated sludge treatment around 1910, anaerobic processes were rarely used in sewage treatment. The need for industrial wastewater treatment, particularly for high COD wastewaters revived interest in anaerobic technology and led the development of high-rate anaerobic reactors such as the fixed film reactor, the UASB reactor, the anaerobic contact process and the anaerobic fluidized bed reactor. The large savings in energy favoured the use of high-rate anaerobic reactors for high-strength industrial effluents. The success of treatment of high-strength effluents led to application of anaerobic technology in medium strength industrial effluents such as papermill and brewery, where anaerobic technology has been very successful. The development of anaerobic reactors for low-strength wastewaters such as sewage has attracted attention particularly for developing countries in warm climates. However, these have not found wide acceptance so far.

In India, high-rate anaerobic reactors were widely adopted in the 1980s and 1990s for the treatment of distillery effluent, where COD exceeds 100,000 mg/l. Although the installation of the reactors were required by regulatory requirements of environment pollution control, companies adopted anaerobic treatment reactors because the biogas fuel generated in such systems allows break-even of investment within 3 years, a remarkably profitable investment. The success of anaerobic treatment in the molasses based distillery sector led to interest in anaerobic reactors in other industries, some of which were similar in nature, such as pharmaceutical industry using molasses as a fermentation substrate, and some of which were having completely different characteristics such as dairy, slaughterhouse, soft-drink, leather tanning, and combined industrial estate ETP. The absence of proper knowledge of process and its

complications has led to the failure of several of the anaerobic reactors. Some of these failures were due to high sulphate concentration, some due the presence of fats and solids, and recalcitrant substances such as lignosulphonates in the effluents. Even in the distillery sector, the presence of high sulphate concentration and the generation of H<sub>2</sub>S in the biogas were seriously considered only later.

The application of anaerobic treatment of solid waste took place later than wastewater treatment. The first application of “anaerobic composting” took place in India in 1920s (“Bangalore process”) where solid waste and farmwaste was buried in constructed trenches. There is currently great interest in anaerobic treatment for the stabilization of municipal solid wastes (MSW). A large number of designs are commercially available, some which are slurry digestion systems, where organic fraction of MSW is separated from other wastes, and slurry to less than 10% solids before digestion. Other designs include “dry digestion” and “leach bed” anaerobic reactor designs. Anaerobic technology for MSW has received impetus because methane emissions by land-filling untreated MSW is considered a significant source of greenhouse gas causing global warming.

### 2.2.1. Wastewater treatment

---

There is a large number of publications on anaerobic wastewater treatment including books<sup>3,4</sup> and series of conference proceedings on anaerobic digestion conducted by the International Water Association. Hence only an outline review of anaerobic wastewater treatment is given here.

Anaerobic technology began to be seriously considered for wastewater treatment first in the treatment of high strength industrial wastewater, as environmental regulations on discharge of effluents were formed and enforced. The main driver for anaerobic technology was the interest in reducing aeration costs of direct aerobic treatment. In India, anaerobic reactors were first applied extensively biogas generation from high strength distillery effluent in the 1980s and 1990s. The biogas generated was enough to run the distillery boiler. The cost of anaerobic digestion in distilleries was recovered within 3 years. The main anaerobic reactor systems for wastewater treatment are described below.

### 2.2.2. Fixed film systems

---

The fixed film reactors have an inert carrier material inside the reactor vessel, on whose surface, microorganisms grow as a biofilm. The physical attachment process prevents biomass washout and leads to high biomass retention times and high biomass concentrations. The reactors can be operated safely at high flow velocities without washout. The major types of fixed film reactors currently used are

- Packed bed reactor.

These reactors have an inert packing media either plastic or stone for biofilm growth. The plastic media is may be random packing, that are dumped into the reactor vessel, or structured packing, which are placed so as to fill the reactor flow cross-section. The plastic packing media used in anaerobic reactors are derived from media used in mass transfer equipment such as distillation columns, absorption columns and cooling towers. Excess biofilm growth can clog packing media and therefore, anaerobic reactor packing media are large size versions of media used in mass transfer applications. The larger sizes reduce the surface area available per unit volume for biofilm growth, but provide larger flow channels.

The direction of flow in packed bed reactor can either be downflow or upflow and suppliers claim various advantages for either configuration, but there are no scientific studies to back these claims. In any case, there is little difference in applicable loading rates in each configuration.

- Fluidized bed reactor

The fluidized bed reactor uses small size inert carriers, typically sand less than 0.5 mm size. The bed is fluidized by the application of an upflow velocity, typically 10 to 15 m/h. The velocity applied is sufficient to achieve around 100% expansion of the bed. Small size media have large specific surface area, and therefore the biomass concentrations achieved in fluidized bed reactors is large compared with fixed film reactors. The biofilm thickness is limited by particle to particle collisions and turbulence. Usually when the biofilm

thickness become large, as in the case of packed bed reactors, the microorganisms deep within the biofilm are starved for substrates and enter the decay phase. Only a thin layer of microorganisms on the surface of the biofilm is active. In the fluidized bed reactor, the constant rubbing of media particles keeps the biofilm thickness small and contains very active biomass. Among all reactors, the fluidized bed reactor has the best mass transfer characteristics. But it is relevant to point out that only the transfer of soluble substrates to biofilm is enhanced in a fluidized bed reactor and there is no advantage in using fluidized bed reactors for complex wastewaters.

### 2.2.3. Suspended growth systems

The continuous stirred tank reactor (CSTR) is the simplest reactor design for wastewater treatment. It does not separate biomass retention and hydraulic retention time. Hence it can be used for complex wastewater provided the hydraulic retention time is sufficiently high - usually 10 to 20 d. The CSTR is a low-rate reactor with no method of enhancing the reactor conversion rate, other than by mixing. The mixing devices can be mechanical paddles or axial flow propellers in draft tube or gas sparging devices. Various technologies for gas sparging are used – uniform sparging, gas lances, gas sparged draft tubes and such devices as slug mixers.

The anaerobic contact process improves the biomass retention times in a CSTR by using a secondary settler to settle and return sludge. It uses the same principle as the well known activated sludge process, but unlike activated sludge, the anaerobic CSTR sludge formed does not settle well because of gas formation. Hence a vacuum degasser and sometimes, a chemical flocculating agent is added before the secondary settler.

The upflow anaerobic sludge blanket (UASB) and expanded granular sludge bed (EGSB) processes are also suspended growth processes. Since the UASB is the most commonly used anaerobic wastewater treatment technology, and since this thesis concerns the development of a reactor that overcomes the limitations of the UASB, in particular, for the treatment of complex wastewaters, the UASB is considered in greater detail in Sections 2.6 to 2.10.

The expanded bed reactor is very similar to the fluidized bed reactor, except that bed expansion is limited to about 50%. The inert media is done away with in the expanded granular sludge bed reactor, with only granular biomass forming the bed. It is essential to provide granular sludge for the start up of the EGSB reactor.

#### 2.2.4. Sludge digestion

---

The objective of anaerobic sludge digestion is the stabilization of wastewater sludges, which can be dewatered and disposed off without putrefaction and odour. Sludge digesters were first introduced at least 100 years ago for the fermentation of sludges obtained from domestic wastewater. Sludge digestors can be mixed or unmixed. The sludge retention time in the reactor controls the degree of sludge degradation. However since the hydraulic retention time is equal to sludge retention time, the design is based on HRT. The retention time for digestion of wastewater sludges is 15 to 20 d and the usual design solids loading is 3.2 to 7.2 kg VS/(m<sup>3</sup>.d). The retention time of 15 to 20 d is required for maintaining requisite population of methanogens in a CSTR. This duration is also sufficient for solubilisation of particulate substrates. Volatile solids destruction of 50 to 60% is achieved within 20 d.

#### 2.2.5. Solids digestion

---

Anaerobic digestion has a long history of application in India as farm biogas units for cow-dung ('gobar gas'). The gobar gas units (usual size less than 25 m<sup>3</sup>) have no power requirements and are capable of stabilizing cow dung while producing fuel for cooking and lighting. Cow dung is relatively homogenous as compared with other solid waste, such as farm wastes, market waste and municipal solid wastes. Digestion of such materials at large scales requires engineered pretreatment systems and reactors and therefore, simple scale-up of gobar gas like units is not sufficient. The development of suitable reactors for solid wastes has made anaerobic digestion a viable option for stabilization of organic fraction of municipal solid wastes<sup>5</sup>.

The situation in solids digestion is more confusing than in wastewater treatment, with reactor designs known by proprietary names rather than by generic classification. In general, we can classify the technologies into one-stage and two-stage digestion systems<sup>6</sup>. The two-stage digestion systems, volatile

fatty acid generation takes place in the first stage and methanogenesis takes place in the second stage. The leach-bed reactor is a 2-stage process. Separation of acid generation and methane generation takes place only when methanogenic population in the first stage is limited. Hence the retention time in the first stage reactor is limited to less than 10 d, preferably less than 5 d.

Most of the reactor designs for solid waste are single stage systems. The 1-stage wet digestion system separates organic fraction from other materials by pulping of the solid waste. A slurry of 10 to 15% total solids is digested in a CSTR. There are technical issues connected with pulping and digestion of the slurry, because of the separation and settling of heavy particles in the digester. The dry digestion technology uses wet macerated solids, up to 40% TS, conveyed using mechanical handling systems such as screws into a plug flow digestion reactor. The very high solids content and viscosity of the mash prevents separation and settling of heavy fraction inside the digester. The recirculation of digested solids to the inlet of the digester is crucial to provide inoculation of methanogens to fresh feed. Horizontal and vertical plug flow digesters are available commercially. The solids conveying, mixing and circulation systems are large size moving machinery, with corresponding cost and maintenance issues. Hence, solid waste digestion requires reactors that are more complex and costly as compared with wastewater treatment reactors or sludge digesters. One of the issues that affect solid digestion, but usually of little consequence in liquid waste, is ammonia inhibition, particularly in the digestion of protein-rich wastes.

## 2.3. Limitations of anaerobic technology

### 2.3.1. Inhibition due to toxic compounds

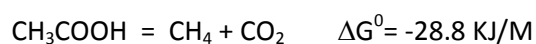
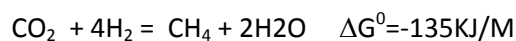
There are many factors inhibiting the rate of methanogenesis. Ammonia, hydrogen sulphide, salt, volatile fatty acids (substrate inhibition) and some tannin monomers are some of the compounds toxic to methanogenic bacteria.

Ammonia inhibition has been noticed during the treatment of gelatine waste, protein wastes and animal wastes<sup>7</sup> such as cow dung. The unionized form of ammonia (free ammonia) is the inhibitory species. Since the pKa of ammonia is 9.3, the fraction of free ammonia at pH 7, (normal anaerobic digester operation pH), is very small. However, the pH of reactors fed with substrates

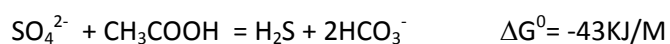
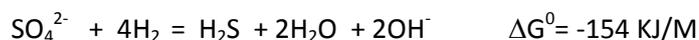
that produce substantial quantity of ammonia, is usually higher and frequently exceeds pH 8, because of the alkalinity contributed by ammonia. In unadapted cultures, ammonia inhibition may occur at free ammonia less than 200 mg-N/l, but in practical situations especially with continuous reactors, we always have adapted biomass. At thermophilic conditions, ammonia inhibition is considerably greater, because of higher unionized ammonia fraction at higher temperatures. In continuous reactors, methanogenesis is not inhibited at ammonia concentration less than 1 g/l. Exceeding this concentration progressively reduces specific methane yield from the substrate, and the VFA concentration in the digester liquor is higher. Higher VFA concentration is required to balance out the higher ammonia concentration and maintain pH conditions conducive to methanogenic activity. There are reports that high ammonia concentration also inhibits hydrolysis and acidification<sup>7</sup>. In the anaerobic digestion model, the Monod-type 50% inhibition constant for acetoclastic methanogens is given by  $K_i = 25 \text{ mg-unionised-NH}_3\text{-N/l}$  corresponding to 1.6 g-NH<sub>3</sub>-N/l at pH7 and 0.52 g- NH<sub>3</sub>-N/l at pH 7.5.

Hydrogen sulphide causes severe inhibition of methanogenesis. H<sub>2</sub>S is formed in anaerobic reactors by sulphate reducing bacteria (SRB). These bacteria occupy the same environmental niche as methanogens, utilizing simple methanogenic substrates like acetate and hydrogen using sulphate as electron acceptor. SRBs are able to outcompete methanogens in the competition for hydrogen and acetate, if sulphate availability is not limiting. Thermodynamically, sulphate reduction is favoured over methane production, for both decarboxylation of acetate as well as for reduction using hydrogen.

Methane generation



Hydrogen sulphide generation



The above reactions are written under standard conditions. The actual free energy changes are dependent upon the activities of the reactants and the

products of each reaction in the reactor. This is very often favourable to SRB<sup>8</sup>. The inhibiting species is un-ionised H<sub>2</sub>S, rather than HS<sup>-</sup>. Both SRB as well as methanogens are inhibited, but methanogens are inhibited at a lower H<sub>2</sub>S concentration than SRB. Hydrogen sulphide is a very soluble gas, and liquid/gas equilibrium is rapidly established in reactors. Therefore, the gas phase hydrogen sulphide concentration is directly correlated to liquid phase unionised H<sub>2</sub>S. It is generally observed that gas phase concentration above 5% causes substantial inhibition of methanogenesis, while complete inhibition occurs above 8%.

Highly saline conditions are inhibitory to micro-organisms because of osmotic pressure. Methanogenic condition occurs in marine sediments and salt marshes and therefore, methane bacteria adapts to fairly high TDS concentrations (~50 g/l). Among the cations, sodium is a stronger inhibitor than potassium<sup>9</sup>. 50% inhibition is seen at Na<sup>+</sup> > 5g/l.

Volatile fatty acids are the main substrate for methane production. Yet anaerobic reactors are inhibited by excess VFA. There are two factors to be considered: 1) high VFA levels can cause acidification and low pH in reactors affecting methanogens, that can grow only within narrow neutral pH band; 2) VFA, in particular the unionized fraction of VFA is inhibitory to growth. Growth of acetogens, particularly on propionate is inhibited. At neutral pH, the unionized fraction of volatile fatty acids is low (<1%) and hence direct inhibition is rarely experienced. VFA inhibition is considered to be reversible. The 50% inhibition constant for un-ionised C<sub>2</sub> and C<sub>3</sub> volatile fatty acids was reported to be 16 and 6 mg-COD/l. A Monod inhibition K<sub>i</sub> value of 1 g-acetate-COD/L and 0.1 g-butyrate-COD/L is taken for acetogen growth on propionate. In practical high-rate anaerobic reactors, there are two classes of methanogens that predominate depending on the steady state concentration of VFA. At low VFA levels, less than 4 mM as per our experience, granule forming methanogens outgrow flocculant methanogens.

Compared with VFA, long chain fatty acids (LCFA) are reported to be more toxic to methanogenic sludge. Long chain fatty acids have low solubility and hence the reported values are difficult to interpret. Lipid and long chain fatty acid degradation are considered the main problems affecting the anaerobic digestion of dairy effluent. Lipids contribute up to 60% of the COD of milk

effluent and its hydrolysis and the subsequent biochemical reactions determines the efficiency of the reactor.

Rinema et al.<sup>10</sup>, is a widely quoted study of LCFA inhibition of granular UASB sludge. It was found that capric acid concentration of 6.7 to 9.0 mol / m<sup>3</sup> is sufficient to be near 100% lethal to both acetogenic and methanogenic sludge. In COD terms, this concentration is only 2.79 to 3.74 kg/m<sup>3</sup> - within the range expected in many fat containing effluents. Therefore, the above result apparently would imply serious limitations of the anaerobic process. But this is contrary to experience of successful operation of anaerobic reactors for fat containing wastewater and fat containing solid wastes. Therefore, the above result is non-representative of actual reactor conditions, particularly as it is based on batch tests with sludge obtained from (fat-free) potato processing wastewater.

Hwu et al.<sup>11</sup>, studied the biosorption of LCFA on UASB sludge in both batch tests as well as continuous reactor studies. The authors used potato processing wastewater sludge in the batch assays. Complex patterns of adsorption and desorption of LCFA are seen in the batch reactor studies. These are likely to be artefacts of the nature of experiment and the use of unadapted sludge. UASB reactor studies<sup>6</sup> using slaughterhouse effluent (expected to be adapted to LCFA) showed complete sludge flotation at loading rate exceeding 0.2 kg fat-COD/m<sup>3</sup>/d. No inhibition is reported at this loading rate.

## 2.4. Mass transfer limitations

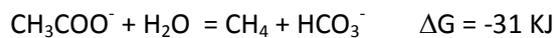
---

### 2.4.1. Efficiency limitations

---

Anaerobic treatment is usually considered a pre-treatment method because the residual COD after treatment is not usually within statutorily acceptable limits (<250 mg/l for land discharge and <100 mg/l for surface water discharge). Aerobic treatment can produce high quality treated effluent with COD less than 30mg/l in the treatment of sewage. At the same time, anaerobic treatment seldom is capable of producing effluent less than 150 mg/l. Therefore anaerobic treatment is followed by aerobic treatment. The poor efficiency of treatment, with regard to residual COD, has not been properly explained in published literature and there are very few developments on improving the efficiency. Furthermore, there has been little comment in literature on why anaerobic

treatment cannot achieve efficiency levels of aerobic treatment. A common classroom explanation of high residual COD is that it is a consequence of the poor energetics of methanogenesis as compared with aerobic mineralization. The thermodynamics of acetoclastic methanogenesis is given below:



If we take initial acetic acid concentration as 1000 mg/l, and proceed to equilibrium, partial pressure of methane and carbon dioxide as 0.5 atm, then the estimated residual acetic acid concentration to initial concentration is less than 1µg/l. A thermodynamic equilibrium model that includes redox, gas-liquid and acid-base equilibria<sup>12</sup> shows that essentially complete conversion of acetate to methane is thermodynamically feasible. While reactions would not proceed to equilibrium because of the need to have enough free energy for production of ATP (ie., an electron generated from the oxidation of acetate should be at potential sufficient to reduce ADP to ATP), it is still true that acetate can be almost completely converted to methane. Hence the classroom explanation for high residual COD from anaerobic reactors is not correct.

#### 2.4.2. Limitations for treatment of complex wastewater

The limitations of current anaerobic reactor design when treating complex wastewater is briefly reviewed here.

The UASB reactor is not particularly suitable for the treatment of suspended-solids rich complex wastewater<sup>13</sup>, because it is difficult to maintain sludge settleability. The presence of suspended fats and lipids are mentioned as heavily promoting sludge flotation and washout of active biomass both in the case of flocculant and granular sludges. Mixing in UASBs is dependent on upflow velocity. The upflow velocity is limited by the need to retain active sludge by settling, an inherent limitation of the UASB design. The fixed film reactors can capture suspended solids and provide adequate retention time for biosolids, "the anaerobic filter", thus satisfying the criterion of decoupling of suspended solids retention time from hydraulic retention time. But fixed film reactors have severe limitations regarding mixing because of its stationary biomass support. Evidently attached films on stationary supports do not facilitate suspended solids - biocatalyst contacting. The fluidized bed reactor has better mass transfer characteristics when compared with the fixed film reactor but unlike in

a fixed film reactor, there is no mechanism available for capture and retention of suspended solids. The 'two-phase' reactor concept improves process stability and efficiency because sensitive and rate-limiting methanogenic phase is protected from substrate inhibition (VFA overloading) by segregation from the acidogenic phase. Ipso facto, phase segregation appears unnecessary when solubilization is the limiting factor, because acid build-up is not expected. On the other hand, low pH conditions in the acid phase reactor can reduce the hydrolysis rate of solids<sup>14</sup>. There solubilisation of fats in acid phase of two-phase reactors is limited<sup>15</sup>.

The following directions for the development of improved anaerobic reactor technology can be identified.

- Enhancing volumetric organic loading rate in the anaerobic treatment of complex wastewater.
- Improving efficiency of removal and efficiency of methanization of fat and lipids in anaerobic reactors so as to avoid pretreatment requirements.
- Improving process efficiency in anaerobic reactors in order to obtain high quality effluent (COD less than 100 mg/l) so as to avoid aerobic post treatment for organic carbon removal.
- Improving pathogen removal efficiency in the case of anaerobic sewage treatment.
- Reducing chemical costs for pH control in anaerobic reactors.
- Developments for avoiding precipitation, deposition and scaling inside anaerobic reactors.

The "Buoyant Filter Bioreactor" (BFBR) is an attempt to enhance the loading rate and treatment efficiency of complex wastewater in anaerobic reactors.

## 2.5. Complex wastewaters and examples

Complex wastewaters are discharged by several industries including dairies, slaughterhouses, palm oil mills, food and fruit processing plants. Although of low-strength, municipal sewage is also a complex wastewater. The

determination of insoluble COD is method dependent. Generally the 0.45 micron filtered COD is taken as soluble COD and the difference from total COD is taken as suspended COD. The suspended COD in sewage ranges from 66% to 79%<sup>16</sup>.

## 2.6. Anaerobic treatment of sewage

---

The standard process for municipal sewage treatment comprises (a) primary settling, (b) secondary treatment by activated sludge, and (c) anaerobic digestion of primary and secondary sludge in a anaerobic digester. Activated sludge treatment step is the main component of the operating cost of sewage treatment plants. Direct anaerobic treatment of raw sewage would considerably reduce operating costs, the number of process steps and the process equipments required. But anaerobic treatment cannot achieve nutrient removal (nitrogen and phosphorous removal) from sewage. Another drawback of anaerobic treatment is that metabolic heat generation in the process is low and hence digesters, unlike aeration tanks, would require to be heated in cold climates. But for third world cities in tropical climates that do not have sewage treatment plants, anaerobic treatment can be an attractive low-cost option, at least in the short term.

Sewage is a complex, partially soluble wastewater. While some of the particulate components are quickly solubilised, the rate of hydrolysis of other particulate components (liquefaction) is slow. Hence, “in the anaerobic treatment of raw domestic sewage, the extent to which suspended solids is entrapped in the anaerobic reactor is of great importance”<sup>17</sup>. The COD strength of sewage is very low (0.3 to 1g/l). The gas yield during sewage treatment is therefore very low. The turbulence created by gas production is a major factor enhancing mass transfer, i.e., substrate and biomass contact. Poor gas production in anaerobic reactors treating sewage does not facilitate contact between biomass and sewage. The problem is accentuated by the fact that methane produced but not transferred to bulk gas phase can be as much as 0.1 g-COD/l. This is frequently as high as 50% of the methane produced. It may be noted that turbulence is primarily a function of specific volumetric gas production rates, rather than gas yield and hence, theoretically, if the reactor volumetric organic loading rate is increased, sufficient turbulence can be created

by gas production. However, nearly all development of anaerobic sewage treatment, has been carried out using the non-agitated UASB reactor.

## 2.7. UASB reactors for the treatment of sewage

The UASB reactor developed by Lettinga and others, was first introduced to optimize the anaerobic treatment of agro-industrial wastewaters. In applications for the treatment of sugar beet, potato, brewery and papermill effluents, the UASB has demonstrated high volumetric loading rates, good COD conversion and low sludge production. This was primarily attributed to the growth of granular sludge with excellent settling properties and high methanogenic activity. Sanitary engineers were therefore motivated to apply the UASB reactor for sewage treatment. The results were not particularly satisfactory. UASB reactors failed to develop granular sludge. Accumulation and slow hydrolysis of suspended solids and low methanogenic activity plagued the reactors. Nevertheless, the UASB reactor remains the only anaerobic reactor tested and applied in direct sewage treatment<sup>18</sup>. It was realised from the beginning that the UASB has best chance of success in hot climates which is where it has been studied intensively<sup>19,20</sup>.

Leitao<sup>19</sup> reports on laboratory UASB steady state experiments on real sewage. He observed that the specific methanogenic activity of sludge was quite low 0.2 gCOD/gVSS/d. But COD-total removal efficiency and COD-settled removal efficiency decreased for lower sewage COD. The ratio of COD\_VFA/COD-dissolved in effluent decreased as the influent COD decreased. It was interpreted as acidification rate being the limiting rate. The solids retention time in the reactor calculated as the ratio of solids in reactor / sludge production where the sludge production was defined as settleable VSS in treated effluent. By this definition the solids retention time decreases as the influent concentration increases. Settled COD removal efficiency increased with increased HRT from 1 h to 6 h, with the efficiency becoming constant for HRT greater than 4 h. At 6 h HRT, methanation of removed COD was nearly complete (74%), close to the biodegradability of the COD (77%). The UASB is very stable with regard to pH and buffer capacity and does not get acidified because of load variability in sewage. The specific methanogenic activity of sludges were greater at lower HRT. COD concentration of the sewage did not affect specific methanogenic activity in the tested range (200 mgCOD/l to 800 mgCOD/l). The

author determines that only sludge produced in UASB reactors with HRT >6h is sufficiently stable to be disposed off without further treatment, whereas at less than 6 h HRT, the sludge contains entrapped suspended solids undergoing degradation. Contrary to expectations, the sludge that forms in the UASB is more voluminous (less compact) when the influent COD is low.

Full scale plants in hot climates were installed and monitored by Dutch companies, in cities like Sao Paulo and Saumare in Brazil, Kanpur and Mirzapur in India, Bucaramanga and Cali in Colombia. The plants were rarely operated at HRT less than 4 h but never exceeded an HRT of 20 h. At higher HRT, removal efficiencies were better. However, the reactor costs are corresponding larger. Start-up of UASB reactors on domestic sewage is simple - self-inoculation by operating the reactor at HRT near 24 h. COD removal efficiencies increase from 60% to 75% after 6 months.

UASB reactors at Kanpur<sup>21</sup> and Mirzapur were operated with upflow velocity 0.75, .92, .61 m/h. The COD-total removal efficiency was 80%, 24-50%, and 49-65%. Under the Yamuna Action Plan, 12 UASB sewage treatment reactors have been set up in India, and are reportedly functional<sup>22</sup>.

Long term full-scale experiments with anaerobic treatment of sewage at Cali, Columbia have been published. UASB reactors for sewage treatment can be started by self-inoculation - a great practical advantage. The hydraulic retention time is the critical factor for trapping sewage suspended solids. The recommended design HRT for sewage treatment in UASB is 4 hr (corresponding to reactor upflow velocity 1 m/h). The velocity in gas-solids separator aperture recommended is less than 4 m/h. The reactor is able to take hydraulic shocks up to 1.75 m/h upflow velocity, which is important since sewage treatment plants have diurnal fluctuations in hydraulic load. The fractional conversion of COD to gas was 0.5 kg CH<sub>4</sub>-COD/ kg COD removed. The excess sludge production in the Cali plant was 0.1 kg COD/ kg CODinfluent. The unaccounted COD is presumably dissolved gas in effluent. The sludge formed in the UASB has rather low methanogenic activity (0.15 kgCOD/kg VSS/d) and while the sludge concentration is 10 kg VSS/m<sup>3</sup>/d. Based on these figures, the maximum loading capacity of UASB reactors is limited to 1.5 kg COD/m<sup>3</sup>/d. These values represent the performance parameters that any new anaerobic reactor design for sewage treatment should surpass.

India is one of the leading countries in the world in application and promotion of UASB for sewage treatment. Sewage is screened and grit is removed before pumping to the UASB.

The Indian sewerage design manual<sup>23</sup> provides the following specification for direct UASB sewage treatment in hot climates:

- Organic loading 1.0 to 2.0 kg COD/m<sup>3</sup>/d
- Efficiency of COD removal 50 to 70%
- HRT 6 to 12 h; Sludge retention time: 15 to 30 d.
- Overflow rate < 1 m/h; Aperture velocity 3 m/h
- Sludge production 0.1 to 0.2 kg dry matter / m<sup>3</sup>
- Gas yield 0.15 to 0.2 m<sup>3</sup>/kg COD removed

An economic analysis of various sewage treatment options in India has been carried out by Sato<sup>24</sup>. The capital cost of UASB is given by the formula:

$$y = 494x^{-0.20}$$

where

y is in USD/(m<sup>3</sup>/d) (2003 prices Rs.48/USD)  
x is in m<sup>3</sup>/d

UASB capital costs are comparable to that of conventional activated sludge plants with sludge digesters of similar capacity.

The annual operating and maintenance costs (mechanical and electrical equipment replacement costs calculated at annual interest cost 5%) for sewage treatment UASB is given by the formula

$$y = 453x^{-0.49}$$

UASB operating costs are only about 25% that of activated sludge plants. However, the COD removal efficiency of UASB is less than 70%, while it exceeds 90% for activated sludge.

The land area requirement for UASB is given by the formula

$$y = 10.2x^{-0.12}$$

where

y is in  $\text{m}^2/(\text{m}^3/\text{d})$

x is in  $\text{m}^3/\text{d}$

The land area requirement for UASB works out to be 2 and 5  $\text{m}^2/(\text{m}^3/\text{d})$ .

Capital costs (excluding land costs, land prices being determined by location) are more than 50% of total annual costs.

In summary, we conclude that the UASB reactor as a method of sewage treatment was developed on the following presumptions:

- It simplified the sewage treatment process train – by producing stabilized sewage sludge, avoiding primary and secondary settling tanks and sludge digesters
- High-rate anaerobic treatment implies small reactor sizes and reduced capital costs. The UASB without any internal packing media for retention of biomass has lower capital costs for low strength effluents. It should be sufficient for less developed countries, looking to implement basic sewage treatment plants, advanced treatment processes for nutrient removal being postponed for the future.

However, the experience in implementation of UASB has been:

- The UASB cannot accommodate high organic loading (of the order of  $10 \text{ kgCOD}/\text{m}^3/\text{d}$ ) as in the case of simple industrial effluents.
- Given the low COD removal efficiency of UASB and capital costs comparable to that of activated sludge plants, it is not clear that the UASB is an economic choice for sewage treatment, particularly in towns in Kerala, with extraordinarily high land values.
- The gas yield in UASB reactors for sewage is severely affected because of leakage with liquid. This has adverse impact on greenhouse gas emissions
- The efficiency of pathogen destruction in UASB is an order of magnitude lower than obtained in activated sludge process. Hence, UASB alone would not suffice as a sewage treatment measure even

for less developed countries. It has to be supplemented by measures such as pond treatment.

UASB technology for sewage is examined in this thesis in some detail, as sewage treatment would be the largest market for a new reactor for complex wastewater. The organic loading of the UASB reactor is necessarily limited in order to trap sewage suspended solids in the reactor sludge. On the other hand, reactors that enable higher organic loading rates, with improved mass transfer, may ultimately, be less expensive because of reduced sizes. These factors will become explicit when we consider later the development of the BFBR reactor.

## 2.8. Removal of suspended solids in UASB reactors

The key issue limiting the loading and removal efficiency of UASB for complex wastewater is its ability to remove suspended solids. The physical mechanism by which suspended solids are retained in sludge bed is complex and not well understood<sup>25</sup>. The main parameters that affect capture of suspended solids is temperature and viscosity of wastewater, the HRT, gas turbulence linked with COD loading rate. In addition there are factors which have not been discussed in literature. These are related to microbiological characteristics of the sludge such as filamentous organisms, exocellular polymeric substances that promote flocculation, higher trophic organisms that may directly consume suspended particulate matter.

## 2.9. Anaerobic sludge digestion

Although wastewater sludge digestion is not usually considered in the context of anaerobic wastewater treatment, it is nevertheless instructive to examine it in this thesis concerning complex wastewater, as sludge has the characteristics of both liquid and solid. Anaerobic digestion of sludge is a technology that has been practised for more than 50 years, and the terminology used in sludge digestion is different from that of wastewater treatment. The volatile solids content of wastewater treatment plant sludges is usually between 3 to 10 g VSS/l. Sludge digestion is successfully carried out only in completely mixed reactors or tank reactors. The various types of digesters differ according to the method of mixing – mechanical, gas stirred, draft-tube, etc., and the shape of the digester – cylindrical, conical bottom, egg-shaped etc.. It may be

noted that no special effort is made in sludge digesters to decouple the retention time of either biomass or solids from hydraulic retention time. The completely mixed reactor, where HRT is identical to SRT is called a “high-rate digester” in sludge digestion terminology. The name suggests that the unmixed digester where layers of settled solids, supernatant and scum layers are distinct and would have different retention times, has a lower volumetric loading rate and volumetric gas productivity. It implies that unmixed sludge digesters are limited by mass transfer, though it is not clear where exactly are the constraints on mass transfer – is it the contact between solids and micro-organisms, contact between exocellular enzymes and solids, contact between scum and micro-organisms or enzymes, gas transfer limitation etc.? The issue becomes clearer in the light of experimental observations described in this thesis.

The process design of sludge digesters is based on solids retention time (SRT) which is equal to hydraulic retention time for completely mixed units. At 30C, the recommended SRT is 14d<sup>26</sup>. The gas yield in anaerobic sludge digesters is usually given in term of VS destroyed. The yield is usually 0.75 to 1 m<sup>3</sup>/kg VS destroyed<sup>27</sup>, with methane ranging from 60 to 70%. The loading rate in high-rate digesters is in the range of 1.6 – 4.8 kg-VSS/m<sup>3</sup>/d. Sludge volatile solids destruction ranges from 50 to 65% in digesters. Ammonia released during the digestion is a potential toxicant during wastewater sludge digestion.

## 2.10. Reactor design for anaerobic degradation of complex wastewater

Reactors for treatment of complex wastewaters are sized according to the hydraulic retention time (HRT), rather than COD loading rate, implicitly assuming that solubilization of particulate COD is the rate-limiting factor in the anaerobic mineralization process. 20 to 30d HRT provides sufficient retention time for the solubilization and degradation of solids. This approach is sufficient in the case of biomethanation of sludges and slurries such as cow-manure. In the case of lower strength complex wastewaters such as dairy effluent (10 to 5 gCOD/l) and sewage (1.5 to 0.5 g COD/l), providing 20-30d retention time, obviously leads to uneconomically large reactors. Reactor design is therefore based on assumed COD loading rates for various wastewaters. When UASB reactors are used for the treatment of dairy wastewaters, fats in retained sludge can cause catastrophic washout. In the case of sewage, problems are seen with build-up of scum. These problems are caused by the slow solubilization of particulate COD.

The design of anaerobic reactors specifically for high-rate degradation of complex wastewater characteristics is not well developed.

### 2.11. Hypothesis

---

My hypothesis is that complex wastewater containing insoluble COD can be treated in a high-rate reactor that is capable of retaining solids. The “Buoyant Filter Bioreactor (BFBR)” is designed to retain suspended solids, along with biomass in well-mixed condition. This thesis presents the development of the BFBR and its performance on complex wastewater.

### 2.12. The BFBR concept

---

The BFBR is based on the concept of decoupling particulate COD retention time from the HRT. This would enable greater retention of particulate COD and thereby allow its solubilization and mineralization. The retention of particulate COD in modern high-rate anaerobic reactors designs is incidental to the design philosophy of retention of biomass. However biomass and particulate COD have different characteristics and therefore the retention of particulate COD is not efficient.

In a UASB, solids separation is effected using gas-liquid-solid separation (GSS) baffles. This enables the settling of particles, with settling velocities greater than  $\sim 5$  m/h. The GSS baffles are well suited to separate granular or flocculant biomass from water. Since the GSS system is able to retain only fast settling sludge, it is a driving force for the development of granular biomass. Particulate COD in complex wastewater can be colloidal and does not settle easily. Particles of fat have density lower than water and therefore do not settle. The UASB design is not designed to retain particulate COD of such nature. At the same time, UASB does provide a degree of separation of particulate COD because of adsorption on biomass and because of coagulation and flocculation of particulate COD in the reactor environment. These mechanisms are not controllable and currently not predictable.

In a fixed film reactor, particulate COD capture in fixed film media is highly unlikely since media is designed to minimize dead zones where particle may settle. In fact, primitive fixed film reactors with rough stone media offers better particulate COD retention than structured or random plastic media

The key issue is therefore the development of a practical reactor which can efficiently retain particulate COD. Filtration is an efficient method of separating fine solids from liquid phase. Deep bed filters are constructed from a porous granular medium, usually of graded sand. It is widely used in water treatment for the removal of suspended solids. The separated solids build up in the granular medium increasing the pressure drop for flow. If the filters are not cleaned, the pressure drop increases and flow ceases. Filters are cleaned by fast reverse flow. Granular media can be fluidized by sufficiently high velocity flow. Backwashing in the regime that causes bed expansion will thoroughly clean the media. In the case of sand filter working by gravity, flow is downward during filtration and upward during backwashing. It is possible to have a floating filter media (buoyant filter) where the filtration flow velocity is upward and backwash is downward. The BFBR uses a deep bed filter to retain particulates inside the reactor. But the major problem in using a granular filter for solids separation from anaerobic reactor liquor is the high solids content ( $> 4 \text{ g/l}$ ) of the liquor. Deep bed filtration of such slurries is very difficult as filter gets choked very quickly, and needs to be backwashed frequently. If backwash interval in water treatment is of the order of hours, the backwash interval with anaerobic digester mixed liquor would be in minutes. An automatic backwash system, capable of expanding the filter bed, becomes essential for the reactor. It is also necessary that the backwash system is economical since backwashing requires high volume flow rate. The key invention in the BFBR is a backwash system which is self-driven by gas pressure developed inside the reactor.

### 3. Scope of work

---

The working hypothesis (Section 2.11) states that a high-rate reactor for complex wastewater requires the ability to maintain a large retention time for the particulates. The BFBR reactor concept (Section 2.12) is based on the hypothesis. The hypothesis is to be established by building and testing a laboratory BFBR, and by elucidating the processes and factors that affect its performance.

The scope of the development of the BFBR is given below:

- Conceptual arrangement of BFBR
- Development of filter media
  - Selection of materials
  - Method of preparation
  - Filtration performance testing
- Development of automatic filter backwash system
  - Conceptual arrangement
  - Fluidization studies
- Experimental BFBR set up
- Selecting a model complex wastewater for performance testing of BFBR
- Reactor operation and determination of
  - Long term performance with milk wastewater
  - Performance with LCFA effluent

- Discussion of performance, microbiological characteristics
- Development of mathematical model of BFBR
- Discussion of aspects of reactor scale-up

## 4. Development of new reactor BFBR

---

### 4.1. Principles

---

The BFBR is a new concept anaerobic reactor<sup>28,30,29</sup> that can separate degradable particulate solids from wastewater and retain it inside a reactor under mixed condition for sufficient retention times. A particulate filter combined with the reactor is able to meet this objective.

The solids that are separated in the filter must be returned to the reaction mixture, where it will undergo anaerobic mineralisation. The filter must be flushed and filtered solids transported to the mixed liquor. A floating filter – ‘buoyant filter’ – has the advantage that gravity will aid return of filtered solids. Conceptually, solids that form a filter cake under the buoyant filter bed may break and fall back into the reactor, although in actual operation, this situation rarely happens.

Since reactor liquor is to be filtered, the filter load will be extremely high. Hence to avoid excessive filter choking, it has to be backwashed frequently. The most successful anaerobic reactor design, the UASB, is a very simple device, with no moving machinery. The separation of liquid, solid and gas are achieved with a simple arrangement of internal baffles. From the exterior, the UASB looks no different from an unattended tank. It is desirable that the new concept reactor is able to match the UASB in simplicity in operation and cost, and exterior features. Therefore the backwashing has to be carried out automatically, at low cost and without extra consumption of water. In addition the system has to be compact. Backwashing is most effective when the filter media is fluidized. This is the only way to prevent growth of biofilm which would inevitably plug the filter media. Fluidized backwash requires high velocity flow. The filter area being large, the flow rate required for backwash is also high, although such flow is

required only as a short pulse. Hence, it is required to hold-up a large volume of filtered effluent and release it in a pulse through the filter, by gravity flow. A method by which this can be achieved is by accumulating gas inside the reactor under pressure and releasing a volume of gas equal to the required backflow. This intent is the genesis of the gas driven backwash system. Biogas is produced at the hydrostatic pressure inside the reactor and therefore, it is possible to accumulate and use the produced biogas for driving the backwash system. In a high-rate reactor, the gas volumetric yields are frequently 4 to 10 times the active volume of the reactor per day. Hence, it should be possible to use gas for driving a large quantity of backwash. The hydraulic loads on high-rate anaerobic reactors are of the order of 2 to 5 times that of the active volume of the reactor. Hence, gas driven backwash can be as much as twice the effluent discharged. But increasing the backwash volume also increases the filter load to several times that of the effluent produced.

Another aspect that needs consideration is reactor mixing. The use of agitators limits reactor shapes and depths, and also makes maintenance difficult. Hence, gas injection agitation is chosen for the BFBR.

## 4.2. Design of equipment

---

The laboratory BFBR design evolved through trial and error. Many ideas were tried and discarded. The Environmental Technology Laboratory at NIIST, Thiruvananthapuram is equipped with multipurpose QVF gas columns, mounting frames, acrylic sheets, tubes and workshops where simple steel, plastic and glass fabrication can be carried out. The other facilities available for reactor development were various sizes of peristaltic pumps, pH controllers, gas flow meters and tanks, agitators, compressed air.

Acrylic sheet and tubes were used to home fabricate the various versions of the filter and backwash system. The reactor vessel was assembled from several 4inch QVF glass column spool pieces with CI flanges. The fabricated filters and backwash systems were fitted between the flanged glass spool pieces. Variable speed peristaltic pumps were used for pumping both liquids and gases. Among the aspects of the BFBR that evolved were, the design of the filter, how it was fitted into the reactor, the automatic backwash mechanism, gas circulation system, the filter media. The filter media was developed through

trial and error. Various grades of EPS resin were tried. Various methods of expansion of the resin such as heating in oven, boiling in water and steaming were tested. It was found that expansion was non-uniform, and sometimes the beads fused together. If the heating is carried out slowly, some of expanded bead begin to contract by losing the blowing agent in the resin. Finally, steaming the resin in a stirred vessel allowed controlled expansion without beads fusing together. The expanded bead density and strength were measured.

It is essential that the backwash system is designed to operate automatically and without large volume pumping. A key innovation is the hold up of gas under pressure in the bottom chamber of the BFBR. When accumulated gas is released, the backflow of liquid can be used to backwash the filter bed. This innovation allows high velocity backwash using the self-generated gas pressure, thus avoiding large pumping systems.

An automatic system is required to trigger backwash, since backwash is required very frequently. An electronic system with level or pressure sensors and electrical solenoid valves may be designed, but is difficult to realise in a laboratory anaerobic reactor. In particular, level sensors are problematic. Sensors that use light or ultrasound may be fouled by the foam and scum that can fill the gas space in a anaerobic reactor. Sensors with moving parts can be jammed by accumulation of solids. The gas is released to the upper chamber through a U-tube containing a liquid seal. When the gas pressure exceeds the liquid seal in the U tube, the liquid in the U tube is pushed out as a slug, and gas is discharged, till the liquid seal is reformed at the smaller arm.

### 4.3. Hydraulic testing

The BFBR went through various tests before it was ready for long duration wastewater treatment operation. Some of the hydraulic tests carried out during the design stage of the BFBR are:

1. Fluidization tests on filter media
2. Filter pressure drop tests
3. Filter bed compression tests
4. Tests on gas siphon discharge system

## 5. Materials and Methods

---

### 5.1. BFBR arrangement

---

The laboratory test BFBR<sup>30</sup> is schematically shown in Figure 1(a). The parts of the BFBR are

- a lower reaction chamber (21) where the wastewater is contacted with anaerobic biomass and where gas generated is collected under pressure
- a filter assembly (30 detailed in Figure 1.b) comprising a buoyant filter media contained in a filter chamber (31)
- a upper chamber (22) where filtered effluent is collected
- a gas siphon assembly (40 detailed in Figure 1.c) between the lower chamber and the upper chamber for periodic discharge of gas from the lower chamber
- a return tube (41) between the lower chamber and the upper chamber

The BFBR is made from two 4 inch diameter glass tubes, with QVF-type flanged ends. The filter holder (internal diameter 2.6 cm, length 43 cm) is made from acrylic tube, and its lower end is capped (33). It is bonded to an acrylic partition plate (23). The plate with the filter holder (31) is clamped in between the two glass tubes, thus forming a lower chamber, (21) and an upper chamber, (22). A gas-liquid-separator, (24), with a peripheral effluent launder was provided at the top of the upper chamber. Biomass and biosolids accumulate in the lower chamber where the reaction proceeds. The upper chamber collects filtered treated effluent, but does not contribute to the active reaction volume as it does not contain biomass. The total volume of the reactor was 11.9 l and

the active volume of the lower feed chamber was 3.5 l. The upper chamber could collect 7.9 l of treated effluent. A gas collection dome was provided on top of the upper chamber.

The filter chamber has holes through which liquid can flow between the upper and lower chambers through the filter bed contained inside. The filter bed, (32), is made from polystyrene balls (porosity 42%, void ratio 0.73, filter bed depth 12.5 cm). It forms a floating granular filter - "Buoyant Filter".

During operation, gas formed due to bioconversion and gas recirculated by pump (3) collect in the lower chamber forcing liquor into the upper chamber through the filter chamber. As a result of filtration action, biosolids and sludge are captured in the buoyant filter. After a predetermined quantity of gas has accumulated in the lower chamber, it is released into the upper chamber automatically by the gas siphon (40) discharge mechanism. Gas release causes a rapid backflow of filtered liquor from the upper chamber to the lower chamber, causing the buoyant filter bed to fluidise and expand downward. Solids captured in the buoyant filter are washed out, "backwashed", into the lower chamber. The interval between successive backwashes is adjusted so as to prevent excessive build-up of filter pressure drop.

The backwash system by automatic gas discharge is shown in Figure 1(c). The system is made from a length of silicon rubber tubing, OD 6mm, ID 4mm, (42) inserted into a 15 mm acrylic tube (41). Acrylic tube 41 called the 'return tube' pass through the partition plate (23). The joint between the return tube 41 and the partition plate 23 is sealed against gas leak. The lower end of tube-42 emerges from hole on the side of the return tube and is bend back to form a U as shown in the figure. The return tube extends about 5 cm below the lowest part of the U and is always immersed in the liquor in the lower chamber. The side hole in the return tube is sealed to prevent gas entry into the return tube through gap between return tube and U tube. We call the shorter leg of the U as 'downcomer' and the longer leg inside the return tube as 'riser'. The end of the riser is well above the liquid level in the top chamber of the reactor.

During initial operation of the BFBR, the gas discharge system was occasionally fouled by scum entering the downcomer. This is prevented by adding a scum baffle (43) around the downcomer.

Also during the course of reactor operation, the BFBR was modified with a scum recirculation facility for the lower chamber in order to improve mixing. A scum collection vessel (270 ml), (27) is connected to the lower chamber through a large nozzle. Scum along with mixed liquor, overflows into the vessel during backwashing. The gas vent facility, (28), ensures quick filling of the scum collection vessel. Scum collected in 27 is pumped back into the reactor through nozzle F, using pump 4. The pumping rate is adjusted so that 27 is emptied before the next filling during backwashing. When empty, pump 4 merely functions to circulate gas in lower chamber, providing additional agitation.

The liquor in the lower chamber is mixed by gas recirculation using Pump 3. The pumping rate of gas, can be adjusted to change the interval between backwashing, so as to provide the longest possible filter run before backwashing.

The BFBR was provided with a pH control facility (not shown), through scrubbing carbon dioxide from the recirculated biogas, which automatically adjusts for acidification. No control was provided against alkalification.

The seed inoculum was obtained from a conventional pilot-scale biogas plant treating kitchen waste. The data was collected after a prolonged start-up and acclimatisation period lasting several months. Synthetic dairy effluent (Table 1) was prepared daily by mixing whole milk with tap water and sodium bicarbonate, and trace elements.  $\text{NaHCO}_3$  was added to maintain an influent alkalinity between 1000 to 1200 mg/l.

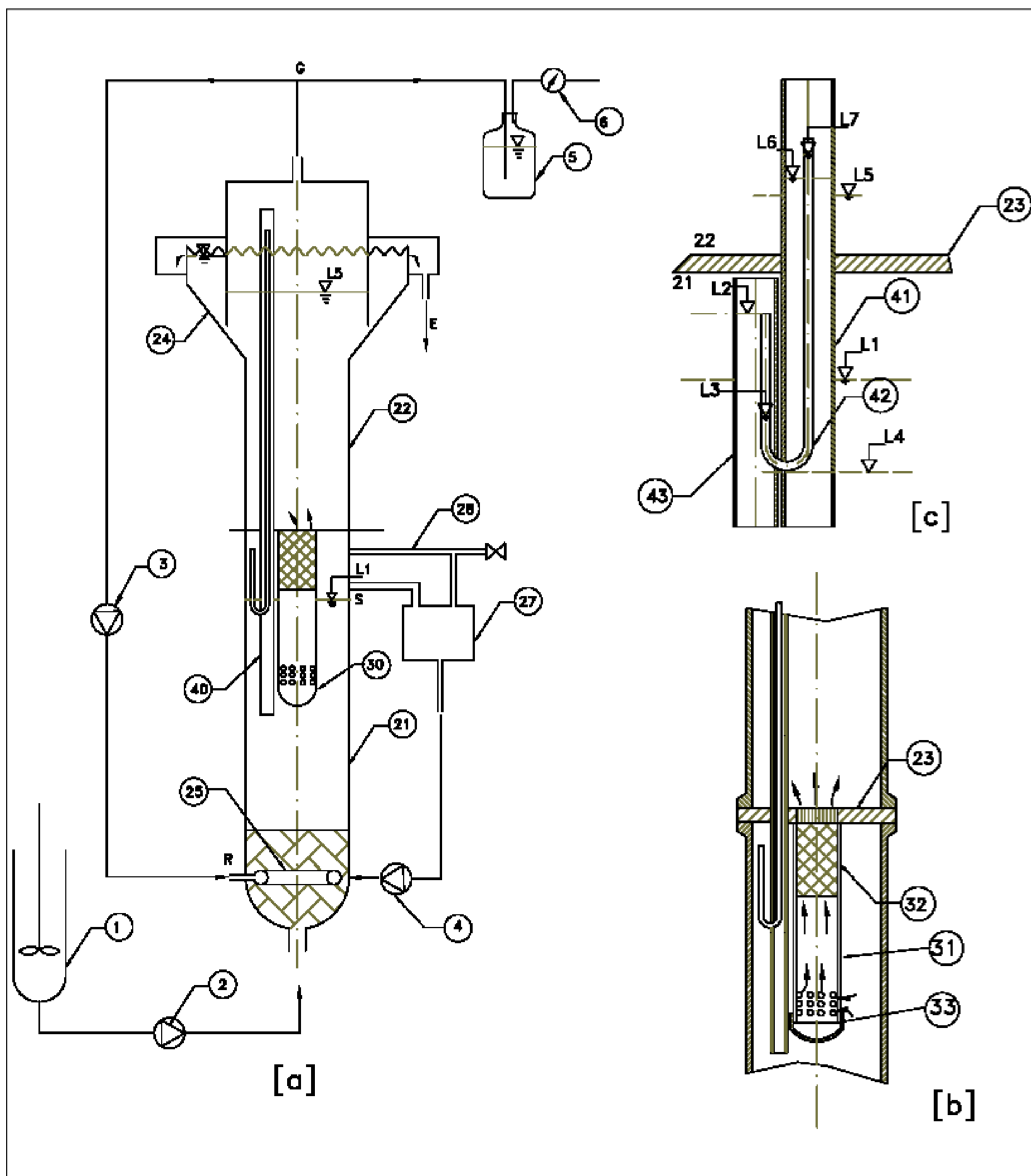


Figure 1. Experimental set-up

(a) (1) 15 litre agitated feed tank; (2) feed pump; (3) gas recirculation pump; (4) scum recirculation pump; (5) water seal; (6) wet gas meter. BFBR reactor assembly: (21) lower chamber; (22) upper chamber; (23) partition plate; (24) gas-liquid-solid separator; (25) inlet for recirculated gas and scum; (27) scum collection chamber; (28) scum collection chamber gas vent; (30) filter module.

Nozzles are denoted as: (F) feed; (E) effluent; (G) gas; (S) scum outlet; (R) gas and scum recirculation inlet.

(b) Filter module assembly: (23) partition plate; (31) filter housing; (32) buoyant filter bed; (33) end cap.

(c) Hydraulic gas release assembly. (41) return tube; (42) U-tube. (42D) downcomer leg of U-tube (42R) riser leg of U-tube (43) scum baffle.

Liquid levels: (L1) level in lower chamber; (L2) maximum liquid level in lower chamber, liquid seal re-forms after backwash; (L3) liquid level inside downcomer limb of U tube; (L4) invert level of U tube. Gas discharge takes place when L3 reaches L4; (L5) liquid level inside gas dome; (L6) liquid level in return tube. (L7) liquid level in riser limb of U-tube.

The difference  $(L6 - L5) =$  filter pressure drop.

## 5.2. Filter design

---

The principal variables in the design of the filter bed are: Filter media characteristics: size, shape, density, specific gravity; filter bed porosity; filter bed depth, filtration rate, allowable head loss and influent wastewater characteristics

The filter media particle size is a compromise between filtration efficiency and pressure drop. Particle size should be small for greater filtration efficiency. The particle size has to be large to limit pressure drop. The density of the media materials is also a compromise. Separation of filtered solids from filter media by fluidization is improved if there is greater difference in density of filter media from that of the filtered solids. This implies lower media density. Lower filter media density also leads to better and faster reformation of filter bed after backwash. An additional advantage is that the filter material mass is lower and hence the filter cost is lower for materials sold by weight. On the other hand, filter media backwash velocity required for fluidization is lower if filter media density is high – as close to density of water as possible. Since filter is backwashed with the filtered effluent, filter productivity is improved if media density is higher. With materials such as expanded polystyrene, filter media becomes highly compressible when media density is low and this leads to sharp pressure increase during filtration. Finally there are practical and economic considerations on manufacture of the media, with commercially available materials that dictate the choice of filter media. Experiments were conducted with various media and expanded polystyrene EPS beads were chosen for fabrication of the filter bed.

The ability to design filters and to predict their performance is based on 1) Understanding of the variables that control the process and 2) A knowledge of the pertinent filtration mechanisms responsible for the separation of particulate matter from the waste water. The complete filtration process essentially consists of two phases: filtration and back washing.

The end of filter run is reached when the suspended solids in the effluent start to increase (break-through) beyond an acceptable level or a limiting head loss occurs across the filter bed. Ideally both these events should occur at the

same time. Once either of these conditions is reached the filtration phase is terminated and the filter is backwashed to remove the material that has accumulated within the granular filter bed.

### 5.3. Filter media preparation

---

Expanded polystyrene beads were prepared as filter media. Expandable polystyrene resins contain a blowing agent which has a boiling point around the melting point of polystyrene. When heated the melted resin expanded because of the vaporisation of the blowing agent. EPS resins in various particle sizes are available from LG Polymers and BASF. These resins are used for manufacture of moulded polystyrene packaging cases, popularly called Styrofoam, which is a proprietary name for the material. The resin is expanded first into beads, packed into moulds and fused by further heating. The reticulated pattern seen on polystyrene packing material shows the boundaries of fused beads.

EPS expanded beads are not commercially available and needed to be prepared from the resin. Several methods of heating the resin for expansion were tried. These included heating in hot air oven, boiling in water, and steaming in a closed stirred vessel. The method of steaming while mixing was easiest for preparing larger quantities of beads and uniform expansion was possible.

### 5.4. filter backwash

---

Filters have to be regularly backwashed to prevent choking. Deep bed filters used in water treatment are backwashed at intervals of several hours. Unlike in raw water filtration, the mixed liquor in an anaerobic reactor has very high suspended solids. Correspondingly, backwash intervals would be very short, (several minutes). The BFBR filter bed is backwashed by fluidization by downward flow of the filtered liquor. The fluidization velocity and bed expansion were measured.

#### 5.4.1. Operation of automatic backwash system

---

The backwash system operates automatically using a hydraulic gas siphon. Gas produced in the lower chamber and gas recirculated from the gas dome collect below the partition plate. The liquid level in the lower chamber as well as

in the downcomer goes down as gas accumulates. When the liquid level in the downcomer reaches L4, the bottom of the U, gas bubbles out through the riser. Since the internal diameter of the U-tube is only 4mm, gas bubbles in the riser fill the cross-section - a 'slug', also called a 'Taylor bubble' - which pushes out the liquid column in the riser. The liquid column in the riser, pushed out by the gas slug, falls into the return tube from where it flows back into the lower chamber. Gas held under hydrostatic pressure in the lower chamber flows into the gas collection dome rapidly through the U-tube. As the pressure in lower chamber decreases, filtered liquid in the upper chamber flows back into lower chamber through the filter bed. When the liquor level in the lower chamber reaches level L2, it enters the downcomer and fills the riser re-forming the liquid seal. The following relations may be noted.

- Filter pressure drop = the difference between liquid level inside and outside return tube ( $L6 - L5$ ). Thus a continuous indication of filter pressure drop can be obtained.
- Backwash volume = (rate of gas production + gas recirculation rate) x backwash interval = liquid volume between L2 and L4, ie., fixed for a U-tube configuration.
- The filter hydraulic load = gas production rate + gas recirculation rate + feed rate.

### 5.5. Reactor mixing

---

In the treatment of high solids effluents, mixing and scum formation are likely issues that can affect the rate of conversion. The experimental BFBR is provided with gas recirculation mixing. The rate of gas circulation is limited - a few bubbles per minutes, released from a 4 mm diameter orifice at the bottom of the reactor liquid pool. The breaking of bubbles generates some turbulence at the surface for breaking of foam or scum.

### 5.6. Reactor pH control

---

BFBR liquor pH was controlled by removing carbon dioxide from the gas phase. BFBR is provided with a gas recirculation system for mixing. The recirculation gas was passed through an absorber comprising of a packed bed of glass beads with sodium hydroxide trickled over the bed. The pumping of

sodium hydroxide to the absorber was controlled by a on-off pH controller. The sodium hydroxide concentration is measured to establish the amount of carbon dioxide absorbed.

## 5.7. Model complex wastewaters for experimentation

Filtration tests were carried out with liquor from a canteen waste biogas plant. The liquor was almost completely bulking with no clear interface forming during 30 minutes of settling time. The sludge contained 13 g SS/l. The liquor was used within the day of collection.

Continuous BFBR operation experiments were conducted with complex wastewater with defined characteristics prepared from components, on a daily basis. The complex wastewaters selected for testing were:

1. Synthetic dairy effluent (milk effluent) prepared from whole milk
2. LCFA effluent prepared from oleic acid effluent

Synthetic dairy effluent (Table 1) was prepared daily by mixing whole milk with tap water and sodium bicarbonate, and trace elements.  $\text{NaHCO}_3$  was added to maintain an influent alkalinity between 1000 to 1200 mg/l.

**Table 1. Composition of synthetic dairy effluent. 10ml of the trace element stock solution was added per litre of the effluent.**

Pasteurised milk (3% fat, 8.5% non-fat solids)	Between 50 and 250 ml per day depending on organic loading rate applied: Average COD of milk 162 g/l; TOC 63 g/l; Non-fat COD of milk 50%; COD of milk fat (experimental value) 2.7 g / g.
Tap water	Between 6 and 12 litres per day depending on hydraulic loading rate applied.
Sodium bicarbonate	1 g / l of feed
NH <sub>4</sub> Cl	60 mg/l
K <sub>2</sub> HPO <sub>4</sub>	20 mg/l
CaCl <sub>2</sub>	50 mg/l
MgCl <sub>2</sub>	100 mg/l
FeSO <sub>4</sub>	15 mg/l
Trace element stock solution	10 ml / l
Composition of trace element stock solution (mg per litre stock solution)	
MnSO <sub>4</sub>	86
CaCl <sub>2</sub>	170
ZnSO <sub>4</sub>	210
NiCl <sub>2</sub>	50
Na <sub>2</sub> MoO <sub>4</sub>	20

Long chain fatty acid effluent was prepared by homogenizing oleic acid with equal moles of sodium hydroxide and making up to required volume. The concentration of LCFA effluent was around 2500 mg COD/l. This effluent was used to study LCFA degradation. Except for milk, all other components of the LCFA effluent are as per Table 1

## 5.8. Feed system

---

There are unique experimental difficulties in laboratory reactor studies with complex wastewater. Typically, prepared slurries have to continuously mixed in feed tanks in order to prevent settling. Peristaltic pumps with narrow bore tubing tend to get choked quickly when pumping slurries. Using larger bore tubing reduces flow velocities and solids settle in tubing. When using fats, the emulsions separate quickly and form a scum layer on top the feed tank. Hence, it is very difficult to achieve uniform composition of feed throughout the day. In the reactor studies carried out, complex wastewater was prepared with diluted milk and starch to simulate sewage, diluted milk to simulate dairy wastewater, and oleic acid with sodium hydroxide to simulate a long-chain fatty acid containing wastewater.

An agitated tank was used to mix the contents of the feed tank, but this was possible only to limited extent.

## 5.9. Analytical methods

---

pH in the digester was continuously monitored and regulated with a pH probe (Cole Parmer) and a on-off control system as previously mentioned. The electrode was calibrated daily.

Total biogas production was recorded with a wet-gas flow meter (Insref, India).

Alkalinity and total volatile fatty acids (VFA) concentration in the BFBR were estimated titrimetrically according to Anderson and Yang<sup>31</sup>.

Individual volatile fatty acids were measured using by gas chromatography (FISONS 8000 series GC, Shimadzu C-R7A computing integrator, FID detector, 6 ft, 2mm i.d. glass column with Supelco CarbowaxWAW, 0.1% phosphoric acid, carrier gas ultrapure helium 20 ml/min, injector 150°C; detector temperature 175°C, oven isothermal 120°C). The detection level was less than 1 mg/l. Column

resolution was maintained by occasional injection of formic acid. Individual volatile fatty acid analysis was carried out only infrequently.

Total organic carbon (TOC) and inorganic carbon (IC) were monitored using total carbon analyzer, Shimadzu TOC-5000 system with detects combustion product carbon dioxide with NDIR adsorption detector. TOC samples (not filtered) were prepared by dilution of with distilled water and sonication for 15 minutes

Biogas composition was routinely measured using the TOC analyser, where the IC value is taken as carbon dioxide and (TC-IC) is taken as methane. The TOC 5000 instrument is designed for measurement of carbon in liquid samples. It can be used for gas sample injection, and does not require further calibration, as both carbon dioxide as well as methane are measured in mass of carbon by NDIR absorption of carbon dioxide. Systematic errors are possible in gas sample introduction and these were avoided by calibration with gas standards. Biogas was collected from the reactor in a homemade glass bulb with an acidified water seal. The automatic injector of TOC 5000 has a capillary suction tube made of teflon, which can be inserted into the gas bulb through the water seal. Initially gas composition was verified against gas chromatography measurements (Fisons 8000, TCD, 2mm i.d. silica gel column, He 150 ml/min, oven 40°C, injector 110°C, detector base 120°C, detector wire 190°C) and found to be accurate. The TOC method was chosen over GC because of ease of operation. The TOC method for gas analysis consistently gave less than 1% coefficient of variation in multiple injections.

Chemical Oxygen Demand (COD) tests were carried out according to the open reflux method as per Standard Methods [20] using a temperature controlled block digester (Tecator 2000).

Long Chain Fatty Acids (LCFAs) in the effluent and mixed liquor were determined by gas chromatography after extraction with hexane and esterification of the acids (Fisons 8000 gas chromatograph, Supelco OV1 capillary column (30m X 0.32mm X 0.2), carrier gas ultrapure helium 2ml/min; carrier gas split ratio of 30:1; injector temperature 250°C; detector 300°C; oven temperature program 150°C hold 4 minutes, 100°C/min to 220°C hold 2 minutes, 70°C/min to 280°C hold 4 minutes). The gas chromatograph was

calibrated with fatty acid methyl ester (FAME) mix standard, C14 – C22 (Supelco, Bellefonte, PA). FAME mix standards were prepared in hexane, sealed with septum caps in standard bottles and stored at  $-40^{\circ}\text{C}$ . LCFA was extracted from mixed liquor as follows: One ml of the sample was withdrawn to a screw-capped vial, 5ml hexane was added and stirred for 30 minutes with a magnetic stirrer 30 minutes. The organic layer was transferred completely to another glass vial and dried off completely by placing the vial in a water bath at  $80^{\circ}\text{C}$ . The dried sample was then cooled to room temperature, 2 ml methylating reagent was added. The vial was tightly capped, sealed and again placed in the water bath for 1 hour for esterification. After methylation, the vials were cooled to room temperature; 2 ml hexane was added and shaken well for 2 minutes. Completeness of esterification was checked using TLC plates. One ml of the esterified sample was pipetted out and capped tightly in a septum lined bottle. Samples were stored in freezer below  $-40^{\circ}\text{C}$ , if not analyzed immediately. LCFA extraction from mixed liquor samples were verified by spiking mixed liquor samples containing no LCFA with oleic acid 200 mg/l. Recovery was 100% +/- 5% and blank samples gave nil reading. This shows that cell wall lipids were not hydrolysed or extracted by the procedure. On the other hand, extraction with solvents such as petroleum ether gave more than 100% recovery.

Ammonia -N was measured using Orion specific ion electrode.

Filter performance testing was carried out in a test filter bed 7cm deep. The filter bed was constructed from two different expanded polystyrene resins, which were expanded to required size by heating. The test liquor was pumped through the bed and pressure development noted by measuring (L6-L5), the rise in liquor level in the return tube.

## **6. Results : BFBR operation and performance**

---

### **6.1. Feed system and pumping:**

---

Feed was prepared everyday. But it is very difficult to keep the feed homogeneous for continuous feeding. Despite the mixing provided, fat separates and sticks on to the side walls and forms scum. Milk coagulates and separates very quickly in the feed. Heavier solids (eg. starch powder, if fed) settle on to the bottom of tank. The pumping tube also gets clogged with solids deposition. It was not possible to increase the agitation efficiency without undue oxygenation and biological oxidation of the effluent. Each day the solids deposited on feed tank surfaced was washed down and pumped to the reactor. This enabled the total daily organic load to the BFBR to kept constant, but the load is not uniform throughout the day. The composition of wastewaters prepared for experimentation is given in Section 5.7.

### **6.2. Filtration**

---

Filtration tests were performed with canteen waste digester sludge. The filter pressure drop development at constant velocity is shown in Figure 2 and Figure 3.

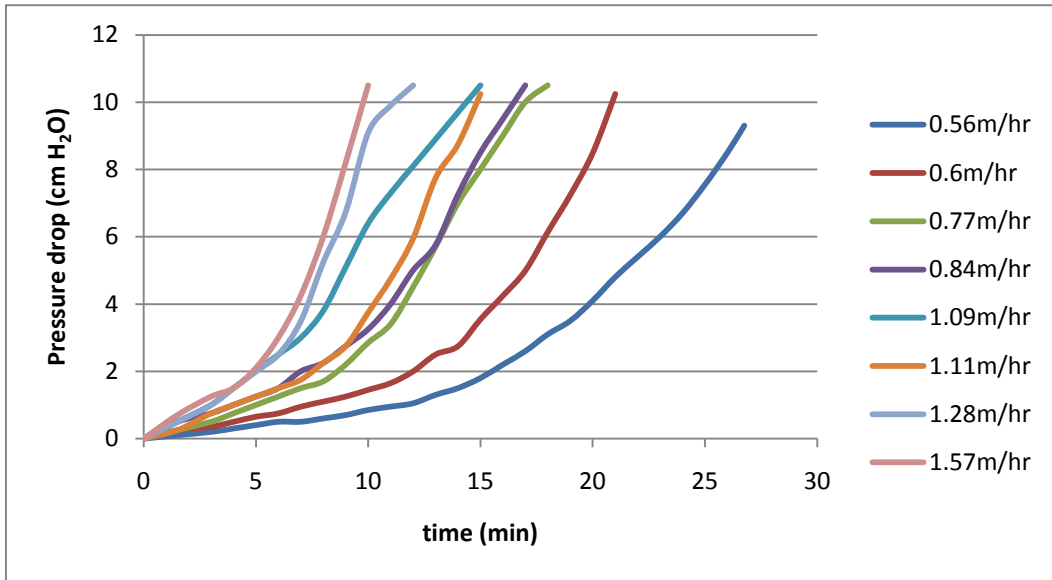


Figure 2. Pressure drop at constant velocity filtration. Filter media: Beardsell EPS, expanded bead size: 1-2 mm, true density: 144.g/l bulk density 81.2 g/l; Method of bead preparation: heating in hot air oven for 20-25 minutes. (Date of experiment: 23/02/05, log book page.11)

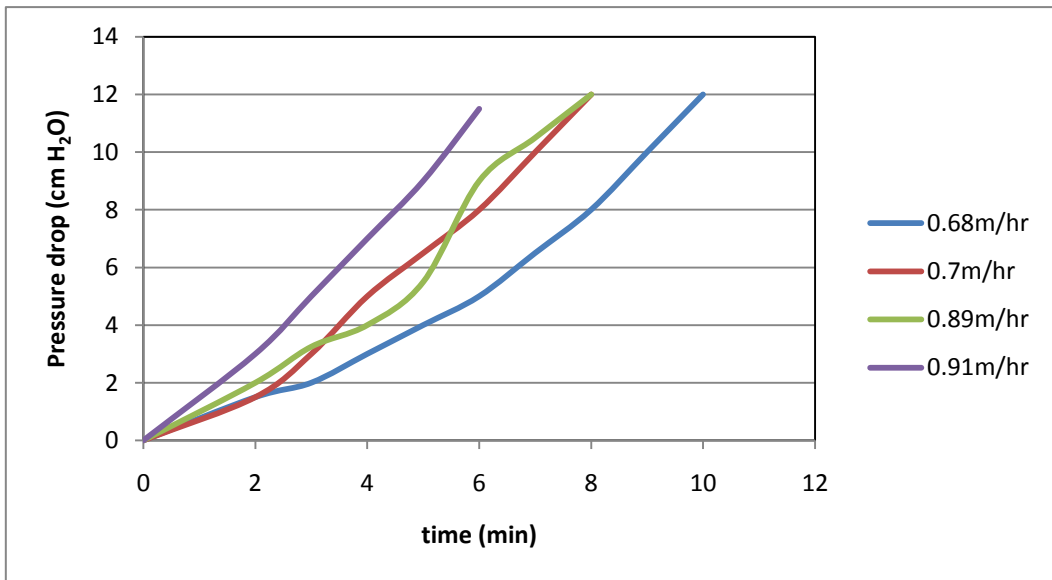
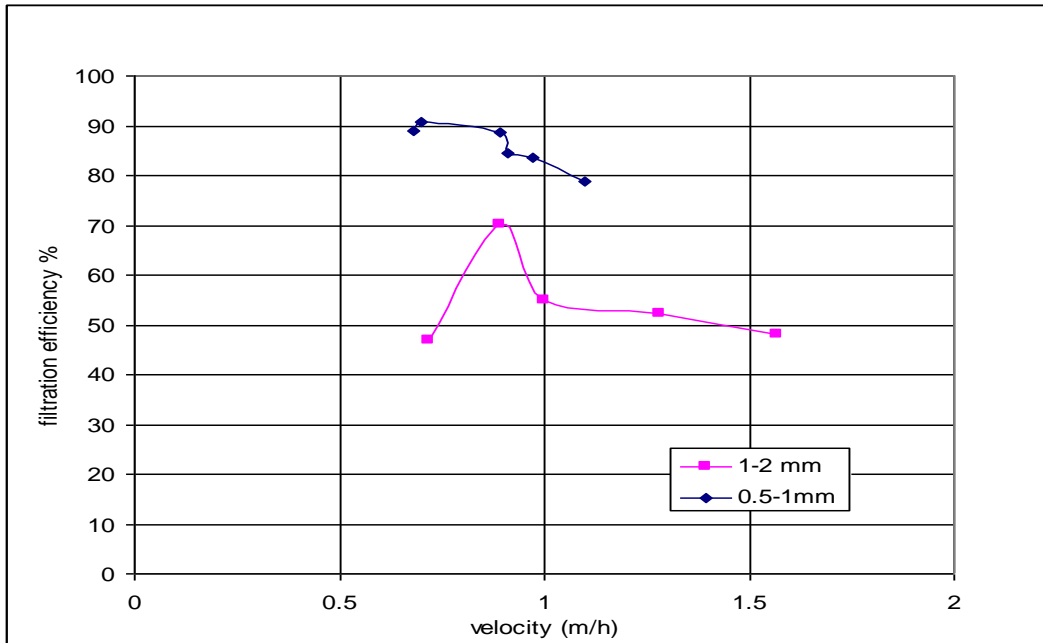


Figure 3. Pressure drop for 7 cm filter bed. Filter media: LGE-625 EPS resin, expanded bead size: 0.5-1 mm, bulk density: 97.6 g/l, true density: 152 g/l; Method of bead preparation: boiling in water for 1-1.5 hours. (Date of experiment 29/03/05, log book page 23).

Filtration efficiency is shown Figure 4.



**Figure 4. Filtration efficiency for filtration of 13 g SS/l bulking sludge for filter beds with 1-2 mm media and 0.5-1 mm media.**

The efficiency of separation of suspended solids varies from 90% for filter bed constructed with 0.5- 1 mm media to 50% for filter beds with 1 to 2mm media. The overall filtration efficiencies does not appear to be high. However the results must be viewed in the context that no solid-liquid separation is possible by settling.

Higher pressure drop operation would improve solids retention by the surface cake filtration mechanism (see page 51). Smaller sized 0.5-1 mm EPS beads have sufficient strength to resist deformation at higher pressure operation. Results of experimental filtration at higher pressure is shown in Figure 5.

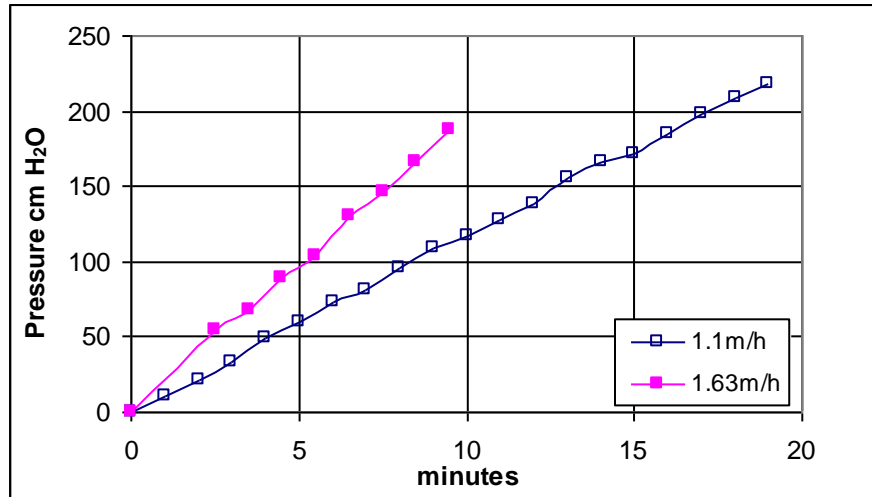


**Figure 5. Filter pressure drop at constant rate filtration of non-settling anaerobic digester sludge.**

The improvement in filtration efficiency, and consequent difficulties of higher pressure drop operation does not automatically lead to higher COD removal efficiency.

Results from BFBR operation with synthetic effluent using filters of different sizes (Figure 6) show only insignificant improvement in COD removal using 0.5-1mm media compares with 1 to 2 mm media. However, COD removal in the case of the smaller filter media is not sensitive to variations as a result of feed or operating conditions. One would expect that improved filtration efficiency with smaller beads would result in improved COD removal efficiency. The reasons for the unexpected results observed are discussed later in the light of model calculations in Section 7.8.

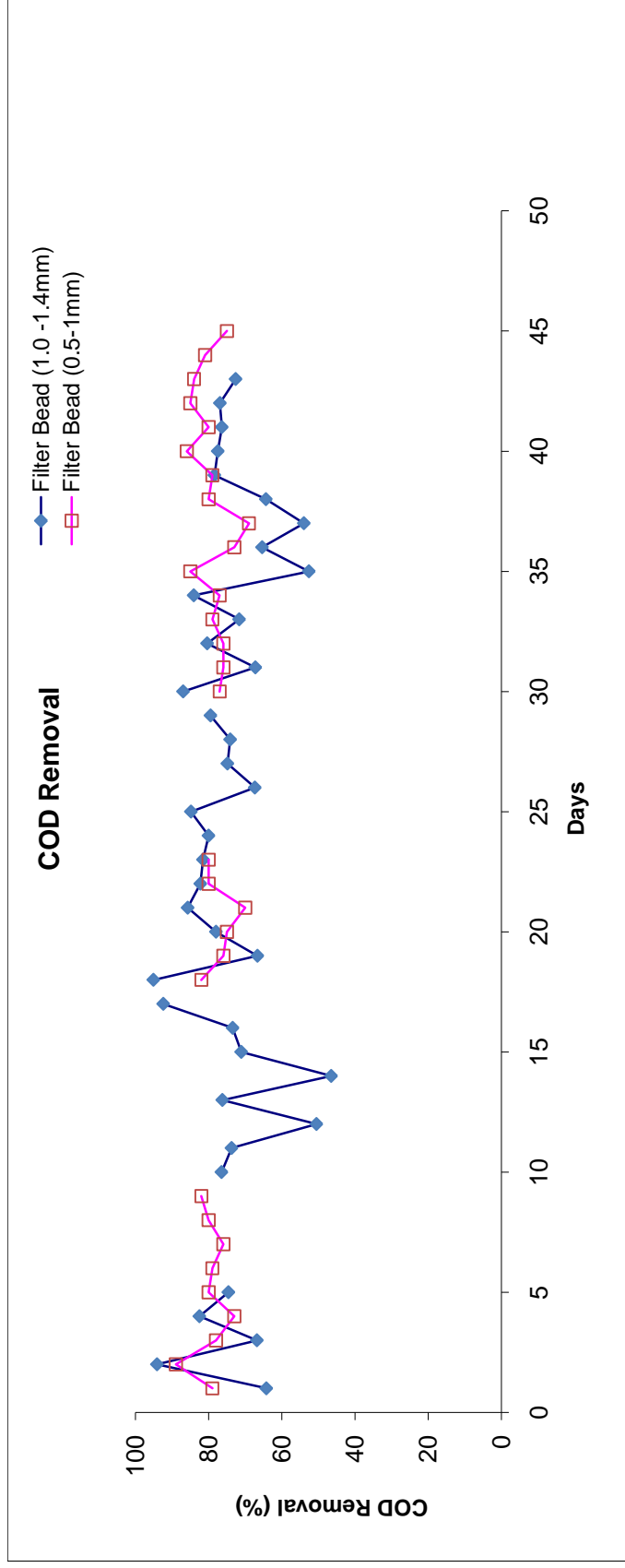


Figure 6. COD removal efficiency in BFBR using different efficiency filters.

The sludge used in the filtration study is a bulking sludge that cannot be separated by gravity settling. Therefore, compared with settling, the separation by filtration is good even with 1mm to 2 mm size media. Filter media size selection is a compromise between better filtration efficiency and the pressure drop build-up which determines the filter run. Selection of filter media size requires further consideration of the wastewater being treated and the sludge formed in the BFBR.

The filtration characteristics of biological sludge, just like its settling characteristics, changes dramatically with the ecology that develops inside a reactor. In an anaerobic system, biological sludge can vary from rapid settling granular sludges that develop in UASB reactors to bulking sludges as in the canteen waste digester. Under the microscope, the bulking sludges are seen to be dominated by long filamentous growth including filamentous fungi. Prior to operation of the BFBR, it is impossible to predict the filterability or settleability of sludge that develops. Furthermore, the characteristics would also be dependent on nature of feed and operational conditions. The filtration tests were carried out with bulking sludge and hence the tests may be taken as presenting a conservative picture of what would happen in sludge that grows in a BFBR reactor.

Filtration was observed to take place via the following mechanisms

- Solids capture in the initial phase within the pore spaces
- Cake formation at the surface of the bed at the later stage, with cake acting as filter

When the pressure drop increases, the cake which forms at the filter surface, begins to compress, leading to non-linear increase in pressure drop. This is the primary reason for limiting filter pressure drop to around 10 cm H<sub>2</sub>O. It was also observed that once sludge cake compacts, it is difficult to break-up during backwashing. At higher pressure operation, the sludge cake and filter beads cement together to form aggregates that do not disintegrate during backwashing. The aggregates are initially a few beads together, and at later stages can become bigger extending across the filter cross section like a plate. This is another reason to limit filter pressure drop to 10 cm H<sub>2</sub>O.

### 6.3. Fluidized filter bed backwash

The velocity required for backwash is presented in Figure 7.

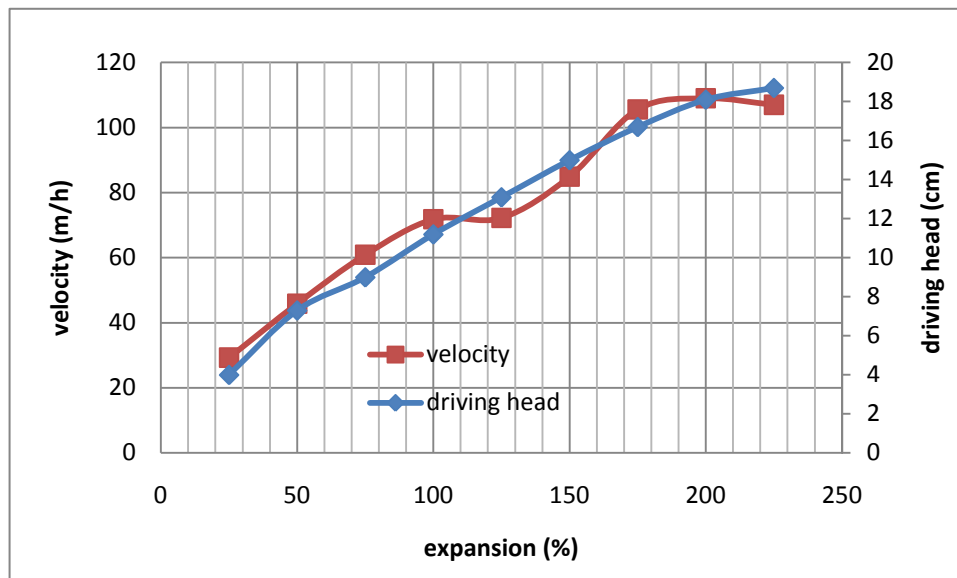


**Figure 7. Superficial velocity and bed expansion during backwash. 8cm deep bed using 0.5mm to 1mm expanded polystyrene beads, made from LG625B EPS resin.**

The driving head for fluidization of the filter bed is also given in same figure. It is evident that velocity of proportional to driving head in the range considered. There are small kinks in the measured velocity which may be attributed to experimental error.

The Richardson-Zaki empirical formula<sup>32</sup> connects bed porosity and fluidization velocity by a straight line on a log graph.

$$v = K_e (\varepsilon)^{n_e}$$

The empirical constants  $K_e$  and  $n_e$  are calculated from packed bed limit porosity at the estimated minimum fluidization velocity.

First the minimum fluidization velocity is calculated using the empirical formula

$$v_f (gpm / ft^2) = \frac{0.00381(d_{60\%})^{1.82}[\omega_s (\omega_m - \omega_s)]^{0.94}}{\mu^{0.88}}$$

where

$d_{60\%}$  = 60% finer size in mm, = effective size x uniformity coefficient

$\omega_m$  is the specific weight of particle

$\omega_s$  is the specific weight of water in lb/ft<sup>3</sup>

$\mu$  is the water viscosity in centipoises.

The effective size is the 10 percentile grain size (10% of sample less than this size)

Uniformity coefficient = 60 percentile size/ effective size.

The dimensionless particle Reynolds number corresponding to particle diameter  $d_{60\%}$  and minimum fluidization velocity  $v_f$  is calculated.

$$\text{Re}_f = \frac{\rho_l v_f d_{60\%}}{\mu}$$

If  $\text{Re}_f$  is greater than 10, a correction factor  $K_R$  for  $v_f$  is applied

$$K_R = 1.775 \text{Re}_f^{-0.272}$$

The unhindered settling velocity (in this case unhindered rise velocity) is given by

$$v_s = 8.45 v_f$$

The Reynolds number based on unhindered rise velocity is calculated

$$\text{Re}_0 = \frac{\rho_l v_s d_{60\%}}{\mu}$$

The expansion coefficient is given by

$$n_e = 4.45 \text{Re}_0^{-0.1}$$

Given  $K_e$ , bed porosity and fluidization velocity are given by:

$$v = K_e (\varepsilon)^{n_e}$$

Constant  $K_e$  for the system is calculated using the values of velocity  $v_f$  and porosity at minimum fluidization.

The equation for  $n_e$  is valid for  $1 < \text{Re} < 500$ .

The fluidization velocity measured and calculated as per the above procedure are shown in Figure 8.

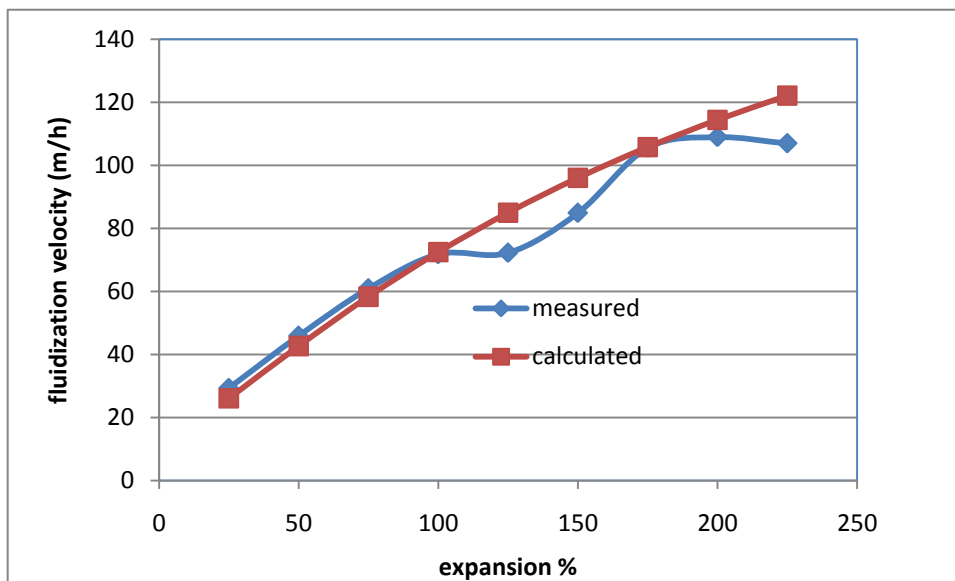


Figure 8. Comparison of measured and calculated fluidization velocities for LGE 625 beads, 0.7mm  $d_{60\%}$ , true density 155 kg/m<sup>3</sup>, porosity 39%.

Figure 8 shows that the Richardson-Zaki formula, along with an empirical formula for minimum fluidization velocity, fits the observed fluidization of the filter bed during backwash. Using this procedure, it is therefore possible to carry out the filter process design scale-up even for filter bed materials that have not been tested. The only data needed are material density, porosity of static bed and particle diameter.

### 6.3.1. Backwash volume

The backwash volume is determined by the volume of liquid between L2 and L3, and is fixed by adjusting the downcomer length. The minimum backwash volume for proper bed cleaning was found to be at least equal to volume of filter bed. The duration of backwash for a filter bed 14cm depth with 1-2mm beads was about 5 seconds for backwash volume equal to filter bed volume.

The backwash interval was fixed at 15 minutes by changing the gas recirculation rate. At this backwash interval, the filter pressure drop did not exceed 10 cm H<sub>2</sub>O.

The filtration velocity (filter hydraulic areal loading) is given by the volume of filtered effluent per unit cross section area of filter.

The filter productivity [(volume of filtered effluent – backwash volume) per square meter per hour], is a process design parameter required to determine the filter area required for a particular reactor application. The filter productivity for filtration of non-settling sludge is presented in Figure 9.

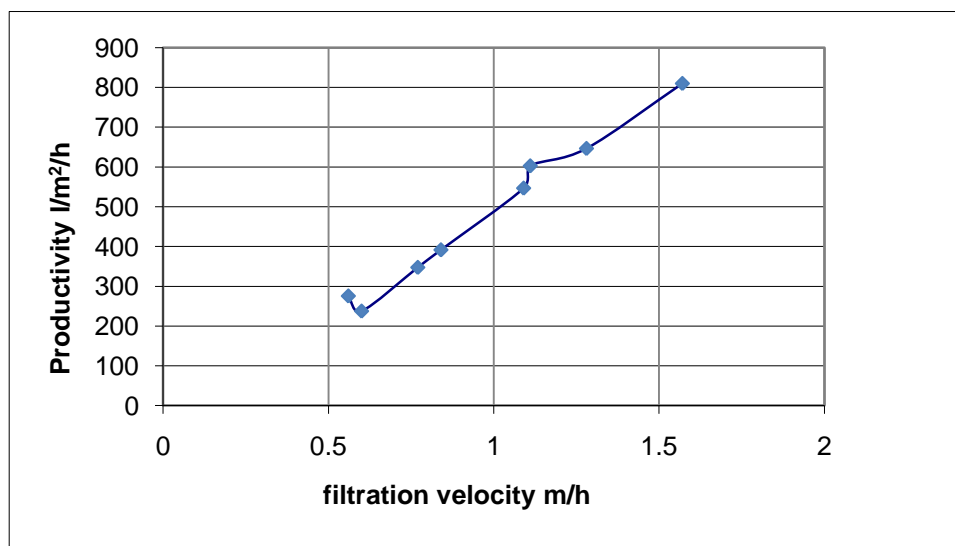


Figure 9. Filter productivity for filter bed 14cm depth, 1-2mm beads. Non-settling anaerobic digester sludge with 13g SS/l was filtered.

The filter productivity increases with the filtration velocity in the range under consideration. This is obvious since the backwash volume was kept constant. It was possible to clean the filter bed with constant backwash volume for the tested range of filtration velocities because the filtered sludge were held weakly within the filter bed. This is a consequence of filter operation at low pressure.

Backwash cleans the filter bed as long as the filtered sludge are not compressed into a solid cake. At higher filter pressures the filter cake is compressed and forms aggregates with filter beads. Backwash eventually fails to fluidize the bed and filter cleaning fails. At intermediate pressures, a few beads at the bottom get cemented together with sludge. The aggregates look like granular sludge, irregular shaped, and 2-5 mm in diameter. But on closer examination the cemented filter beads and occluded gas bubbles could clearly be seen.

These aggregates fail to break up during backwash. The aggregates behave like larger size particles with different fluidization behaviour. Fluidization causes the filter bed starts to segregate, since the cemented beads have higher rise velocities. The filter bed begins to loose its filtration properties. It is possible to break up weaker aggregates by providing wires against which the aggregates impact. Disintegration of aggregates is better at higher backwash velocities. At lower backwash velocity, the momentum of the aggregates is not sufficient to cause fracture on impact. The mechanism is weaker for smaller sized filter media. Reliable disintegration of aggregates is possible only with mechanical agitation. However, implementation in full scale would be rather impractical because of complexity and cost. It would be better to limit the filter pressure drop.

#### 6.4. Reactor mixing

---

Mixing, or mass transfer, was considered an important factor in determining the rate of degradation of particulate COD. Since particulate COD has to be degraded by exocellular enzymatic action, enzymes need to diffuse onto the particle surfaces. In real situation, this is not so important, as bacteria colonise the surface of the particle, and produce enzymes to solubilise and utilize the

solubilised substrate. The production of free enzyme to diffuse to particle surface and uptake of soluble compounds that diffuse to the microbial cell is obviously a costly strategy as compared with colonisation of the particle surfaces. Mixing is not so important in colonisation of the particle surface. The relevance of mixing lies in breakup of agglomerations of particles. It is particularly important in the case of fats, which being hydrophobic, agglomerates into thick scum. Mixing to break-up scum therefore becomes important. The scum mixing device to recirculate scum back into the liquor was devised to test this hypothesis. A definite comparative study of scum mixing versus no mixing could not be tested, because of the observation of development of scum degradation in the unmixed reactor as well.

#### 6.4.1. milk effluent

---

The composition of feed prepared for the BFBR is shown in Table 1. The feed was prepared daily. It was pumped from a agitated, dished bottom tank. The load on the BFBR was changed both by changing the concentration and by changing the flow rate. However, the flow rate was relatively constant and the main changes were applied through changing the composition. The loading applied is shown in Figure 10. Since this is a very long term experiment, there are breaks where the reactor was shut down. There are also intervals where the reactor was had to be restarted from a lowered load. Even when the synthetic feed composition is unchanged, (same quantity of milk is used to prepare the synthetic feed), it is possible that the COD load on the BFBR varies, because of the tendency of the feed to separate and stick to surfaces.

#### 6.4.2. LCFA effluent

---

Since LCFA is expected to be the slowest degrading intermediate, during the treatment of milk effluent, at the end of the milk effluent test, the BFBR was tested in continuous operation with LCFA as the sole carbon source. LCFA effluent was prepared by homogenizing oleic acid with stoichiometric quantity of sodium hydroxide to form the sodium salt. It was then diluted to form an emulsion of the required COD strength. All other mineral components were retained as in Table 1.

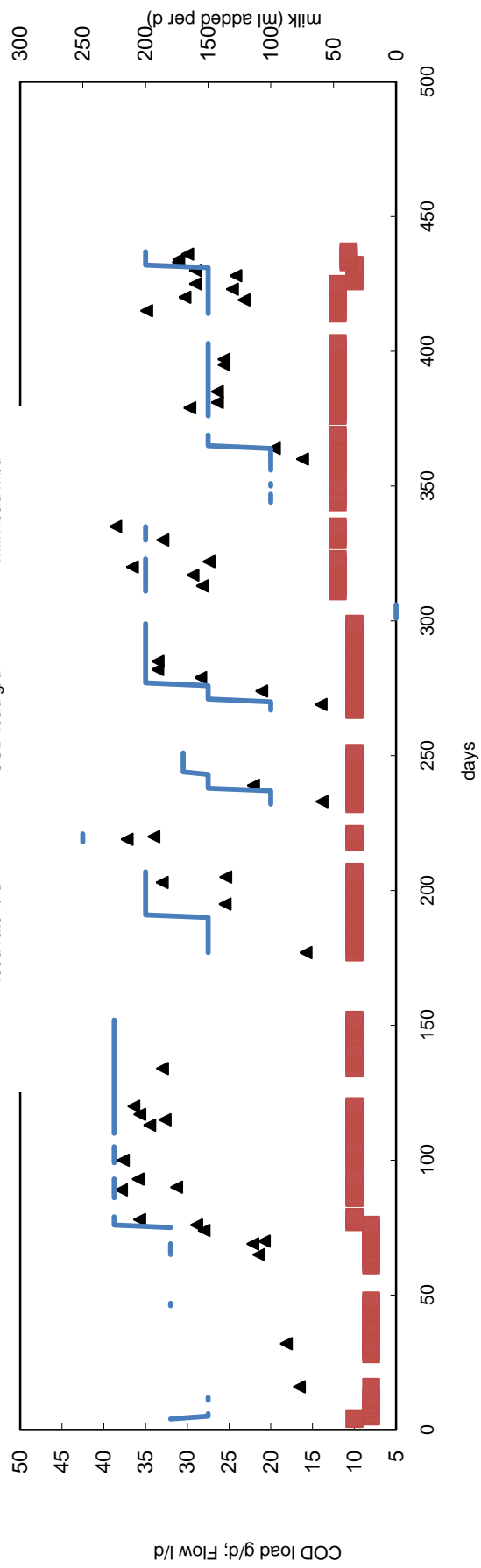


Figure 10. Loading history of BFBR with synthetic milk effluent composition given in Table 1.

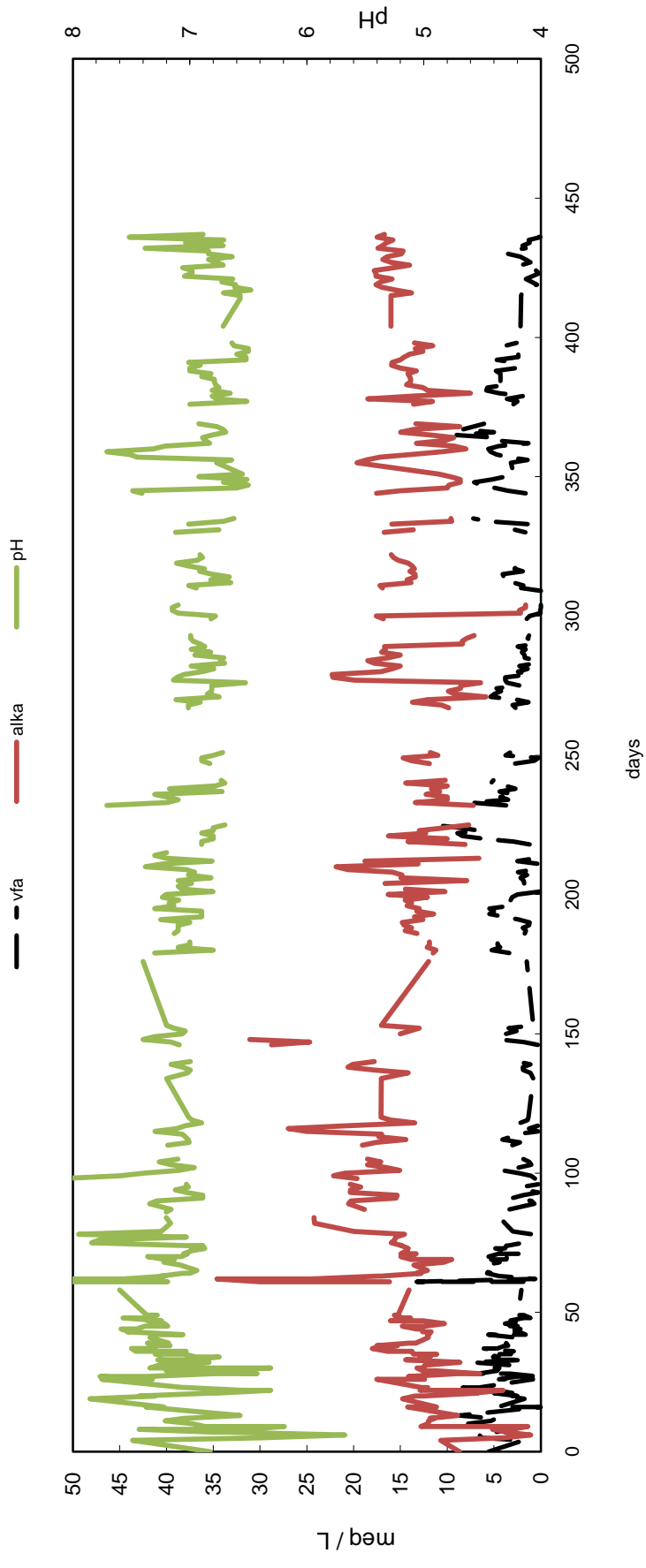


Figure 11. pH, VFA and alkalinity history

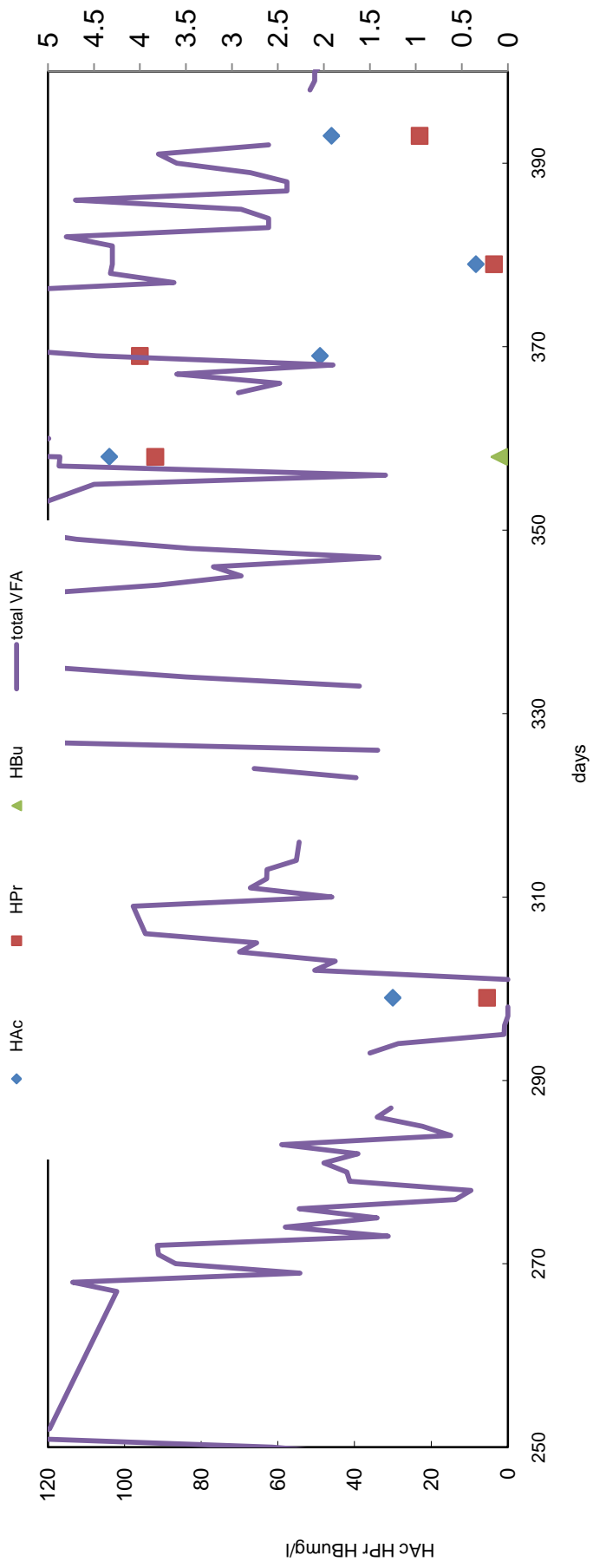


Figure 12. Acetic, propionic and butyric acid in BFBR. Total VFA in mM is plotted on right-hand y-axis.

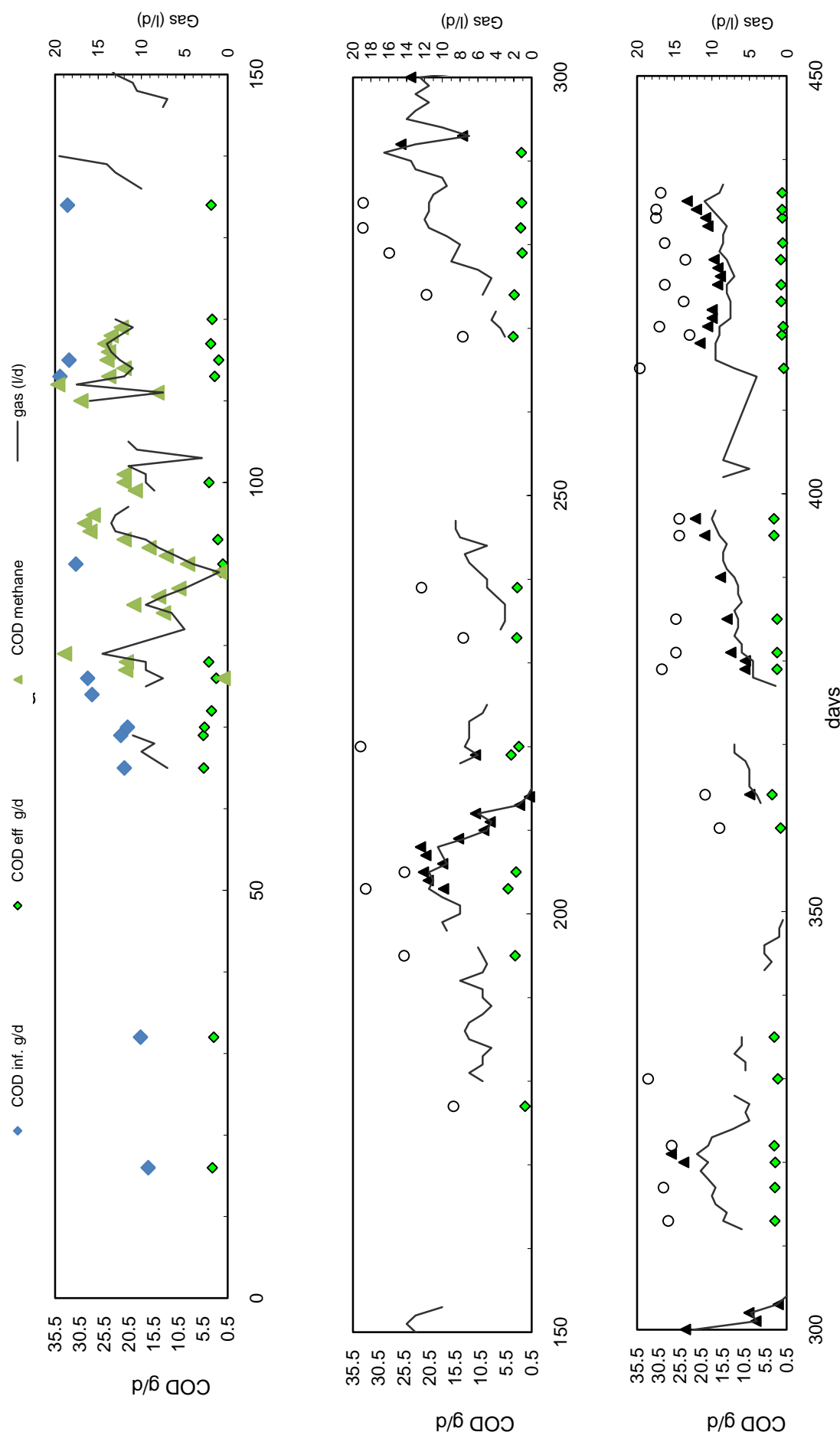


Figure 13. BFBR time series history of COD load, COD effluent and COD recovered as gas for milk effluent

## 6.5. Milk effluent: Discussion of experimental results

---

### 6.5.1. pH and alkalinity

---

Figure 11 illustrates the variation of pH, alkalinity and total volatile fatty acids in the digester. After the initial start-up period, when there was overloading and acidification, reactor pH was nearly always stable in the range of 6.8 to 7.0 at various organic loading rates. The active pH control system was responsible for preventing acidification of reactor. During low loading conditions, the reactor pH rose above 7.4. Throughout the reported period, the alkalinity in the reactor ranged between 800 to 2000 mg/l. The alkalinity of the effluent was provided mainly by 1 g/l sodium bicarbonate added in the feed wastewater. System pH would be sensitive to changes in VFA concentration, without the active pH control system. The VFA to alkalinity ratio in the digester was always between 0.01 to 0.4 during stable operation. After achieving stable methanation, the total VFA concentrations in the reactor never rose above 4 meq/l (256 mg/l as acetic acid).

The concentrations of individual volatile fatty acids are shown in Figure 12. Data on individual volatile fatty acids could be generated only in the later stages of the reported period. However, some general trends in VFA generation could be drawn. During steady methanization conditions, only acetic acid was detected in the reactor effluent. Propionate and butyrate were detected in liquor during changes in load. Interestingly, these VFAs are not seen immediately on increase of load, but after a lag period of several days, signifying the end of Stage 2 (discussed later) of the scum accumulation and degradation process that occurs on load increase in the BFBR.

### 6.5.2. COD removal

---

The COD history of the BFBR is illustrated in Figure 13. At all the OLRs applied, the steady-state COD removal efficiency was above 85%. The maximum organic loading rate applied during the period reported is 10 kg COD/(m<sup>3</sup>.day). COD removal efficiency during steady state at this loading was 90%.

Through out the operation of the BFBR, effluent COD was less than 450 mg/l. During pseudo-steady state at all loading rates, the effluent COD was less

than 250 mg/l. It was found that COD removal efficiency gradually improved with aging of the sludge when steady loading was maintained for long duration extending to 8 weeks. On prolonged steady operation, effluent quality improved and very low COD was obtained even at high organic loading rates. For example, at the end of the reported period, with feed COD was in the range of 3200 to 3500 mg/l, the effluent total COD was only 120 mg/l total of which soluble COD was 80 mg/l. The TOC in the effluent at this stage was in the range of 30 to 50 mg/l and the VFA in the effluent was less than 20 mg/l. Apparently other soluble compounds contribute to the COD of the effluent, but these could not be determined. While dissolved and supersaturated methane are an important constituent of low-strength anaerobic liquor, we could not confirm whether the open reflux COD test quantitatively oxidizes this component. During step increases of COD load to the reactor, only small increases in effluent COD were observed. The effluent obtained from the BFBR was also remarkable for its lack of suspended solids and its clarity, resembling activated sludge treated effluent

### 6.5.3. Methane yield and biogas production

Methane production ( $\text{CH}_4$ -COD) is also shown in Figure 13. The recovery of COD as methane was close to 100% at each steady state. During step increases in load, gas production increased slowly, taking 3 to 4 weeks to reach steady state values. The reactor passes through three stages during step increase in COD load. During Stage 1, COD recovery as methane production was less than COD removed as determined by analysis of feed and effluent liquid. During Stage 2, COD recovered as methane exceeds 100% of daily COD removal. During Stage 3, methane yield decreases and reaches steady state values. Excess gas yield is obtained because of mineralisation of accumulated biosolids.

### 6.5.4. Scum accumulation and degradation

Scum accumulation in the BFBR was visually observed during startup and during step increases in load. In general, scum accumulation and degradation before achieving steady state, can be seen as passing through 3 stages:

#### *Stage 1: Initial buildup of scum and biosolids.*

This period may last 10 to 30 days from time of step increase in load. Visual observation shows thick and dense scum, which may capture most of the sludge in the liquor. The scum does not have flowing nature and very few occluded gas

bubbles are seen. The scum circulation system is largely ineffective and mixing requires vigorous mechanical agitation.

*Stage 2: Methanization of accumulated scum.*

During this phase, gas production and gas yield increase. COD of methane produced exceeds liquid COD removal rate. The length of this phase depends on the amount of degradable scum accumulated in the reactor. In our reactor, it did not extend more than 7 days. The nature of scum changes showing gas bubble occlusions. Towards the end of this phase, scum becomes increasingly foamy, with large gas bubbles and thin liquid walls of bubbles.

*Stage 3: Steady state.*

During this state methane production decreases from Stage 2, and reaches steady state methane yield matching with liquid COD removal. The quantity of scum in the reactor is much less than in Stage 1 and 2. The nature of scum in this stage is more hydrophilic, and can be mixed into the liquor relatively easily as compared with scum in Stage 1 and Stage 2.

The quantity of biosolids accumulated in the BFBR can be determined in terms of COD from a COD balance calculation, as the difference in COD removed and COD recovered as methane. While solids accumulation includes both biomass growth and scum accumulation, biomass growth is much smaller than COD accumulation as scum. It is theoretically possible to estimate net biomass growth from the steady state COD balance of the system, but requires the determination of COD balance to better than 1% accuracy and keeping variations in steady state to less than 1%. We could not maintain such low variability in COD loading in our experiment using real milk and therefore, estimates of biomass growth are not derived.

From Figure 13 data, the amount of accumulated scum / biosolids during a transition period was estimated. The reactor was shut down on day 365 and restarted at same loading rate on day 370. Scum accumulated in the BFBR for 20 days, total quantity was 42 g COD. From 20th day, scum degradation rate exceeded accumulation and COD recovered as CH<sub>4</sub> exceeds COD removal.

The rate of degradation of scum forming compounds in the BFBR was determined by measuring methane production, on stopping feed to the reactor.

Methane generation is measured till gas production ceased after stoppage of feed to the reactor. Two experimental runs were carried out at organic loading of 7 g COD/l.day and 10 g COD/l.day. Feed to the digester was stopped when a layer of scum was present in the reactor. At the end of cessation of gas production, the reactor liquor is clear and separates into a fast settling sludge and very clear supernatant.

Figure 14 shows the cumulative methane production as a result of scum degradation when reactor was stopped at two different times (day 203 and day 297) when operating at a steady load of 200 ml milk per day (corresponding to pseudo-steady state organic loading of 8.6 g COD/l.day). The results are summarised in Table 2.

**Table 2. Starvation tests to determine accumulated scum**

feed stopped (day)	Load before stopping (ml milk/d; gCOD/d)	Methane production rate before stopping (g COD /d )	COD removal (%)	Scum (g COD)	Biomass (g)	Mixed liquor LCFA mg/l before stoppage
203	200; 30	25	86	92.3	10	
297	200; 30	24	92	19.6	20.9	C18:0 = 8 C16:0=10
408	150; 25	24	86 to 90		12.8	

When the reactor was stopped on day 203, a thick layer of scum was present in reactor whereas on day 297, it was much less. The quantity of scum accumulated was determined as 92.3 g-COD and 19.6g-COD respectively. When methane production stops, the reactor is free of scum. The microbial biomass present in the reactor was almost twice as high during the shutdown on day 297 as compared with day 203. On day 297, the reactor contains mostly biomass (20.9 g) rather than degradable solids (7.0 g; scum and methanisable biosolids conversion ratio of 2.79g COD = 1 g VSS). The superior reactor performance, meaning less accumulation of particulate substrates, during the second instance was possibly because of increased biomass present in the reactor and greater adaptation of sludge to LCFA degradation.

LCFAs were determined in the reactor mixed liquor for 3 consecutive days prior to shut down on day 297. Only stearic and palmitic acids (C18:0 and C16:0) were detected in the liquor at low concentrations. It is noted that oleic acid

(C18:1), the main hydrolysis product LCFA of milk fat was not detected in the liquor. This shows that conversion of unsaturated LCFAs was not rate limiting during the time of shutdown.

The rate of removal of scum forming matter is obtained from the slope of the plot of cumulative CH<sub>4</sub> production versus time (Figure 14). The average rate of methanization of scum solids (SMR) obtained in the two experimental runs of different loading rates was 3.5 lit\_CH<sub>4</sub>/ day (volumetric SMR = 1 lit\_CH<sub>4</sub>/ l.d) and the specific methanization rate of scum solids was 0.167 lit\_CH<sub>4</sub>/g\_VSS.day. The SMR was independent of the input fat concentration. If we assume that scum forming matter is fat and LCFA, the volumetric SMR = 1 lit\_CH<sub>4</sub>/ l.day corresponds to a conversion rate of fat COD in BFBR of 2.62 g fat COD/l.day. This is much higher than usually recommended for the treatment of dairy effluents in anaerobic reactors e.g.. Perle et al<sup>33</sup>. The scum degradation study demonstrated that fat degradation is the rate limiting step in the methanization of dairy waste. Other control parameters monitored showed that there was no accumulation of VFAs and LCFAs in the BFBR at steady state and at unsteady state. The slow hydrolysis of fat facilitated fatty acid degradation and oleic acid was not detected in the effluent and in the mixed liquor.

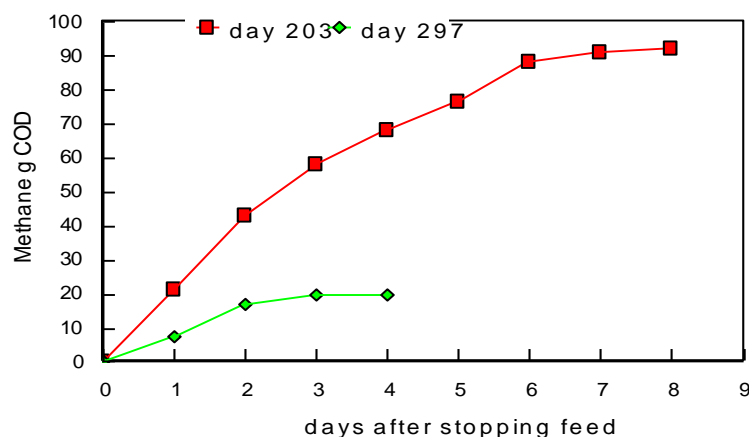


**Figure 14. Methane production at no feed condition gives the quantity of degradable COD (scum) accumulated in the BFBR. The amount of scum on day 297 is only 20% of that on day 203.**

## 6.6. LCFA effluent: microbiological aspects

---

A reactor develops its own microbial ecology. The BFBR creates an environment, characterised by high solids retention time, and selective pressures causing washout of dispersed micro-organisms. The microbiology that develops in the BFBR would have characteristics that suit its own environment. The study on treatment of milk in a BFBR, showed excellent performance with regard to COD removal at high loading rates. About 60% of the dairy waste COD is contributed by milk fat, and COD balance showed that fat methanation was essentially complete. The performance of the BFBR is curious as it is generally acknowledged that long chain fatty acid degradation is difficult and rate-limiting in the anaerobic degradation of complex wastewaters. Hence it was possible that the BFBR sludge has interesting microbial characteristics.

The BFBR was operated continuously with oleic acid (sodium salt) emulsion as the sole COD source to investigate the phenomena of protozoa growth. COD removal data was collected and the liquor in the BFBR was examined microscopically. Microscopic examination of the sludge in the reactor showed, most unusually, the presence of protozoa (Figure 15 to Figure 18). Figure 15 shows stalked ciliate vorticellae attached to a floc, feeding on particulates being swept into its gullet by a ring of cilia. At first, it was thought that there must be some mistake as protozoa are not reported in anaerobic reactors. Furthermore, the kinds of protozoa seen in the sludge were very much like those present in aerobic activated sludge. But repeated tests showed that this was not an artefact and the BFBR sludge showed consistently, a large and varied population of protozoa, which are obviously capable of fully anaerobic metabolism.



**Figure 15. Sludge from the anaerobic BFBR shows vorticella, a ciliated protozoan, grazing while attached to a bacterial floc.**

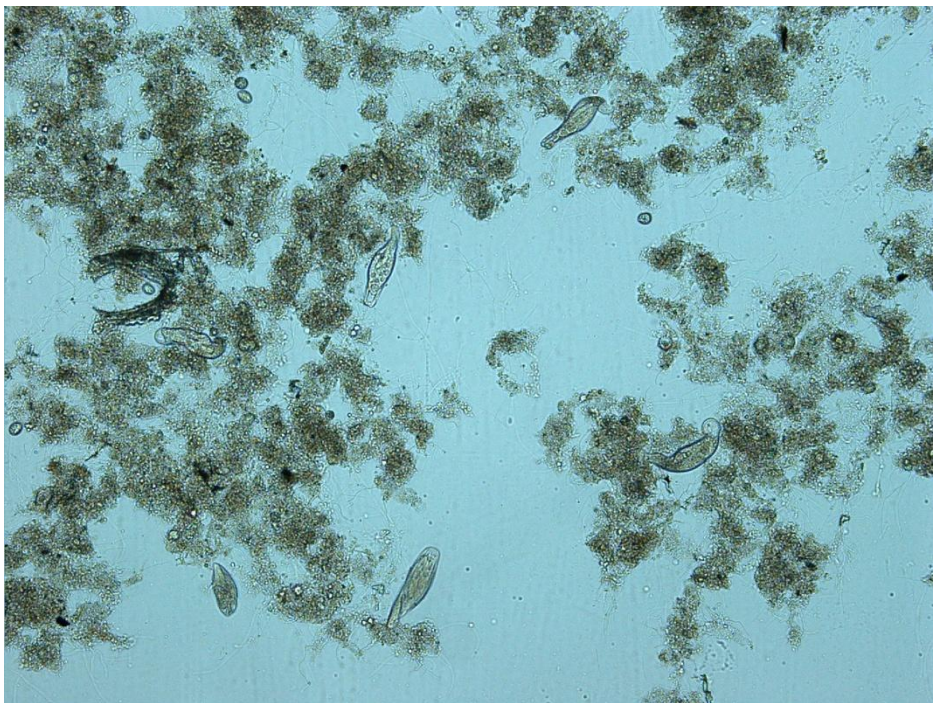


**Figure 16. Metopus grazing on BFBR sludge flocs**



Figure 17. Spiostomum in BFBR sludge, seen in phase contrast microscopy. The spiral cilia leading to the gullet, and injection of particles can be distinguished in this picture. ((Courtesy: Nimi Narayanan, B. Krishnakumar)

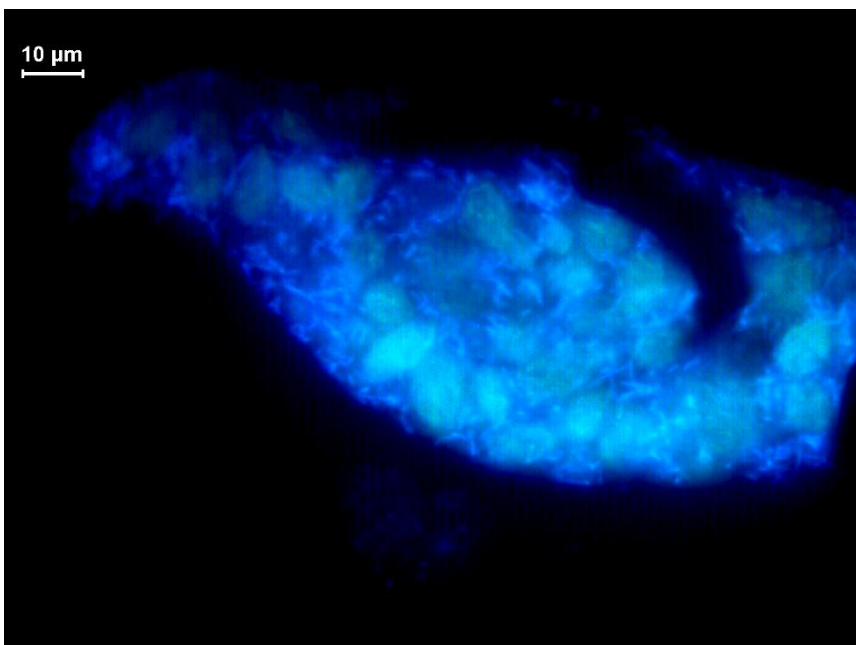


Figure 18. Metopus in BFBR sludge seen under fluorescence microscopy. The bright blue fluorescent rods are interpreted as endosymbiotic methanogens. (Courtesy: Nimi Narayanan, B. Krishnakumar)

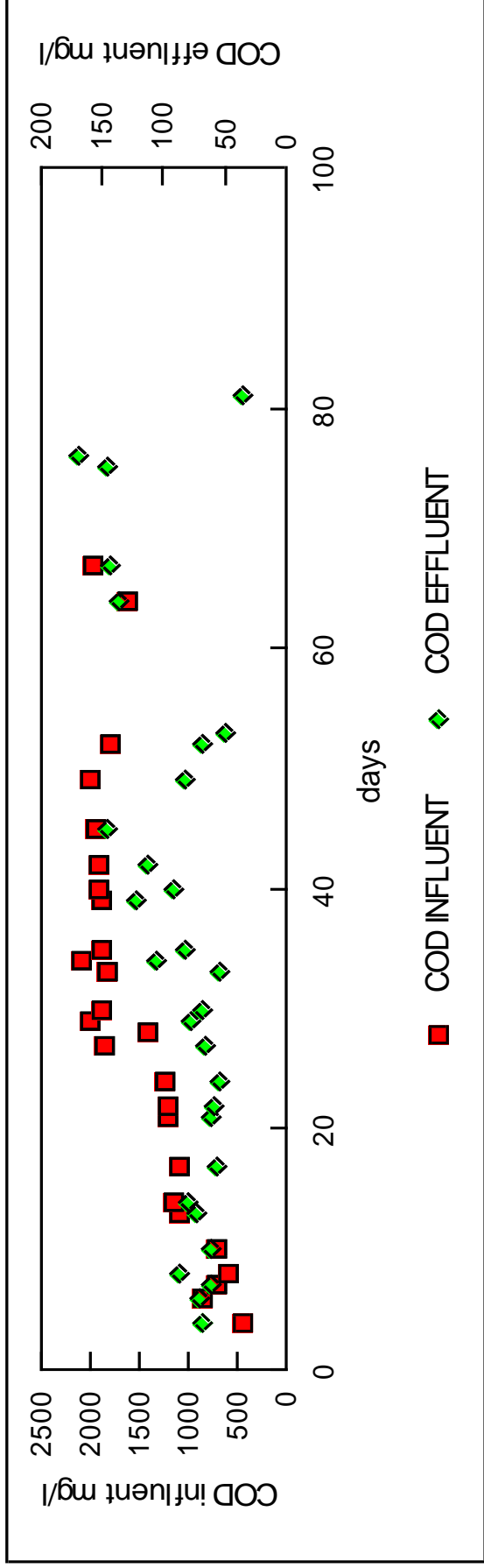


Figure 19. COD removal in BFBR with LCFA effluent

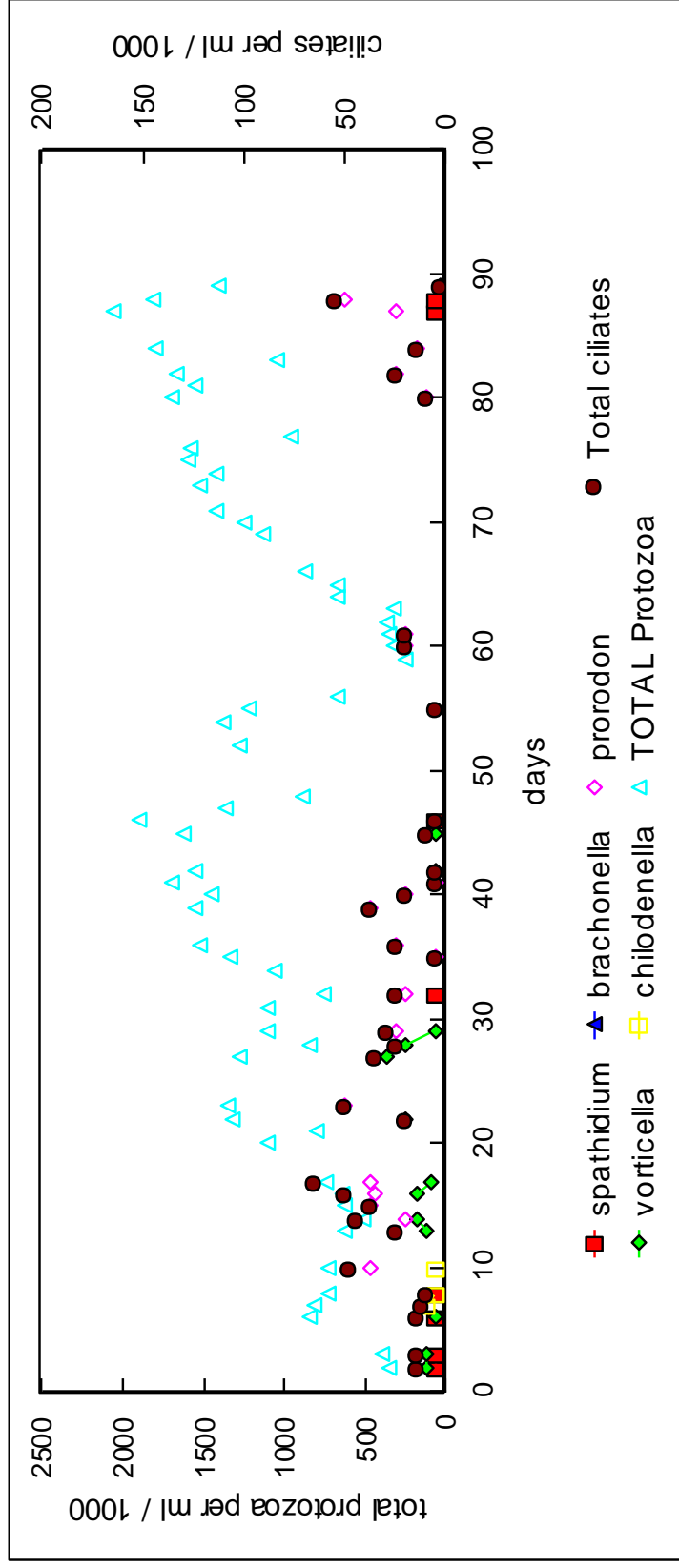


Figure 20. Changes in population of various protozoa in BFBR. The total protozoa numbers reduce when ciliate numbers increase, because of size selective predation.

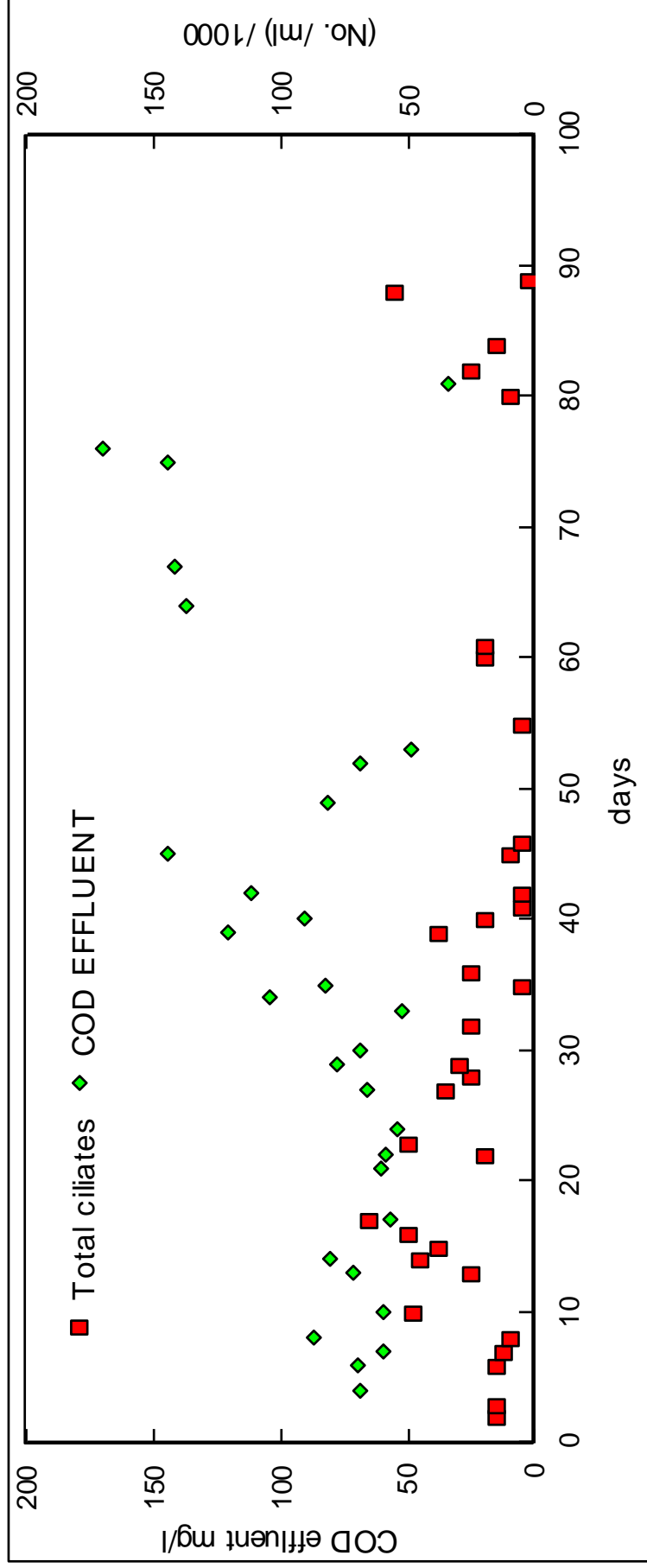


Figure 21. Effluent COD and total ciliates in mixed liquor

### 6.6.1. Discussion of microbiological characteristics of LCFA fed BFBR

---

Most of the LCFA in the feed liquor are present as micron sized globules. The BFBR once again showed high efficiency (97%) removal of COD, at organic loading rate of 7 kg COD/(m<sup>3</sup>/d). Further, it is shown through a COD balance that COD conversion to methane in the BFBR is essentially complete. Treated effluent quality was remarkable: COD 120 mg/l (avg.) (Figure 19) and free of turbidity.

Total protozoan counts varied from  $0.5 \times 10^6 \text{ ml}^{-1}$  to  $2 \times 10^6 \text{ ml}^{-1}$ . The protozoan diversity included small round amoeba, ciliates and flagellates. The highest number of ciliates found was  $3 \times 10^5 \text{ ml}^{-1}$ . The quality of effluent (COD, turbidity) produced from the BFBR is weakly related to the number of ciliates in the liquor in the reaction chamber. The number and diversity of protozoa in the BFBR were not steady during the duration of this experiment, even when steady feed of oleic acid was given to the reactor. In general, small, round protozoa and amoeboid population increase first when oleic acid load is increased, while the COD of the effluent and its turbidity increase. This is followed by increase in flagellated and ciliated organisms as the reactor stabilizes. When the reactor is overloaded, (evidenced by scum build-up), the number of ciliated protozoa is less. The BFBR filter used in this study is not fine enough to directly retain free swimming protozoa and retention is dependent on nature of sludge produced. Protozoa are found anchored to biomass or mobile within flocs. The results show a negative correlation between ciliate count and effluent COD, and a positive correlation between total protozoa and effluent COD.

The standard theory of the mineralisation of complex, insoluble COD in an anaerobic reactor postulates only bacterial or archaeal mediation for the breakdown process. The presence of more than one trophic layer of organisms in an anaerobic reactor environment has scarcely ever been reported. The microbial diversity is limited essentially to fermentative bacteria and methanogenic archaea, all of which depend on soluble COD for energetics. However, our study correlates protozoan population and diversity with the performance of the BFBR anaerobic reactor.

In analogy with activated sludge, we can hypothesize that protozoan activity in the anaerobic BFBR leads to improved performance, especially in the treatment of wastewater with insoluble COD. Protozoan activity could have the following effects

- predation of free swimming bacteria leading to improved clarity of treated effluent and formation of flocs and granules.
- direct consumption of fat / lipid globules or insoluble COD of certain size fractions leading to increased removal rates. This was confirmed in later studies by Priya<sup>34</sup>

Anaerobic protozoans generate energy through fermentative pathways. Fermentation products like hydrogen are scavenged by methanogens which are invariably found as endosymbionts or ectosymbionts associated with anaerobic protozoans. The endosymbionts are visible inside protozoa using a fluorescence microscope, since methanogens contain enzymes that fluoresce when illuminated with UV light (Figure 18. Metopus in BFBR sludge seen under fluorescence microscopy. The bright blue fluorescent rods are interpreted as endosymbiotic methanogens.).

It is easy to see that anaerobic protozoa have a competitive advantage over bacteria in using insoluble COD. Bacteria require exocellular enzyme activity to utilize LCFA globules but protozoa can directly consume the globules. The internal nature of the enzymatic processes and the richer portfolio of hydrolyzing and liquefying enzymes that protozoa have, allow faster rate of utilization of insoluble COD, compared with bacteria. An anaerobic reactor treating complex wastewater and producing low residual COD effluent is a COD limited (energy source limited) environment, and COD available is likely to be in the form of insoluble particulates. The mobility of protozoa gives it further competitive advantage over bacteria in harvesting particulate COD sources.

Fluctuation in population of various types of protozoa is expected in a predator-prey relationship between smaller protozoa and larger ciliates. The net effect of predation in an anaerobic system is the conversion of biomass to methane. Thus, counter-intuitively, instead of reduced efficiency of COD removal, such processes would evidence itself as increased sludge

methanogenic activity. High sludge methanogenic activity has been seen in BFBR sludge.

Grazing and predation can lead to formation of biomass flocs and granules because of selective elimination of free swimming bacteria. The BFBR sludge formed fast-settling irregular shaped granules, particularly upon stopping feed to the reactor.

The data gives indications but is not strong enough to conclude that lack of trophic layers is the reason why anaerobic reactors do not achieve residual COD, turbidity and pathogen levels achieved routinely in aerobic activated sludge processes. It is topic deserving attention at centres of anaerobic R&D as it holds promise to generate pathogen-free, odour-free anaerobic treated sewage for direct irrigation.

## **7. Development of a mathematical model of BFBR**

---

Practical application of the anaerobic digestion processes for wastewater treatment has been marred by its reputation of being difficult to operate, slow to start and prone to instability. There are several full-scale installations where anaerobic reactors have failed to operate satisfactorily. The failure of anaerobic reactors can be attributed to lack of understanding of the process – at the design stage as well as at the operation stage. Often in India, anaerobic reactors are installed by suppliers who have licensed the mechanical design from a foreign developer. The supplier usually lacks the 'know-why' on the process design and its dependence on waste characteristics while executing the order for the anaerobic system. In the design of an anaerobic reactor, the process design and start-up are the critical issues, while the mechanical design of the system is straightforward. The situation is compounded by the reactor buyer who invariably lacks the expertise to evaluate technically the system he has been offered.

Ideally the rational process design of an anaerobic reactor, should follow from: (a) a knowledge of the reaction stoichiometry (b) the intrinsic microbial kinetics of the interacting groups of anaerobic bacteria (c) the hydrodynamics of the system and (d) the mass transfer characteristics of the system. It is possible to simplify the problem and assume uniform spatial distribution of reactants, biomass and products within most anaerobic reactors because of the time scales of hydrodynamic variation are much shorter than the reaction time scales.

In actual practice, because of the extremely complex nature of the reaction process, it was not practical to carry out calculations based on intrinsic microbial kinetic of the interacting groups of bacteria<sup>35</sup>. However, the rapid fall in computational costs and the development of powerful software tools has made

now it possible to carry out these calculations with much less effort and cost. Some notable previous attempts at modelling of the anaerobic process may be mentioned<sup>36,37,38</sup>.

The anaerobic process model can throw light into the dynamic behaviour of a reactor. Hence, the combination of an sufficiently detailed anaerobic process model with a suitable reactor model having the features of the BFBR can give insight into the dynamics of the BFBR. This chapter develops a model for a BFBR anaerobic reactor for the treatment of complex wastewater. Degradable particulate COD is described as composed of only proteins, fats, and carbohydrates<sup>39</sup>. This description is adequate for effluents discharged by dairies, slaughterhouses, gelatine plants, food processing units, edible oil processing units etc. As per this definition, sewage can also be termed a complex wastewater. Materials such as municipal solid waste or animal manure require more detailed description for modelling. In particular, it is required to distinguish between easily degradable carbohydrates difficult to degrade polysaccharides such as lignocellulosic biomass.

The breakdown of insoluble COD to soluble COD is usually the rate limiting step in anaerobic digestion of complex wastewater. The BFBR reactor is characterized by its ability to separate and retain insoluble COD particles till it undergoes solubilization – termed, in this thesis, as decoupling solid retention time from hydraulic retention time.

The model is used for simulating the application of BFBR in treatment of sewage and the experimental observation of treatment of dairy effluent in BFBR. The results are analysed to learn more about the nature of the process that occur within the BFBR

## 7.1. Model concept

---

The configuration of a BFBR reactor is schematically shown in Figure 22. The BFBR is represented as a completely mixed reactor (CSTR), provided with a filter that passes dissolved substrates while retaining solid substrates. The CSTR assumption implies concentrations of all components are functions of time only. The efficiency of retention is given by parameter  $\alpha_i$  for substrate  $i$ , where  $\alpha_i = 0$  for dissolved substrates. Thus the concentration of insoluble substrate  $i$  in the BFBR reactor is increased by fraction  $1/\alpha_i$  compared with a normal CSTR.

Making  $\alpha_i$  a property of insoluble substrate component  $i$ , allows the model to be flexible enough to model the digestion of materials where differentiated retention is expected. For example, in the digestion of cow dung slurry containing chopped straw or newsprint, we may expect these materials to be retained in a coarse filter while the liquefied slurry is free to pass through the filter.

The reactor has active liquid volume  $V_r$ ,  $Q$  is the flow rate,  $Q_{gas}$  is the gas production rate and  $C$  the concentration of components (either chemical or microbial species) in the reactor. The buoyant filter (zero volume) passes  $\alpha$  fraction of the insoluble concentration and 100% of the soluble concentration inside the CSTR. The model admits varying flow rates and time varying concentration of feed substrate. This allows the study of reactor response to short interval shocks, hydraulic and organic. The model equations also include a water balance and therefore  $V_r$  can be varying as in the case of a BFBR reactor operated as a sequencing batch reactor.

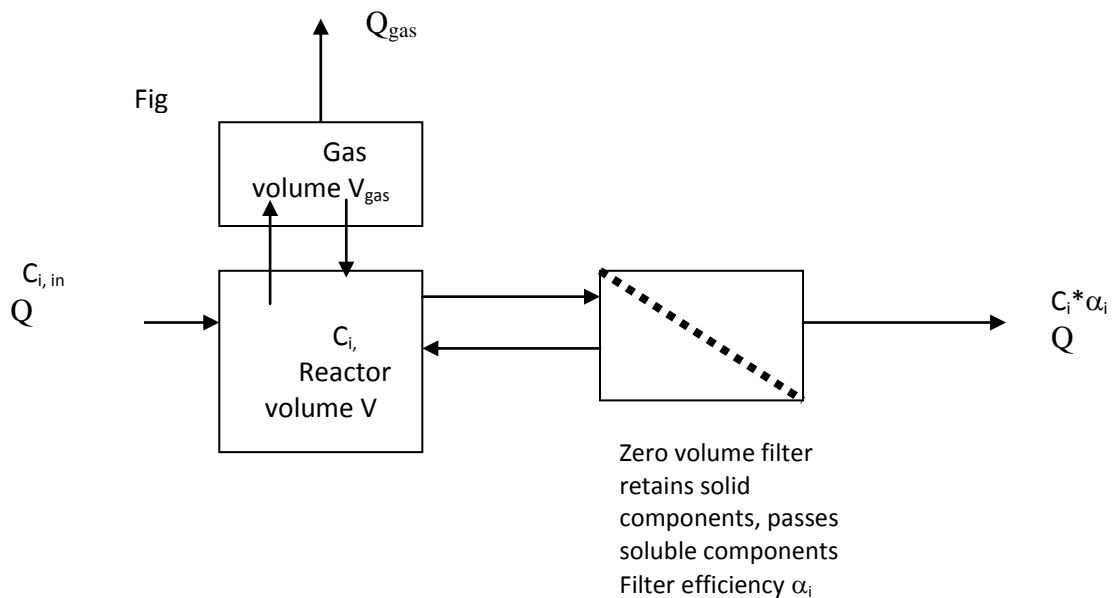


Figure 22. Schematic representation of BFBR

## 7.2. Model equations and matrix representation

---

Material balance equations can be written for each species in the system as below:

$$\frac{\partial VC_i}{\partial t} = Q_{in} C_{in,i} - Q_{out} \alpha_i C_i + V \sum_j Y_{ij} r_j$$

1

where

$C_i$  is the concentration of component  $i$  in the reactor

$V$  is the (time varying) volume of the reactor

$Q_{in}$  is the flow rate of liquid into the reactor (given function of time)

$Q_{out}$  is the flow rate of liquid from the reactor (given function of time)

$\alpha_i$  is the fraction of species  $i$  not retained by the retention device (filter)

$r_j$  is the rate of reaction  $j$ , (the rate production of component  $m$  per unit time per unit volume)

$Y_{ij}$  is the yield of component  $i$  for reaction  $j$  (the stoichiometric ratio of production of component  $i$  per unit production of component  $m$  produced in reaction  $j$ ).

The material balance equation 1 is valid for time varying flow and time varying concentration of feed. It is also valid when rate of inflow is not equal to rate of outflow causing change in reactor volume. Hence, the equation can simulate fed batch and sequential batch operation of the reactor. The material balance equation is written so that each component can have different retention times within the reactor by giving a different  $\alpha$ , where  $(1-\alpha)$  would be efficiency of retention of the component. In practice, however,  $\alpha$  for all soluble components is taken as 1, and therefore equal to hydraulic retention time. The concept of retention time is itself rather ill-defined when simulating time varying flow rates in reactors where the active volume is itself changing, and the traditional definition of retention time becomes a time varying function. Equation 1 can be rewritten as below:

$$\frac{\partial C_i}{\partial t} = \frac{(-C_i \frac{\partial V}{\partial t} + Q_{in} C_{in,i} - Q_{out} \alpha_i C_i + V \sum_j Y_{ij} r_j)}{V}$$

The overall liquid balance in the reactor is written as

$$\frac{\partial V}{\partial t} = Q_{in} - Q_{out}$$

2

Hence, the material balance for component i becomes

$$\frac{\partial C_i}{\partial t} = \frac{-C_i(Q_{in} - Q_{out}) + Q_{in}C_{in,i} - Q_{out}\alpha_i C_i + V \sum_j Y_{ij}r_j}{V}$$

3

Equations 2 and 3 represent the material balance for the liquid phase including insoluble solids which are assumed to be spatially homogenous in the reactor. These are supplemented by gas phase material balance equation. There is no gas inflow into the reactor, only generation and outflow. Hence, the gas phase material balance can be written as.

$$M_{gas} \frac{\partial P_i}{\partial t} = -Q_{gas}P_i + V \sum_j Y_{ij}r_j$$

4

where

$Q_{gas}$  is mole flow rate of gas

$M_{gas}$  is the molar gas holdup in the reactor (in moles of gas phase in reactor)

$P_i$  is the mole fraction of gaseous component i

$r_j$  is the rate expression of reaction j, producing component m per unit volume of reactor liquid volume

$Y_{ij}$  is the stoichiometric ratio in mol gas produced per unit mass COD of reaction component m produced in reaction j.

The yield coefficient matrix written in terms of COD is such that, for each reaction j, the sum of the coefficient over all components should give the COD balance, i.e.,

$$\sum_i Y_{ij} = 0$$

5

Equation 5 is valid only if yield coefficients are converted to consistent units. Since the yield coefficient of methane is given in terms of moles of methane

produced per g COD converted, the conversion factor 64 gCOD/mol methane must multiply the the coefficient corresponding to methane gas. In the implementation of the model, we carry out COD balance for liquid phase soluble and insoluble organic components all of whose yields are given in terms of COD only, thus avoiding the conversion factors. Equation 5 would then be valid for all process, except transfer of dissolved methane to methane gas.

Equations 2, 3 and 4 together form the material balance of reactor. Formally, it is a system of first order differential equations, the number of equations being equal to the number of chemical and biological species of interest. The equations are conveniently expressed in matrix format, with component concentrations  $\{C_i\}$  as  $1 \times n$  dimensional matrix of  $n$  unknown variables.  $[Y_{ij}]$  representing the  $n \times m$  dimensional matrix of stoichiometric constants coupling the unknown variables.  $r_j$  is the  $m \times 1$  dimensional rate vector for  $m$  processes.  $r_j$  is nonlinear in  $C_i$  and therefore, numerical methods are necessary to solve the system of equations.

The ASM (activated sludge model of International Water Association) format of the model has yield coefficients in matrix form with components (S for soluble substrates, X for particulate materials including microbial biomass) as columns, processes as rows. Each material balance equation sums the product  $Y_{ij}r_j$  column-wise. Row-wise sum of the matrix for all terms in terms of COD should give zero as per COD balance. The matrix format is used in IWA's ADM1 model<sup>40</sup> also. The model developed in this thesis follows ASM, in using growth and decay of relevant classes of organisms as the processes being modelled. ADM1 uses substrate consumption and production as processes being modelled.

The yield coefficient matrix must be normalized so that the stoichiometric coefficient of the component whose rate of production is given by the expression is 1. Hence the yield coefficient for growth of acetoclastic methanogen is  $1 \text{ gCODacetoclasticmethanogen/gCODacetoclasticmethanogen}$  for component XCH<sub>4</sub> representing acetoclastic methanogen biomass and  $-10 \text{ gCODAcetate/gCODacetoclasticmethanogen}$  for  $S_{\text{acet}}$  representing acetate concentration.

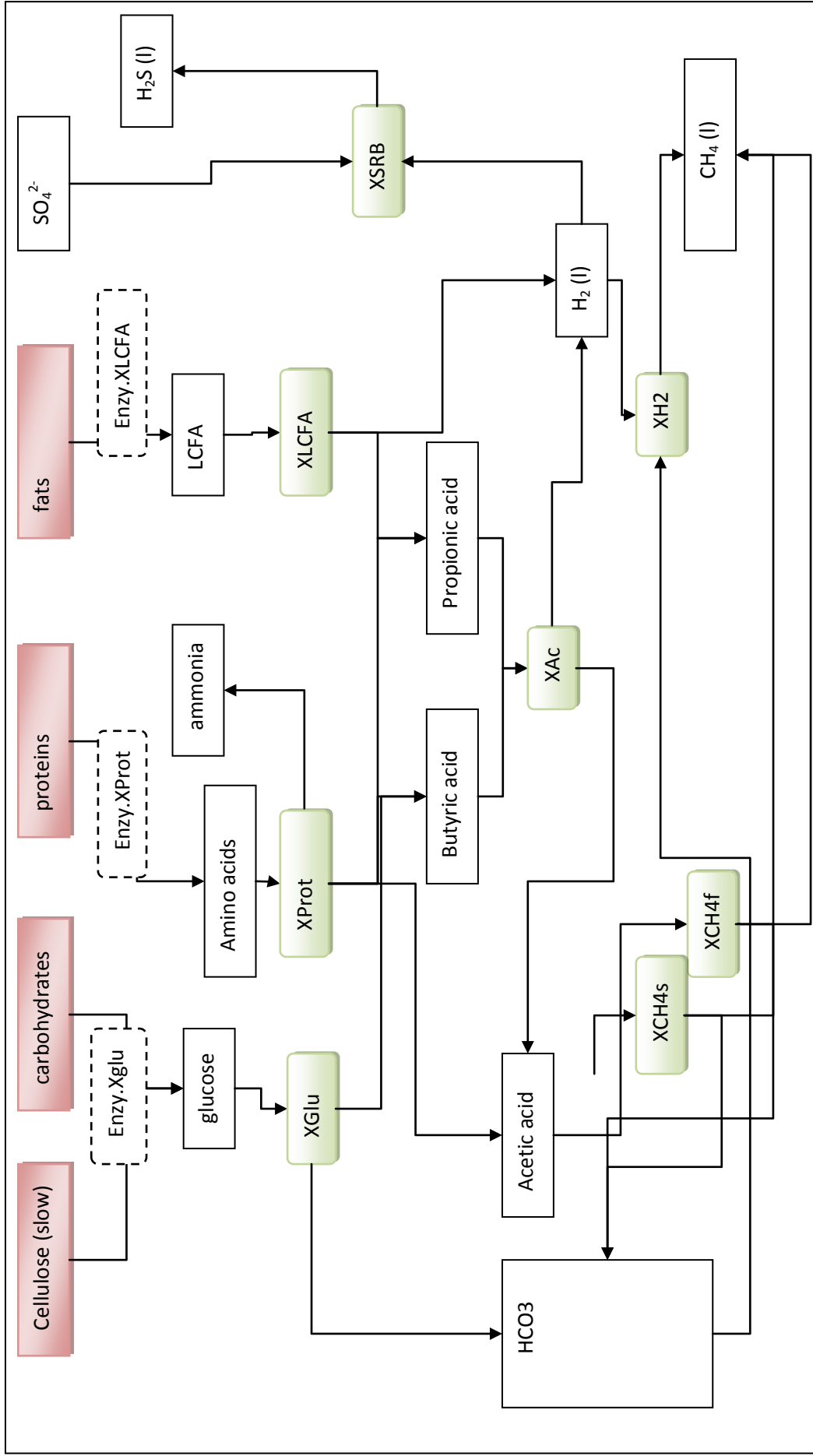


Figure 23. Process model for anaerobic digestion. Arrows showing generation of inorganic carbon in each process step, and gas transfer to gas phase components is not shown. Components in green boxes are subjected to growth and decay, red boxes are subjected to enzymatic processes.

### 7.3. Rate expression

---

The various processes that change the concentration of component species are

- microbial growth,
- microbial decay
- enzymatic reactions
- interphase mass transfer (gas transfer)

We choose microbial growth and decay are taken as the principal rate process rather than rate of production or consumption of substrates. This implies that the  $Y_{ij}$  for growth of microbial species  $i$  is 1 for all the various process by which such growth takes place. It may be noted that a organisms may grow on multiple substrates. Each can be represented as a process. For example, one differential equation may represent the growth of acetogens on butyrate, and another differential equation represents the growth of acetogens on propionate. We can eliminate one of the processes by a rate expression combining the multiple substrates, but we choose to use independent equations.

The components chosen for the model are the mass of various micro-organisms grouped by function, various dissolved, gaseous and particulate substrates. The anaerobic digestion process model used is shown in Figure 23. The process model is a idealized model. It is not meant to accurately show all that is known about anaerobic digestion. The shaded boxes are components. Only liquid phase components are shown. Inputs and outputs of each box is shown. Processes cannot be identified easily in this type of figurative representation.

The model construction using microbial growth as the principal rate process is a departure from the IWA ADM1 model where substrates utilization is taken as the principal rate processes. The two are related by modification of yield coefficient. The advantage of using microbial growth as the principal rate process, is that it is simpler when more than one species carry out a particular conversion. For example, the competitive growth of *Methanosarcina* and *Methanosaeta* fermenting acetate to methane is more naturally represented in the microbial growth based model than in the substrate utilization based model.

The maximum specific growth rates for various broad classes of bacteria and archae fall within a certain range and can be guessed. On the other hand, experimental measurement of masses of various bacterial classes modelled is almost impossible in an anaerobic reactor consortia, while it is comparatively easy to monitor the concentration of various substrate, particularly the soluble substrates.

### 7.3.1. Microbial growth

---

The Monod function<sup>41</sup> is the standard two parameter method of expressing microbial growth in terms of a single limiting substrate.

$$r_g = \mu X$$
$$\mu = \frac{\mu_{max} S}{K_s + S}$$

where:

$\mu$  is specific growth rate

X is the microbial concentration

S is the limiting substrate concentration

$\mu_{max}$  is the maximum specific growth rate

$K_s$  is the affinity constant

The Monod function (**Figure 24**) reduces to first order growth at low substrate concentration and zero order growth at high substrate concentration. The maximum growth rate is obtained when substrate is provided in excess. The affinity constant is the concentration of the limiting substrate at which the growth rate is half the maximum growth rate.

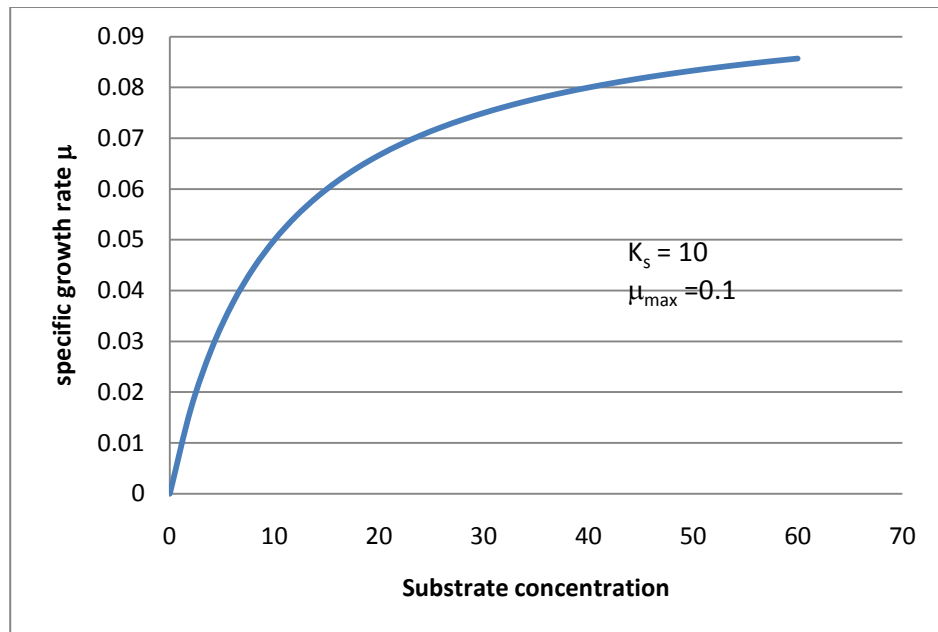


**Figure 24: Monod function for a limiting substrate**

The logical construct of the Monod function is illuminating. Under steady-state conditions, obtained in a chemostat, when amount of substrate is limited, microbes double in number at fixed time intervals. The doubling time is seen to be inversely proportional to the availability of food. When food is available in excess, no further decrease in doubling time is observed. This implies that the rate of increase in microbial number is a linear at low substrate concentration, and when food is available in excess, the rate of growth is constant.

Substrates are transported inside the cell by passive diffusion through the cell membrane and by active transport using energy. The cell membrane is permeable to gases and low molecular weight non-polar substances. Diffusive transport of substrates implies that cell internal concentrations are less than cell outer surface concentrations. On the other hand, using active transport, substrates can be transported against concentration gradient and cell internal concentrations may greatly exceed outside concentrations. In substrate limited growth for many substrates, the cell surface concentration is not so high as that diffusive transport exceeds internal utilization by cell at its maximum rate<sup>42</sup>. By Fick's law, the rate of diffusion is proportional to the concentration gradient. Since cell membrane thickness can be considered as effectively constant, the

rate of diffusion may be considered as proportional to the difference between substrate concentrations on either side of the cell membrane. If we consider cell internal substrate concentration is effectively zero, as when all substrates are utilized as soon as it diffuses into the cell, the rate of diffusion is proportion to cell surface concentration and thereby to bulk substrate concentrate. Hence, when diffusive transport is limiting, the rate of cell growth is a linear function of substrate concentration. On the other hand, when sufficient substrate is available at the cell surface, internal biochemistry will limit cell growth. In this case, growth rate is no longer a function of substrate concentration. We need to note that with increasing substrate concentrations, particularly for substrates that diffuse freely into the cell, internal cell machinery can be damaged and growth will be inhibited. This is particularly important in anaerobic reactors, where the main methanogenic substrate, acetic acid, is inhibitory to methanogenic organisms at concentrations that are frequently encountered in real reactors.

The same arguments to show linear dependence of growth on limiting substrate concentration can also be made for active transport of substrate. The cell has to expend more energy for transport of substrate at lower substrate concentrations and hence less energy is available for growth. The analogy between Michaelis Menten kinetics for enzymatic reactions and growth kinetics has often been drawn and it can be explained by active transport using enzymes to transport substrates across membrane<sup>42</sup>. The difference between passive transport and active transport becomes relevant when considering inhibition at above growth saturation substrate concentration. Here substrate that are actively transported are much less likely to impact growth adversely. Indeed, it is noted that un-ionised fraction of many substances such as volatile fatty acids, ammonia, hydrogen sulphide are transported by diffusion through the cell membrane and at high concentration inhibit growth of the anaerobic consortia.

The Monod function may be generalised in several ways to include the effect of various substrates and nutrients that may limit microbial growth. For example, a generalised Monod function can be formulated as the product of various Monod terms for each growth substrate. The  $K_i$  for each substrate  $S_i$  represents the affinity constant for that substrate.

The effect of inhibitory substrates is modelled by an complementary form of the Monod expression. The effect of pH and hydrogen partial pressures are modelled using hat functions.

$$r_j = \mu_m X_j \prod_i \frac{S_i}{K_i + S_i} \prod_m \frac{Kin_m}{Kin_m + Sin_m} \cdot fpH \cdot fp_{H_2}$$

6

The generalised Monod product function reduces to the single substrate Monod function, when all other growth essential substrates are present in excess and the concentration of all inhibitory substances are very small compared with their affinity constants.

This generalised Monod product expression can model many of the conditions that occur in a anaerobic reactor. But there are instances where the expression is deficient. For example, it is not able to model the growth of organism on two alternate substrates, one of which is preferred over the other.

The generalised Monod product function is a linear function of the limiting substrate, and a constant function of the non-limiting substrate, and hence models very well the limiting cases. But intermediate response may not be accurate. For example, let  $S_1 = K_{s1}$  and  $S_2 = K_{s2}$ , and all other growth substrate / nutrients are in excess; we get a specific growth rate  $\mu = \mu_m/4$ , which may not be accurate. In fact, we may expect a specific growth rate closer to  $\mu_m/2$ , as it is more likely that only one substrate is growth limiting and the other is already in excess even if its concentration is smaller than its saturation level. The unnatural product terms can be removed using minimum functions as given below:

$$r_j = \mu_m X_j \underset{i}{\text{Min}} \left[ \left( \frac{S_i}{K_i + S_i} \right) \right] \cdot \underset{m}{\text{Min}} \left[ \left( \frac{Kin_m}{Kin_m + Sin_m} \right) \right] \cdot fpH \cdot fp_{H_2}$$

7

In Equation 7, the rate is a simple Monod function of the rate limiting substrate alone and rate limiting inhibitory substrate. An expression containing maxima and minima may appear difficult to evaluate but is actually quite simple using built-in functions using programming software like MATLAB.

Other rate expressions have also been proposed for growth limited by multiple limiting substrates. In particular, growth modelled as a Monod function

of the ratio of limiting substrates<sup>43</sup> is logically elegant. However, there is little reported data on microbial growth kinetics with multiple growth limiting substrates and therefore there is little to choose between the various functions when experimental data is missing.

### 7.3.2. Microbial decay

---

Assuming that a constant fraction of microbial numbers lyse or become otherwise unviable, microbial decay can be modelled as first order decay. It can be shown from thermodynamic arguments that microbes consume energy even when there is no growth, merely to maintain cell structure and concentration gradients across the cell wall. This energy is called maintenance energy. Accounting for maintenance energy leads to the same rate expression as first order decay.

$$r_{dj} = -k_{dj}X_j$$

8

The above equation is written for each microbial species  $j$  included in the model.

### 7.3.3. Enzymatic reactions

---

In modelling the degradation of complex effluents where COD as insoluble substrates is significant, enzymatic reactions responsible for solubilisation are particularly important. Enzymes that are responsible for hydrolysis and solubilisation are produced by bacteria, that can utilize the product of enzymatic reactions. Enzymatic reactions are also surface based reactions and enzyme production is generally initiated after the bacteria responsible for attach on the surface of particulate substrates.

In contrast to microbial growth reactions, there is less consensus in literature about rate expressions for enzymatic reactions<sup>44</sup>. Logically, we expect the rate of hydrolysis to be proportional to the population density of organisms producing hydrolytic enzymes when substrate are in present in excess. Similarly, when organisms are in excess of insoluble substrate (surface area) the rate of hydrolysis should be proportional to the substrate (surface) available. In the intermediate regime, the rate of hydrolysis may be modelled as a Monod function of the ratio of substrate to hydrolytic microbes. When the ratio is large, substrate is in excess, and rate of hydrolysis is proportional to the concentration

of hydrolytic organisms. When the ratio is small, the rate of hydrolysis is proportional to substrate concentration. This model is called the Contois model of enzymatic reactions<sup>45,46</sup> shown below:

$$r_n = \left( \frac{k_{max} \frac{S_n}{X_j}}{K_s + \frac{S_n}{X_j}} \right) X_j$$

9

where

$r_n$  is the rate of hydrolysis of insoluble substrate  $S_n$  by organism  $X_j$

$k_{max}$  is the maximum specific rate of hydrolysis of insoluble substrate  $S_n$  by organism  $X_j$

$K_s$  is the ratio of substrate to organism, at which the specific rate of hydrolysis is  $k_{max}/2$ .

#### 7.3.4. Gas mass transfer rate processes

---

Usually, anaerobic reactor modelling makes the following assumptions: (a) carbon dioxide in equilibrium with dissolved  $CO_2$  and (b) methane completely non-dissolved. The assumption of equilibrium for gases is not strictly valid and it is preferable to model the evolution of all gases as rate process<sup>47</sup>. Thus,

$$r_j = (k_L a)(C_j - C_j^*)$$

10

where

$r_j$  is the rate of gas transfer of gaseous species  $j$

$C_j^*$  is the concentration of gas phase

$C_j$  in equilibrium with partial pressure of gas species  $j$

$(k_L a)_j$  is the overall (liquid film) mass transfer coefficient<sup>48</sup> of gas species  $j$ .

Measured  $(k_L a)$  in anaerobic reactor is very low. The  $(k_L a)$  of various gases are in proportion to the square root of its molecular diffusivity. The gas phase material balance can be related to liquid phase dissolved gas concentration at steady state.

It may be noted that in the anaerobic digestion process, gas evolves at molecular level within cell, and diffuses out into the liquid phase. Gas bubbles at nucleation will be in the form of microbubbles, of sizes comparable with the microbial cell. Tiny bubbles have high gas pressure inside because of surface

88

tension. The pressure difference between inside and outside of a bubble is given by the Laplace equation.

$$\Delta P = \frac{2\sigma}{R}$$

where

$\sigma$  is the surface tension  
 $R$  is the radius of the bubble

An order of magnitude calculation shows that the pressure inside a bubble  $10^{-6}$ m diameter would be  $2 \times 70 \times 10^{-3} \text{N/m}^2 / (10^{-6} \text{m}/2) = 3 \times 10^5 \text{ Pa}$  above hydrostatic. In order to transfer gas from liquid into tiny bubbles, the dissolved gas concentration must exceed the equilibrium concentration of the gas in the bubble. As bubbles grow, gas pressure and the equilibrium concentration also reduces. Hence bubbles may be expected to have a rapid growth phase at very small sizes followed by linear size increase. Our observations show tiny bubbles about 0.1mm diameter, rising through the liquid column.

Under steady state condition, the material balance for gas phase, Equation 4, reduces to

$$M_{gas}P_i = V(k_L a)_i(S_i - S_i^*) \tag{11}$$

where

$S_i$  is dissolved gas concentration of gas species  $i$   
 $P_i$  is mole fraction of gas  $i$  in reactor gas volume  
 $M_{gas}$  is total gas holdup in moles in bulk gas phase in reactor  
 $V$  is total liquor volume in reactor

The equilibrium gas concentration  $S_i^*$  corresponding to bulk gas concentration  $P_i$  is given by Henry's law

$$S_i^* = K_{Hi}P_i$$

where

$K_{Hi}$  is Henry's law constant in (mol/litre)/(molfraction)

12

Substituting 9 into 8, we get

$$\frac{S_i}{S_i^*} = 1 + \frac{M_{gas}}{K_{Hi}V(k_L a)_i} \tag{13}$$

Equation 13 shows the ratio  $(S_i/S_i^*)$  is closer to 1 when gas transfer coefficient is larger or when  $K_{Hi}$  is larger (soluble gas species). The volumetric gas transfer coefficient is dependent on system parameters such as turbulence and gas production rate.  $K_L a$  is dependent on nature of gas only to the extent of square root of diffusivity. The relative change in diffusivity for various relevant gases is small when compared with change in Henry's constant (Table 3). In the anaerobic reactor, this implies that gases such as ammonia, hydrogen sulphide and carbon dioxide are close to equilibrium concentration calculated from bulk gas concentration, while for methane, hydrogen and nitrogen, the dissolved gas concentration may be much larger than equilibrium values estimated from bulk gas concentrations.

**Table 3: Diffusivity and Henry's law constant (ref: Chemisty Webbook, NIST) for various gases of relevance in anaerobic reactor. Henry's law constant at 35°C for methane and hydrogen from Perry's Chemical Engineer's Handbook.**

Gas	Diffusivity $m^2/s$	Henry's constant atm/mol.fr
Methane	$1.57 \times 10^{-9}$	$4.8 \times 10^4$
Carbon dioxide	$1.98 \times 10^{-9}$	$2.1 \times 10^4$
Hydrogen	$4.65 \times 10^{-9}$	$7.42 \times 10^4$
Hydrogen sulphide		$7.1 \times 10^3$

## 7.4. Equilibrium processes

---

### 7.4.1. Acid base reactions

---

Several physicochemical processes relevant to anaerobic digestion are so fast, that they are essentially in equilibrium. Acid-base ionic equilibrium is invariably established.

The pH of the anaerobic liquor is estimated from charge balance. The main components affecting the charge of the system are bicarbonate, volatile fatty acids, ammonia and hydrogen sulphide. In the range under consideration, all these species are monoprotic. However, for evaluation of reactors performance under extreme high pH, the bicarbonate-carbonate equilibrium has to be considered. The charge balance equation may be written as:

$$\sum_i z_i \alpha_i C_i = 0$$

where

$z_i$  is the charge on ions,

$\alpha_i$  is the fraction of total concentration of component  $i$  which is charged

$C_i$  is the total concentration of component  $i$

For monoprotic negative ions (acetate, propionate, butyrate,  $\text{HCO}_3^-$ ,  $\text{HS}^-$  etc),

$$\alpha_i = \frac{1}{1 + 10^{pK_i - pH}}$$

15

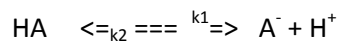
and for monoprotic positive ions (only  $\text{NH}_4^+$ )

$$\alpha_i = \frac{1}{1 + 10^{pH - pK_i}}$$

16

It may be noted that in modelling of anaerobic reactors treating low strength wastes such as sewage, ammonia<sup>49</sup> and diprotic carbonates can be significant in determining the reactor pH equilibrium and therefore should not be neglected in formulating the charge balance equation. The charge balance equation is a non-linear function of pH, given the total concentration of components affecting charge balance, which needs to be solved separately at every step when integrating the ODEs representing material balances.

It is possible to avoid the solving the non-linear function, by formulating each equilibria as a rate processes comprising forward and backward reactions. For example, consider the dissociation of HA:



The rate of formation of  $\text{A}^-$  is given by

$$r_{\text{A}^-} = k_1\{\text{HA}\} - k_2\{\text{A}^-\}\{\text{H}^+\}$$

Substituting the material balance for total HA,

$$\{\text{HA}\} + \{\text{A}^-\} = C_t$$

and using the equilibrium constant  $K_{eq} = k_2/k_1$ ,

$$r_{\text{A}^-} = k_1 \left( (C_t - \{\text{A}^-\}) - K_{eq}\{\text{A}^-\}\{\text{H}^+\} \right)$$

17

A differential equation may now be written for  $A^-$  where the rate expression is given by 17.

The algebraic equilibrium equation is converted into differential equations<sup>50</sup> at the cost of additional components. For example, instead of the ionic equilibrium between bicarbonate and dissolved carbon dioxide, we could write

$$r_{CO_2,liq} = k_{CO_2}([HCO_3^-][H^+] - K_{eq}[CO_{2,liq}]) \quad 18$$

and write material balance equations for both bicarbonate and  $CO_{2,liq}$ , whereas using the algebraic expression we only have a material balance for total inorganic carbon.

If the rate constants are chosen large enough, the reaction proceeds to essentially equilibrium conditions during the time scales of the order of HRT. The  $[H^+]$  appearing in equation 17 is again calculated from the charge balance equation, but in this case, it is an explicit function - the algebraic sum of charged species concentration already known.

In our model, we do not use the differential equation approach to estimate pH. We directly solve the non-linear algebraic charge balance equation as described in Section 7.6.3.

#### 7.4.2. Precipitation reactions

Dissolution and precipitation reactions affect pH. In the case of precipitation reactions, such as the formation of calcite and struvite deposits, equilibria are not fully established and rate processes may be used to model the change. The formation of calcium carbonate precipitate is particularly important in anaerobic reactors. Calcium carbonate occurs in different polymorphic forms which, in order of increasing solubility, are calcite, aragonite, vaterite, hydrated and amorphous calcium carbonate. Calcite is the most stable structure, while amorphous calcium carbonate is the least stable. Table 4: gives the solubility product of calcium carbonate forms.

**Table 4:  $K_{sp}$  for calcium carbonate; Source: Thermodynamic database included with VMINTEQ (free downloadable thermodynamic equilibrium estimation software from CEAM, USEPA)**

	$-\log K_{sp}$
Calcite	8.48
Aragonite	8.34

Vaterite	7.91
Hydrated calcium carbonate	7.14
Amorphous calcium carbonate	

Amorphous calcium carbonate precipitates first in the reactor. The rate of precipitation is shown to be driven by concentration difference between solubility product and the ion-activity product in the bulk liquor<sup>51</sup>. It is also seen that the rate of growth of precipitate is inhibited by adsorbed substances such as phosphate and iron. A slow conversion of amorphous calcium carbonate to calcite takes place in the reactor and calcium deposits as hard cementation can fully choke reactors such as fixed film reactors. Hence we have additional components  $S_{ca}$ ,  $X_{CaCO_3}$ ,  $HPO_4^{2-}$  for the modelling of calcium precipitation. The rate of precipitation of amorphous calcium carbonate is modelled as a second order dependence on the supersaturation:

$$r_{CaCO_3} = k_{CaCO_3} \frac{1}{K_I + S_I} (\sqrt{IAP} - \sqrt{K_{sp}})^2$$

19

where

$k_{CaCO_3}$  is the crystal growth rate constant at zero inhibition (90 to 200 litre.  $mol^{-1}s^{-1}$ ) (reference 51).

$IAP = \{Ca^{2+}\}\{CO_3^{2-}\}$  is the ion activity parameter

$K_{sp}$  is the solubility product for amorphous calcium carbonate

$[S_i]$  = concentration of crystal growth inhibitor, here  $S_i = 1 \times 10^{-3}$  mM for inhibiting species  $[CaHPO_4]$

$K_i$  is the half saturation constant for the crystal growth inhibitor, which can be related to reciprocal of the Langmuir adsorption constant in the Langmuir monolayer adsorption model.

The inhibitor species is taken as  $CaHPO_4^0$  which is thought to deposit on the growing crystal and thereby hindering growth. Phosphate species in the reactor may be taken as  $HPO_4^{2-}$ , and  $PO_4^{3-}$ , neglecting the presence of  $H_2PO_4^-$  in view of pH range expected in anaerobic reactors.

If one desires to model the growth of calcite, additional equations for the conversion of amorphous calcium carbonate to calcite are required. Calcite will be another insoluble species in the reactor, besides amorphous  $CaCO_3$  and soluble  $Ca^{2+}$ . It is reported<sup>51</sup> that soluble  $Fe^{2+}$  inhibits calcite formation. Then one more component enters the material balance. One can easily see that the

number of components quickly increases as we try to bring in greater precision into the model.

Similarly, another hard mineral that precipitates in anaerobic reactors is struvite, which has the formula  $\text{MgNH}_4\text{PO}_4 \cdot 6\text{H}_2\text{O}$ . Struvite precipitation takes place at elevated pH. Under ideal conditions, struvite formation is completed in minutes and nearly in equilibrium. The kinetics of formation of struvite is not well elucidated, but there is little doubt that it does not reach equilibrium in the time scale of the hydraulic retention time of the reactor.

Other precipitation reaction of interest are the formation of insoluble metal sulphides as a result of sulphate reduction. Metal sulphides presumably can be modelled as equilibrium processes.

## 7.5. Parameter values

---

The choice of parameter values is an art considering the very large number of parameters that the model requires. But fortunately, most parameters fall within a narrow range of realistic values. It is also known that the model is not overly sensitive to these values.

For many microbial metabolic pathways, thermodynamic free energy considerations can be used to guess at yield values<sup>52,53</sup>. In general, only about 10% of the COD utilized is converted to biomass in anaerobic reactors. The yield coefficient matrix  $[Y_{ij}]$  is shown split into Table 5 to Table 8 for legible printing within the limited page size. The reaction stoichiometry can be recovered from  $[Y_{ij}]$  after automatic correction of C, N, and S balances.

While protozoa growth is not included in the model, LCFA degradation yields include a part as methane, to account for the observed action of methanogenic endosymbionts in protozoa in BFBR.

**Table 5. Yield coefficients (unshaded cells), empirical formula, initial values, ionisation constants for soluble components.**

Component-> formula	Glu	CH4	H2	HAc	HPr	Hbu	AA	HS
hydrolysis Protein	0	0	0	0	0	0	1	0
hydrolysis Lipid	0	0	0	0	0.063	0	0	0
hydrolysis CarbEasy	0.59	0	0	0	0	0	0	0
hydrolysis CarbsSlow	0.5	0	0	0	0	0	0	0
Growth Xprot	0	0	0	5	2	2	-10	0
Decay Xprot	0	0	0	0	0	0	0	0
Growth acetoXCH4 fast	0	9	0	-10	0	0	0	0
Decay acetoXCH4 fast	0	0	0	0	0	0	0	0
Growth acetoXCH4 slow	0	9	0	-10	0	0	0	0
Decay acetoXCH4 slow	0	0	0	0	0	0	0	0
Growth Xac:Hbu	0	1.8	3	4.2	0	-10	0	0
Decay Xac	0	0	0	0	0	0	0	0
Growth Xglu	-10	0	0	0	4	5	0	0
Decay Xglu	0	0	0	0	0	0	0	0
XAc: HPr growth	0	3.86	3	2.14	-10	0	0	0
LCFA degraders growth	0	5.4	4	9.6	0	0	0	0
LCFA degraders decay	0	0	0	0	0	0	0	0
XH2 growth	0	9	-10	0	0	0	0	0
XH2 decay	0	0	0	0	0	0	0	0
SRB growth	0	0	-10	0	0	0	0	9
SRB decay	0	0	0	0	0	0	0	0
CH4 stripping	0	-64	0	0	0	0	0	0
CO2 stripping	0	0	0	0	0	0	0	0
H2S stripping	0	0	0	0	0	0	0	-80
CO2 absorption	0	0	0	0	0	0	0	0
charge (z/gCOD or z/mol)	0	0	0	0.016	0.009	0.006	0	0.0125
plus (1=+, 0= -)	0	0	0	0	0	0	0	0
K (10^-pK) or Khgas	0	0	0	5E-05	6E-05	4E-05	0	1.3E-07
filter efficiency fe	0	0	0	0	0	0	0	0
Cinitial ( Initial values)	0.045	0	0	0.045	0.045	0.04	0	0.001

**Table 6. Yield coefficients (unshaded cells), empirical formula, initial values for suspended particulate components.**

Component-> formula	XAc	Xglu	XCH4f	XCH4s	XH2	XLcFA	Xprot	XSRB	Prot	Lip	CarbE	Carbs	LCFA	Inert
hydrolysis Protein	0	0	0	0	0	0	0	0	-1	0	0	0	0	0
hydrolysis Lipid	0.007	0	0	0	0	0	0	0	0	-1	0	0	0.93	0
hydrolysis CarbE	0	0	0	0	0	0	0	0	0	0	-1	0	0	0.41
hydrolysis Carbs	0	0	0	0	0	0	0	0	0	0	0	-1	0	0.5
Growth Xprot	0	0	0	0	0	0	1	0	0	0	0	0	0	0
Decay Xprot	0	0	0	0	0	0	-1	0	0.4	0.32	0	0.08	0	0.2
Growth acetoXCH4f	0	0	1	0	0	0	0	0	0	0	0	0	0	0
Decay aceto-XCH4f	0	0	-1	0	0	0	0	0	0.4	0.32	0	0.08	0	0.2
Growth acetoXCH4s	0	0	0	1	0	0	0	0	0	0	0	0	0	0
Decay aceto-XCH4s	0	0	0	-1	0	0	0	0	0.4	0.32	0	0.08	0	0.2
Growth Xac on Hbu	1	0	0	0	0	0	0	0	0	0	0	0	0	0
Decay Xac	-1	0	0	0	0	0	0	0	0.4	0.32	0	0.08	0	0.2
Growth Xglu	0	1	0	0	0	0	0	0	0	0	0	0	0	0
Decay Xglu	0	-1	0	0	0	0	0	0	0.4	0.32	0	0.08	0	0.2
Growth XAc on HPr	1	0	0	0	0	0	0	0	0	0	0	0	0	0
LCFA degraders growth	0	0	0	0	0	1	0	0	0	0	0	0	-20	0
LCFA degraders decay	0	0	0	0	0	-1	0	0	0.4	0.32	0	0.08	0	0.2
XH2 growth	0	0	0	0	1	0	0	0	0	0	0	0	0	0
XH2 decay	0	0	0	0	-1	0	0	0	0.4	0.32	0	0.08	0	0.2
SRB growth	0	0	0	0	0	0	0	1	0	0	0	0	0	0
SRB decay	0	0	0	0	0	0	0	-1	0.4	0.32	0	0.08	0	0.2
CH4 stripping	0	0	0	0	0	0	0	0	0	0	0	0	0	0
CO2 stripping	0	0	0	0	0	0	0	0	0	0	0	0	0	0
H2S stripping	0	0	0	0	0	0	0	0	0	0	0	0	0	0
CO2 absorption	0	0	0	0	0	0	0	0	0	0	0	0	0	0
Charge (z/gCOD or z/mol)	0	0	0	0	0	0	0	0	0	0	0	0	9E-04	0
plus (1=+, 0= -)	0	0	0	0	0	0	0	0	0	0	0	0	0	0
K (10^-pK) or Khgas	0	0	0	0	0	0	0	0	0	0	0	0	5E-06	0
filter efficiency fe	0.98	0.98	0.98	0.99	0.98	0.98	0.98	0.98	0.95	0.95	0.95	0.95	0.95	0.95
Cinitial	0.03	0.03	0.03	0.03	0.03	0.03	0.03	0.01	0.04	0.04	0.13	0.008	0.07	0.04

**Table 7. Yield coefficients (unshaded cells), ionisation constants and initial values for inorganic components.**

Component-> formula	NH3 gmol/l	IC gmol/l	Alk eq/l	SO4 gmol/l
C	0	1	0	0
H	3	0	0	0
O	0	2	0	4
N	1	0	0	0
S	0	0	0	1
hydrolysis Protein	0	0	0	0
hydrolysis Lipid	0	0	0	0
hydrolysis CarbE	0	0	0	0
hydrolysis Carbs	0	0	0	0
Growth Xprot	0	0	0	0
Decay Xprot	0	0	0	0
Growth acetoXCH4f	0	0.140625	0	0
Decay aceto-XCH4f	0	0	0	0
Growth acetoXCH4s	0	0.140625	0	0
Decay aceto-XCH4s	0	0	0	0
Growth Xac on Hbu	0	-0.034375	0	0
Decay Xac	0	0	0	0
Growth Xglu	0	0.049375	0	0
Decay Xglu	0	0	0	0
Growth XAC on HPr	0	0.01625	0	0
LCFA degraders growth	0	-0.1	0	0
LCFA degraders decay	0	0	0	0
XH2 growth	0	0	0	0
XH2 decay	0	0	0	0
SRB growth	0	0	0	0
SRB decay	0	0	0	0
CH4 stripping	0	0	0	0
CO2 stripping	0	-1	0	0
H2S stripping	0	0	0	0
CO2 absorption	0	0	0	0
charge (z/gCOD or z/mol)	1	1	1	0
plus (1=+, 0= -)	1	0	1	0
K (10^-pK) or Khgas	5.012E-10	5.012E-07	0	0
filter efficiency fe	0	0	0	0
Cinitial	0.001	0.0037	0.0034	0.001

**Table 8. Yield coefficients in moles/gCOD converted for gas components (unshaded cells); the Henry's constant (K<sub>Hgas</sub>) is in (mol/l)/atm.**

Component-> formula	C	H	O	N	S	PCO2	PCH4	PH2S
hydrolysis Protein						0	0	0
hydrolysis Lipid						0	0	0
hydrolysis CarbE						0	0	0
hydrolysis Carbs						0	0	0
Growth Xprot						0	0	0
Decay Xprot						0	0	0
Growth acetoXCH4f						0	0	0
Decay aceto-XCH4f						0	0	0
Growth acetoXCH4s						0	0	0
Decay aceto-XCH4s						0	0	0
Growth Xac on Hbu						0	0	0
Decay Xac						0	0	0
Growth Xglu						0	0	0
Decay Xglu						0	0	0
Growth XAc on HPr						0	0	0
LCFA degraders growth						0	0	0
LCFA degraders decay						0	0	0
XH2 growth						0	0	0
XH2 decay						0	0	0
SRB growth						0	0	0
SRB decay						0	0	0
CH4 stripping						0	1	0
CO2 stripping						1	0	0
H2S stripping						0	0	1
CO2 absorption						-1	0	0
charge (z/gCOD or z/mol)						0	0	0
plus (1=+, 0= -)						0	0	0
K (10 <sup>-pK</sup> ) or K <sub>Hgas</sub>						0.025	0.001	0.04
filter efficiency fe						0	0	0
Cinitial ( Initial values)						0.03	0	0

### 7.5.1. Rate expressions and kinetic constants

The formulation of appropriate rate expression that encapsulate our present state of knowledge about anaerobic digestion and our experience of the complex behaviour of an anaerobic reactor is part of anaerobic digestion modeller's art. The rate expressions used have been formulated intuitively for easy input of maximum rate and half-velocity (affinity) concentrations based on general understanding. For example, we know that methanogenic reactor fail when H<sub>2</sub>S reaches about 8%. Hence, the 50% inhibition by K<sub>i,H<sub>2</sub>S</sub> for acetoclastic methanogens is set as 0.04 atm corresponding 0.04% H<sub>2</sub>S concentration in gas phase. The initial case studies carried out were used to mildly tweak the parameters to mimic behaviour seen and expected. Siegfried\_2002<sup>55</sup> is main reference taken for rate parameters.

**Table 9. Rate expressions and parameter values for rate processes in the model. The variable names are explained in Table 10. The rate expressions are given in the statement format used in the computer programme. The units for maximum growth rate  $\mu$ , first order decay coefficient kd, and hydrolysis rate k and gas transfer coefficients KLa are in (d<sup>-1</sup>). Units of K<sub>s</sub> and Ki in gCOD/l unless otherwise specified. (CO<sub>2</sub> absorption process is not used in the cases modelled; it is provided for modelling BFBR reactors with gas recirculation automatic pH control – see section 5.6)**

Process	Rate expression	Parameter
hydrolysis Prot – proteolysis by enzymes secreted by amino acid degraders XProt; Contois model: rate is proportional to XProt at low XProt and proportional to Prot at low Protein concentration; hydrolysis is inhibited amino acid concentrations exceeding 0.1 gCOD/l.	$k * Prot * XProt / (Ks * XProt + Prot) * (Ki2 / (Ki2 + AA)) * pHinhib2;$	k = 4*fT(1) Ks = 0.5 Ki2 = .1
hydrolysis Lip –( lipid hydrolysis by enzymes secreted by LCFA degraders) (Contois model; rate proportional to Lip at high XLCFA concentration and proportional to XLCFA at high Lip concentration; Inhibited by LCFA and H <sub>2</sub> .	$k * Lip * (XLCFA / (Ks * XLCFA + Lip)) * (Ki2 / (Ki2 + LCFA)) * Ki3 / (Ki3 + H2) * pHinhib2$	k = 2.5*fT(1) Ks = .25 Ki2 = 0.5 Ki3 = .01
hydrolysis CarbE – easily degraded carbohydrates by enzymes secreted by acidogens represented by XGlu (Contois model; rate proportional to CarbE at high	$K * CarbE * (XGlu / (Ks * XGlu + CarbE)) * (Ki2 / (Ki2 + Glu)) * pHinhib2;$	k = 3*fT(1) ; Ks = 0.25 ; Ki2 = .1;  % calibration k=2 matches Moller 2004 <sup>54</sup> fig 4 test

XGlu concentration and proportional to XGlu at high CarbE concentration;

hydrolysis CarbS – hydrolysis of slow degraded celluloses – similar to easily degraded carbohydrates except for rate constant	$k * CarbS * (XGlu / (Ks * XGlu + CarbS)) * (Ki2 / (Ki2 + Glu)) * pHinhib2$	$k = 0.2 * fT(1)$ $Ks = 0.5$ $Ki2 = .1;$
Growth Xprot – amino acid degraders inhibited by total ammonia	$\mu * XProt * (AA / (Ks + AA)) * fNH3 * pHinhib1$	$\mu = 5.0 * fT(5)$ $Ks = .128 * fT(5)$
Decay Xprot	<b>kd* XProt</b>	<b>kd = 0.02</b>
Growth XCH4f – fast growth acetoclastic methanogens, growth limited by acetate, total ammonia, inhibited by un-ionized NH <sub>3</sub> and H <sub>2</sub> S	$\mu * XCH4f * (HAc / (Ks + HAc)) * fNH3 * pHinhib3 / (1 + freeNH3 * 14 / Ki) / (1 + (PH2S / KiPH2S))$	$\mu = .7 * fT(5)$ $Ks = .3 * fT(7)$ $Ki (mgN/l) = 25e-3 * fT(6)$ $KiPH2S (atm) = 0.04$
Decay XCH4f	<b>kd* XCH4f</b>	<b>kd = 0.02</b>
Growth XCH4 slow – slow growth acetoclastic methanogens	$\mu * XCH4s * (HAc / (Ks + HAc)) * fNH3 * pHinhib3 / (1 + freeNH3 * 14 / Ki) / (1 + (PH2S / KiPH2S))$	$\mu = .35 * fT(5)$ $Ks = .04 * fT(7)$ Other parameters as in Growth XCH4f
Decay XCH4s	<b>kd* XCH4s</b>	<b>kd = 0.02</b>
Growth Xac:Hbu – growth of acetogens on butyrate; inhibited by acetate; limited by total ammonia and butyrate	$\mu * XAc * (Hbu / (Ks + Hbu)) * (Ki / (Ki + HAc)) * fNH3 * pHinhib1$	$\mu = 0.68 * fT(5)$ $Ks = 0.05 * fT(5)$ $Ki = 1.5 * fT(5)$
Decay Xac	<b>kd* XAc</b>	<b>kd = 0.02</b>
Growth Xglu – growth of acidogenic bacteria on glucose or simple sugars	$\mu * XGlu * Glu / (Ks + Glu) * fNH3 * pHinhib2$	$\mu = 5.0 * fT(5)$ $Ks = 0.5 * fT(5)$ $Ki = .8 * fT(5)$
Decay Xglu	<b>kd* XGlu</b>	<b>kd = 0.02</b>
Growth XAc: HPr – growth of acetogens on propionate; inhibited by butyrate, acetate and hydrogen	$\mu * XAc * (HPr / (Ks + HPr)) * (Ki / (Ki + Hbu)) * (Ki2 / (Ki2 + HAc)) * fNH3 * pHinhib1 * Ki3 / (Ki3 + H2)$	$\mu = 0.54 * fT(5)$ $Ks = 0.02 * fT(7)$ $Ki = 2 * fT(5)$ $Ki2 = 1.5 * fT(5)$ $Ki3 = 16e-4 * fT(6)$
LCFA degraders growth; limited by ratio of LCFA/XLCFA; inhibited by H <sub>2</sub> , acetate; (note that LCFA degradation is not inhibited by H <sub>2</sub> as much as propionate degradation)	$\mu * XLCFA * (LCFA / (Ks * XLCFA + LCFA)) * Ki / (Ki + HAc) * fNH3 * pHinhib1 * Ki2 / (Ki2 + H2)$	$\mu = 0.6 * fT(5)$ $Ks = 0.5 * fT(2);$ $Ki = 1.5 * fT(5);$ $Ki2 = 16e-3 * fT(6)$

LCFA degraders decay	kd* XLCFA	kd = 0.02
XH2 growth; inhibited by H <sub>2</sub> S gas pressure	$\mu * H_2 * \frac{XH_2}{(K_s + H_2) * (1 + (PH_2S/K_iPH_2S))};$	$\mu = 2.0 * fT(5)$ $K_s = 0.001 * fT(6)$  % calibration $\mu = 2, K_s = .001$ as per Siegrist 2002 <sup>55</sup>
XH2 decay	kd* XH2	kd = 0.02
SRB growth; limited by availability of H <sub>2</sub> and sulphate	$\mu * XSRB * \frac{H_2}{(K_{s1} + H_2)} * \frac{SO_4}{(K_{s2} + SO_4)}$	$\mu = 3.0 * fT(5)$ $K_{s1} = 0.0005 * fT(6)$ $K_{s2} = 1e-5;$ % $K_{s2} = 1e-5M$ $SO_4$
SRB decay	kd* XSRB	kd = 0.02
CH4 stripping	$KLa * \frac{(CH_4/64 - PCH_4 * P/KH)}$	$KLa = 40;$ Overall vol.gas tr coeff (1/d) units $KH = 800;$ Henry's constant as atm / (mol/l)
CO2 stripping	$KLa * \frac{(\alpha_{CO_2} * IC - PCO_2 * P/KH)}$  where $\alpha_{CO_2}$ is the fraction of inorganic carbon as un-ionised CO <sub>2</sub> = $1 - \frac{1.585e-6}{(1.585e-6 + 10^{-pH})};$	$KLa = 40$ $KH = 40$ $KH$ is in atm/(mol/l)
H2S stripping	$KLa * \frac{(\alpha_{H_2S} * H_2S/80 - PH_2S * P/KH)}$  where $\alpha_{H_2S}$ is unionised fraction of sulphide = $1 / (1 + 10^{(pH-6.9)});$	$KLa = 40;$ $KH = 20;$
CO2 absorption	$pH < 6.8;$ $rCO_2abs = Q_{gascir} * PCO_2$ $6.8 < pH < 7.5;$ $rCO_2abs = Q_{gascir} * (PCO_2) * \text{linear interpolation of pH}$ $pH > 7.5 \quad rCO_2abs = 0$	

## 7.6. Model implementation

---

### 7.6.1. MATLAB programming language

---

The model was implemented using the MATLAB programming language. MATLAB is an interpreted language and therefore debugging is simplified. ADM1 is usually implemented with higher level software using graphical interfaces (eg. SIMULINK), thus avoiding code-writing. But in this thesis, the model is programmed using only MATLAB primitives, giving greater flexibility in programming and speed, at the cost of user friendliness.

The MATLAB is a vector oriented programme language i.e., each variable is automatically taken to be a vector, and common vector operations such as vector addition, matrix multiplication, transpose etc., are defined at primitive level. MATLAB also provides a large number of built-in subroutines to solve several types of mathematical problems. Several subroutines are available for solution of systems of ordinary differential equations and graphing of results. The vector nature of the variables allows generation of compact and legible code and fast computation.

The model is a set of first order ordinary differential equations representing material balances and an algebraic equation (polynomial) representing charge balance. It is an explicit initial value ODE problem of the form:

$$y' = f(y, t)$$

$$y(t_0) = y_0$$

where

$y$  is a dependent variable vector of a single independent variable  $t$ ,

i.e.,  $y = \{y_1, y_2, \dots\}$ , each  $y_i$  being a function of  $t$

$y'$  is a vector denoting the  $dy/dt$

$y_0$  is given data at  $t_0$  (initial value)

If the function  $f(y,t)$  is sufficiently smooth, the initial value problem has only one solution. In our case the function is sufficiently smooth when using Eqn 6 for rate expressions but could be non-smooth (discontinuity in derivatives) if using Eqn 7.

### 7.6.1.1. *Stiff ODEs*

---

The model equations are a set of ordinary differential equations with widely varying rates. In mathematics, the set of equations is termed stiff. It refers to time dependent systems where the dependent variables have widely different time scales, or where the solution has regions of slow evolution in time and spurts of rapid change. When solving stiff differential equations, the solutions do not converge unless time steps are chosen very carefully. A change is termed rapid, if the time scale of the change is very short compared with the time scale of integration. For instance, in anaerobic digestion, the time scale for the acid-base reaction, the formation of carbon dioxide from bicarbonate is very short, as compared with bacterial growth or enzymatic hydrolysis. Hence modelling carbon dioxide formation from bicarbonate as a rate process rather than as an equilibrium ratio could make convergence very slow or impossible for some numerical solvers. The use of stiff ODE solvers (eg. ODE23s of MATLAB) can, to an extent, speed up the solution. However, it is observed that it is best to formulate the problem in such a way as to reduce stiffness as far as possible. The formulation of acid-base reactions as equilibria instead of forward and reverse rate processes reduces the stiffness of the model considerably.

Another source of unmatched time scale is the hydrogen gas formation and conversion. The solubility of hydrogen is very low (few mg/l). Hence the total pool of hydrogen gas in a reactor is of the order of a few mg per litre of reactor. On the other hand, as much as 50% of the COD converted to methane may go through hydrogen as an intermediate product. COD turnover in the range of a few grams per litre per day. In other words, the flow of hydrogen in the process is of the order of 1 g COD/l/d. Hence the retention time of hydrogen is of the order of  $10^{-3}$  d, while biological processes have time constants of  $10^{-1}$  day. This is another source of stiffness.

The MATLAB ODE solver ODE23s for stiff differential equations was used in problems with rapidly varying hydraulic and organic loads. Such instances occur when sharp peak loads such as on a small sewage treatment plants. Under normal loads, steady or slow varying as in start-up, the ODE45 solver is able to converge to solution more rapidly than ODE23s.

### 7.6.2. Data input interface

---

The BFBR model, besides being an exercise in generating insight into the BFBR processes, can be a useful tool in process design. In order to enhance utility, the following features were incorporated in the model implementation.

- the capability to handle wide range of situations with varying inflow, outflow and varying concentrations.
- The BFBR filters can have varying filter efficiency in retaining various components.
- The ability to estimate inputs which are may not be available explicitly. For eg., feed alkalinity is a model input but is not an usually available effluent characteristic. It can be estimated from feed pH and compositions.
- the flexibility to add components and new processes without excessive re-coding.
- the data input interface was clean and easily understood.

The data for the model is entered through a Excel worksheet, which is a user-friendly data input interface. The worksheet reading capability of MATLAB is used to read the data into the code. The following data are required for the model are input through Excel worksheets

1. components are classified as soluble, insoluble, soluble-inorganics, gas. The component names are entered as columns in the worksheet.
2. Under each component, the following data is given in rows empirical formula for each component in terms of C,H,O,N,S; charge of each component as 0,+1,-1, the ionisation constant pK value or  $-\log(K_H)$   $K_H$  is the Henry's law constant, the filter efficiency for the component  $fe$  (for soluble components,  $fe=0$ ), and the initial value.
3. The processes are entered as rows and under each component the Yield coefficient for the process is entered.

On execution, the model checks the given data for material balance consistency and makes automatic adjustments as described below.

### 7.6.2.1. COD balance check.

---

The sum of yield coefficient matrix rows for all soluble and insoluble components is calculated. It should be zero for all processes except gas transfer of methane, which should give -64gCOD/mol. The calculation of theoretical COD requires careful attention, in order to satisfy COD balances. In particular, the following points, usually neglected, need to be considered to avoid errors in COD balances.

The theoretical COD of the organic compounds containing N can be calculated as follows. Since nitrate is the highest oxidation state of N in the biological environment, COD of nitrate should be 0 g/mol-N and therefore the COD of organic nitrogen is assigned  $3 \times 16 = 48$  g/mol-N. However, the anaerobic mineralisation of organic nitrogen produces  $\text{NH}_3$  and ammonia is not oxidized in the dichromate test procedure for the determination of COD. Hence, for the purpose of modelling, we can, without loss of generality, assign COD of  $\text{NH}_3$  as zero and therefore N will be -24 gCOD/molN. Since COD balance will be satisfied independent of the yield of ammonia, ammonia yield of each process can be independently adjusted to satisfy nitrogen balance. Nitrate is not a component in the model. If denitrifying processes are also added to the model, then nitrate should be assigned 0 gCOD/mol-N.

The COD of sulphur containing compounds is calculated theoretically by assigning sulphate 0 gCOD/mol and hence S is 64 gCOD/mol. Sulphur containing compounds are reduced to  $\text{H}_2\text{S}$ . In the anaerobic model also, COD of  $\text{SO}_4$  is assigned zero and hence organic S has COD 64 gCOD/mol-S. Sulphide is oxidized by dichromate, and therefore the COD of  $\text{H}_2\text{S}$  should be calculated from the conversion  $\text{H}_2\text{S} + 2\text{O}_2 = \text{H}_2\text{SO}_4$ . But during the experimental determination of sulphide containing samples,  $\text{H}_2\text{S}$  escapes during acidification and hence experimental value will be lower than theoretical value. In model implementations without  $\text{SO}_4$  and  $\text{H}_2\text{S}$  as components, S is assigned -16 gCOD/mol-S. This trick implies stoichiometric production of  $\text{H}_2\text{S}$ , without affecting COD balances.

#### 7.6.2.2. Carbon balance

---

The program removes inconsistencies in carbon and other elemental balances. The yield of inorganic carbon (bicarbonate) for each process is calculated so that the total carbon balance is established. The yield of inorganic carbon can be adjusted independent of COD, N, S balances.

#### 7.6.2.3. Nitrogen balance

---

The yield matrix data inconsistency in nitrogen balance is removed by the program. Nitrogen balance is established for each process by adjusting the yield of ammonia. Adjusting the yield of ammonia does not change COD, C or S balances of the process because of the trick assigning  $N = -24 \text{ gCOD/mol-N}$ .

#### 7.6.2.4. Sulphur balance

---

The yield matrix data inconsistency with regard to sulphur balance is removed by the program. Sulphur balance is obtained by adjusting the yield of sulphate in each process. Adjusting the yield of sulphate does not change the COD, N or C balances. The yield of sulphate is unreal as sulphate is not a product of anaerobic dissimilation of sulphur containing organic compounds. The mineralized products are sulphur containing simple organic compounds such as dimethyl sulphide and methyl mercaptan that are finally converted to  $\text{H}_2\text{S}$ . It would be more realistic to specify  $\text{H}_2\text{S}$  yield directly in the model for sulphur containing organic compounds. The model representation produces sulphate which undergoes reduction to  $\text{H}_2\text{S}$  by the action of SRB. Hence the model would overestimate SRB growth, although the error introduced is not significant because the quantity of organic sulphur entering the system is small compared to the quantity of mineral sulphates. If SRB and  $\text{H}_2\text{S}$  are not components in the model, it is assumed that all org-S is converted to  $\text{H}_2\text{S}$ . In this case, in order to satisfy COD balance, organic sulphur is assigned a COD value - 16 g/molS.

#### 7.6.3. pH calculation

---

A trial and error method is required for the solution of differential-algebraic equations. A trial solution of the algebraic equation  $f([\text{H}^+]) = \sum_i z_i \alpha_i C_i$  with given initial values of concentration gives the pH. Using this value the ODEs are

solved to get the trial concentration of various components at the next time step. The algebraic charge balance equation is solved again for pH. The procedure is repeated till the solution converges adequately.

The charge balance function  $f([H^+])$  is a non-linear function of  $[H^+]$ . There are several values where the function becomes zero, but the zero of the function corresponding to the real  $[H^+]$  is required to be determined. The MATLAB built-in function *fzero* is used to find the zero a function of one variable  $[H^+]$ . The *fzero* procedure finds a root within an interval where the function changes sign at the interval limits. We can reduce the guesswork needed to bracket the required root using of knowledge of the chemistry of the system. Functioning reactors to work in the pH range 6 to 8, where buffering is provided by the weak anions and their protonated forms. With this assumption, the charge-balance function can be shown to be monotonic increasing with  $[H^+]$  in this range. Hence, if  $f([H^+]) < 0$  at guess pH,  $f([H^+]*j)$ ,  $j=2,3,\dots$  is calculated till the function becomes positive to get a bracketing value. Similarly, if  $f([H^+]) < 0$  at the initial guess pH,  $f([H^+]/j)$ ,  $j=2,3,\dots$  is calculated till the function become negative to get the bracketing values.

#### 7.6.4. Output data presentation

---

Program execution may take several hours to complete depending on the variability in data. During execution, calculated concentration vector is displayed graphically, showing the evolution of the state of the reactor. The execution can be aborted with a software button control if the results are not converging or if the reactor gets upset. The iterations required at each time step to bracket the zero of the charge-balance function is also displayed. If the iterations required are large, it is sign that the system is runaway and needs to be aborted. If it is impossible to find a zero within the range of  $[H^+]$  tested, the system returns an error.

Data presentation after execution is crucial to evaluating not only the behaviour of the system, but also to verify whether the results are consistent. Evaluating the material balances, in particular, COD and TC balance, is a definite check on the model calculations. In an unsteady system, material input does not need to match material output instantaneously because of accumulation. In reactors where a steady state biomass composition is established, long term

averages input should match with long term average output. Long term cumulative input material quantity would be close to long term cumulative output material quantities. In reactors subject to periodic variations, such as daily load changes, input should equal output in moving-average material balances, where average is taken over intervals larger than the time period of load variations.

## 7.7. Simulations

---

The model parameters need to be adjusted to meet expected behaviour. The application of BFBR for sewage treatment was simulated in a series of runs designed to arrive at an acceptable parameter set. The main unknown parameter which affects reactor performance is the filtration efficiency,  $f_e$ . It cannot be measured *a priori*, because the filtration behaviour of sludge changes during operation. It is reported that sewage treatment UASB can be started by auto-inoculation and minimum HRT of 8 h is required for acceptable COD removal. Therefore BFBR should also be capable of auto-inoculation start-up and HRT less than 8 h. The filtration efficiency of various biomass and particulate substrates were adjusted in a series of runs to obtain the expected performance. Cases 1 to 4 were carried out to study auto-inoculation start-up of a sewage treatment BFBR. The load applied was not changed in Cases 1 to 4, but various parameters are adjusted to obtain effective treatment at HRT < 8h. In Case 1 to 3, the component filter efficiencies, both of particulate degradable solids as well as biomass were adjusted. In Case 4, the kinetic parameters of fat degradation are tweaked to reproduce observed scum accumulation and disappearance behaviour of BFBR.

In Case 5, the parameters were left unchanged and the dynamic behaviour of the BFBR under diurnal periodic variable loads was studied. This simulates the performance of a small sewage treatment plant.

In Case 6, the model is expanded to include growth of sulphate reducing bacteria. The filtration efficiencies and kinetic parameter were not changed.

In Case 7, the model is used to simulate performance of the experimental laboratory BFBR using synthetic milk effluent.

### 7.7.1. Simulation of sewage treatment

One of the potential applications of BFBR is in sewage treatment. The model was used to simulate BFBR operation with a complex wastewater composition that represents sewage.

**Table 10. Complex wastewater composition simulating sewage characteristics. The component names and corresponding MATLAB variable names used are given. All organic component are in gCOD/l, Alk, IC are in mol/l, PCH4 and PCO2 are in mole fractions. Black and greywater are combined in ratio of flow to derive the composite characteristics. Component-wise filter efficiency (fe) values used in Case 1 are shown.**

	Variable name	composite	blackwater	greywater	Filter efficiency (fe) Case 1
Glucose	Glu	0.05	0.05	0.045	0
Dissolved methane	CH4	0	0	0	0
Dissolved hydrogen	H2	0	0	0	0
Total acetate	HAc	0.045	0.01	0.044	0
Total propionate	HPr	0.045	0.01	0.044	0
Total butyrate	Hbu	0.05	0.01	0.049	0
Total amino acids	AA	0	0	0	0
Acetogen biomass	Xac	0.001	0.01	0.00	0
Glucose fermenting acidogens	XGlu				.95
Acetoclastic methanogens fast growth $\mu_{max}$ strategists	XCH4f	0.001	0.01	0.00	.95
Acetoclastic methanogens slow growth $K_s$ strategists	XCH4s	0.001	0.01	0.00	.95
Hydrogenotrophic methanogens	XH2	0.001	0.01	0.00	.95
LCFA $\beta$ -oxidizers	XLCFA	0.001	0.01	0.00	.95
Amino acid fermenters	Xprot	0.001	0.01	0.00	.95
Proteins not biomass	Prot	0.15	1	0.05	.95
Lipids not biomass	Lip	0.1	0.6	0.04	.95
Carbohydrates easily degradable (s)	CarbE	0.1	0.6	0.04	.95
Carbohydrates slow degradable (cellulose)	CarbS	0.008	0.08	0.00	.95
Long chain fatty acids	LCFA	0.1	0.3	0.07	.95
Organic inert materials	Inert	0.02	0.1	0.01	.95
Total ammonia nitrogen	NH3 mol/l	0.002	0.001	0.0019	0
Inorganic carbon	IC mol/l	0.0067	6.7E-03	6.7E-03	0

(HCO <sub>3</sub> <sup>-</sup> and CO <sub>2</sub> -l )					
Alkalinity meq/l	Alk	0.0055	6E-03	5.5E-03	0
CO <sub>2</sub> (g) mol fraction	PCO2	0.06	0.03	0.03	0
CH <sub>4</sub> (g) mol fraction	PCH4	0	0	0	0
	pH	7.2	7	7.2	
Total COD (g/l)	CODtot	0.675	2.83	0.392	
Soluble COD (g/l)	S	0.19	0.08	0.182	
Suspended COD (g/l)	X	0.485	2.75	0.21	
Quantity ratio (l/d)	Q	1000	100	900	

#### 7.7.1.1. Case 1. Start-up and steady load.

The first simulation was carried out for a BFBR reactor under steady hydraulic and organic load of composite sewage given in Table 10. It is a low strength sewage (675 mg-COD/l), as is common in developing countries. Sewage contains all kinds of micro-organisms including methanogens.

The simulation was used to test auto-inoculation start-up and the maximum loading possible before performance begins to deteriorate. The initial sludge in the reactor was not enriched methanogenic sludge containing biomass other than in raw sewage. The sewage used in simulation is assumed to contain 1 mg/l (as COD) of each of the groups of micro-organisms considered in the model. The total biomass in sewage is 7 mg-COD/l out of total COD of 675 mg/l. There is no quantitative mass data on microbial biomass in raw sewage in literature, the mass assumed is reasonable, considering that feces is largely composed of microbial biomass.

The load imposed on the reactor is shown in Figure 25. The sewage strength is constant and given in Table 10. The reactor active volume is taken as 1000 m<sup>3</sup> and gas holdup volume in reactor is 0.2 m<sup>3</sup>/m<sup>3</sup>. The simulation was carried for 200 d. It takes 5 minutes to complete the simulation on a Intel Core2-duo-T6750 CPU, 4GB, 32bit Windows Vista notebook PC using Matlab 7.01 with its ode23s stiff differential equation solver.

The minimum filter efficiency (fe) required for reactor auto-inoculation start-up was 95%. This efficiency includes separation by the mechanism of filtration and settling for separation of particulates and biomass from liquid. Since measured filter efficiency in filtration tests with bulking sludge were much less (Figure 4), it may be concluded that auto-inoculation is possible only if sludge in BFBR develops better filterability than bulking sludge. The observations

during long term experiments show that filterability improves dramatically as the sludge characteristics change.

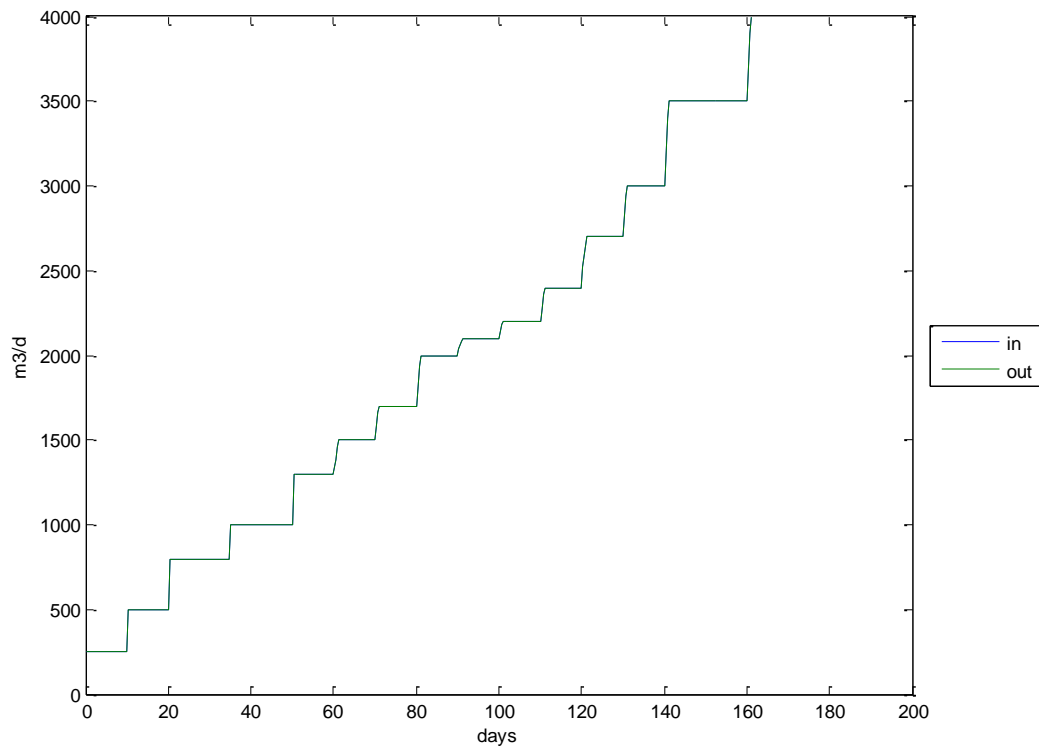


**Figure 25. Hydraulic load applied on reactor in simulation case 1 to 4. Inflow and outflow are equal and hence reactor liquor volume remains constant ( $1000\text{m}^3$ ). The composition of sewage is held constant.**

The soluble components in the effluent are shown in Figure 26. Soluble components in reactor effluent in simulation case 1. Note the increase in volatile fatty acids from day 70; ie., flow  $> 1500\text{ m}^3/\text{d}$  or HRT  $< 16\text{h}$ . Hence, at filter efficiency of 0.95, the BFBR cannot be operated at less than HRT 16h, without reduction in removal efficiency.

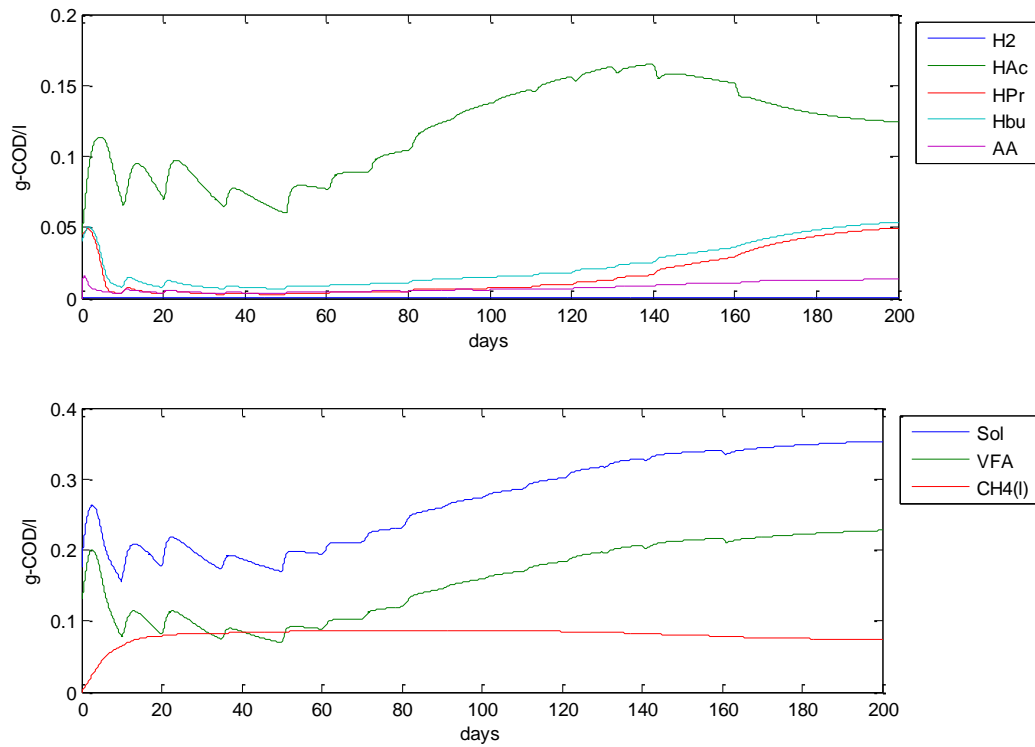


**Figure 26. Soluble components in reactor effluent in simulation case 1. Note the increase in volatile fatty acids from day 70; ie., flow > 1500 m<sup>3</sup>/d or HRT <16h.**

The solids in the reactor liquor are shown in Figure 27. At HRT > 16h, (before day 70), the MLSS contains mainly biomass and inert COD, and the concentration of particulate substrate COD (MLSS – biomass – inerts) is very small. The increase in soluble COD corresponds to decrease in biomass holdup from day 70. It is most interesting to note that from day 70, the concentration of suspended COD ie., proteins, lipids, carbohydrates, LCFA and inerts continues to increase with increased loading. At 95% fe, the retention of particulates is sufficient but the retention of biomass is not sufficient.

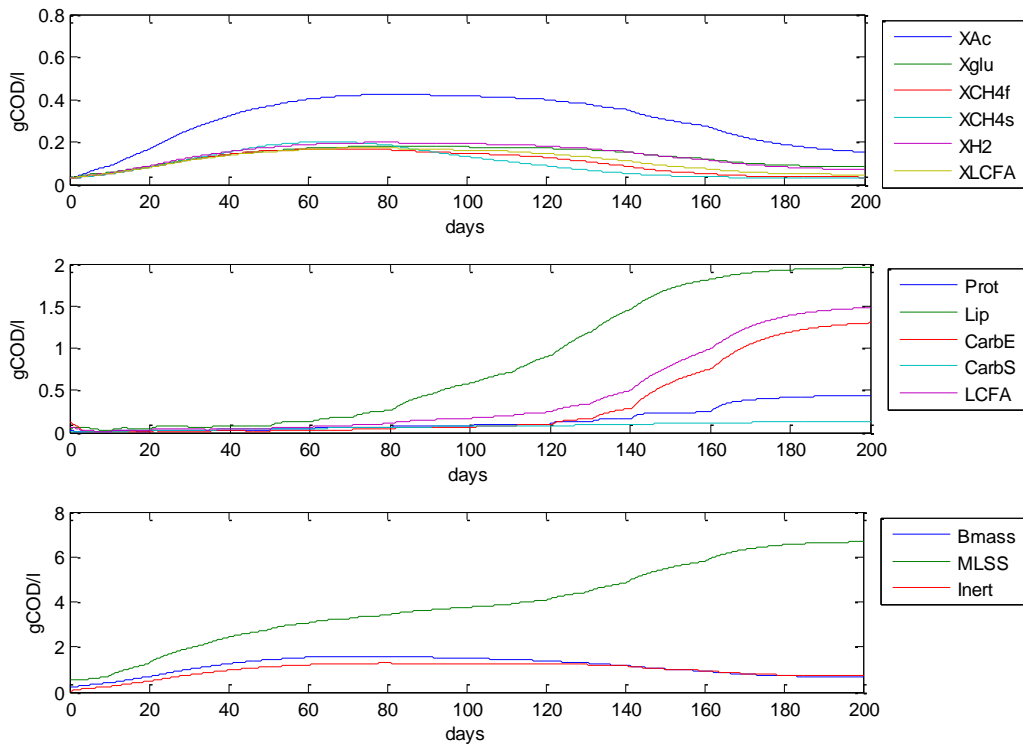


Figure 27. Solids concentration in mixed liquor for simulation case 1. MLSS refers to total solids in reactor liquor (biomass + particulates substrates).

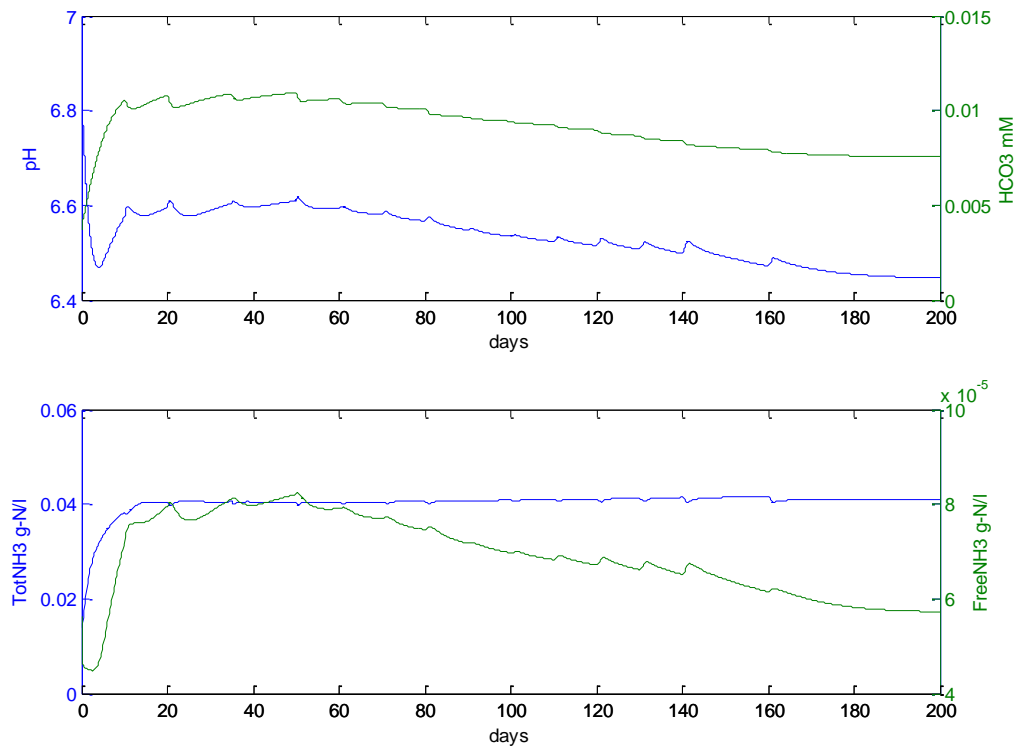
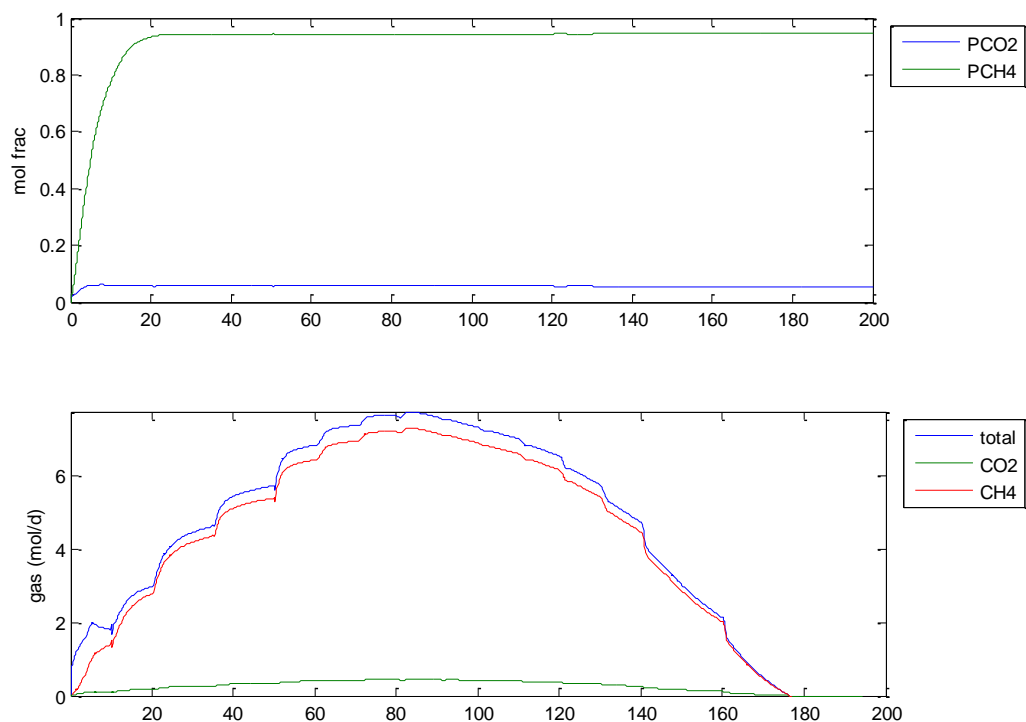


Figure 28. pH profile and ammonia concentration in reactor. The pH does not change substantially even when HRT <16h, (beyond day 70). The total ammonia concentration is steady, and nitrogen balance is satisfied.

Even when the reactor HRT < 16h, the overload condition do not cause acidification of the reactor (Figure 28).

The gas production and composition is shown in Figure 29. The maximum gas production is obtained around 70d (HRT 16h). Clearly the reactor fails at 180 d. The corresponding HRT is 6h. During operation, the methane percentage in the gas is very high(95%). This is because of the relatively high alkalinity of the sewage, as a result of which carbon dioxide produced exits the system as dissolved bicarbonate.



**Figure 29. Case 1. Gas production and composition.**

The COD and TC balances are checked (Figure 30) to determine whether the consistency of results. The COD balance also shows that substantial amount of methane exits the system as dissolved methane. The TC balances are satisfied. This is a test of the accuracy of calculation of pH through charge balances. Every time there is a load increase,  $COD_{diff} = COD_{input} - COD_{output}$  shows a small positive peak. This difference is the accumulation of biomass in the reactor.

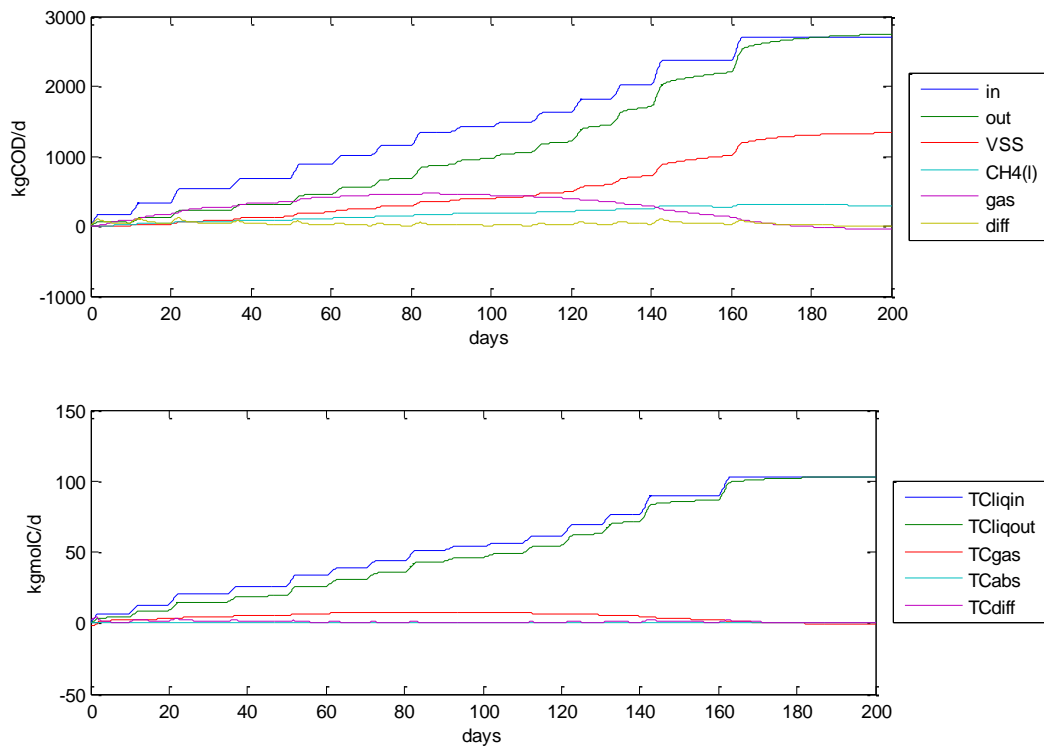


**Figure 30. COD and carbon balance for results of simulation case 1.**

Figure 31 summarizes the findings from previous results as the conversion of COD to methane. This includes methane as gas and as dissolved methane. It once again shows that deterioration of performance at HRT < 16h. At optimal performance, 60% of incoming sewage COD is mineralized to gas.

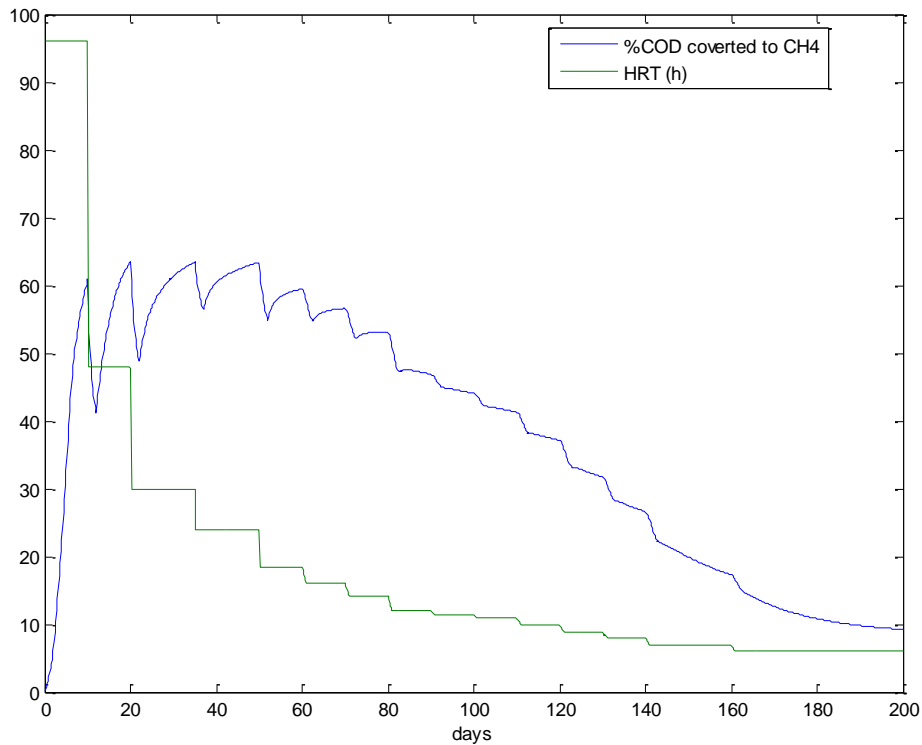


**Figure 31. COD mineralized, (converted to methane), in the reactor simulation case 1, and the corresponding hydraulic retention time (h).**

The simulation show that autoinoculation start-up is feasible but HRT cannot be lower than 16h because of washout of biomass.

#### *7.7.1.2. Case 2. Steady load and start-up; increased filter efficiency*

An analysis of Case 1, shows that biomass washout is the reason for process failure of the BFBR when HRT is below 16 h. The model was used to simulate BFBR operation when filter efficiency of biomass retention is increased to 0.98 while the filter efficiency for retention of particulate COD components was left unchanged from Case 1 ( 0.95).

Figure 31 shows that autoinoculation start-up is quickly established, but when HRT is decreased below 10 h, the VFA begin to increase. It is also seen that washout of slow growing acetoclastic methanogens XCH4s starts to occur at this hydraulic load. The proportion of particulate substrate COD (MLSS – Bmass – Inert) increases slowly after day 120. At day 200, the particulate substrate COD in reactor liquor is mainly lipids (0.7 gCOD/l) and LCFA (0.2 g/l).

Figure 32 shows that optimum mineralization occurs when HRT >10 h, and 65% of incoming COD is converted to methane. Even at HRT= 6 h, 50% conversion of incoming COD to methane is obtained.

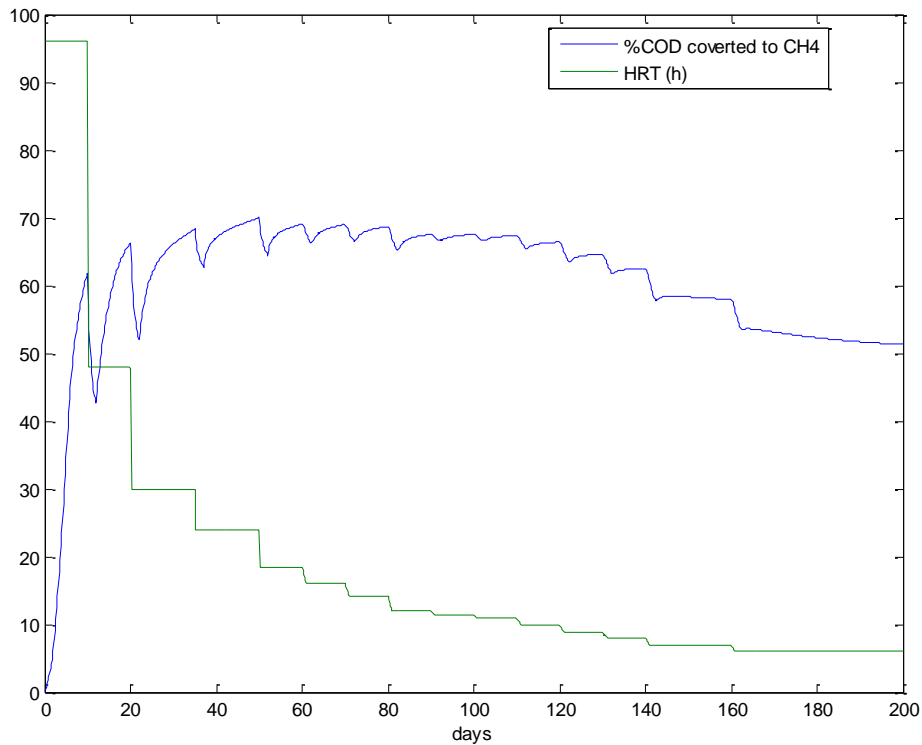


**Figure 32. Case 2: Mineralization of sewage COD (conversion to methane) and corresponding HRT in BFBR.**

On day 200, the biomass concentration in the reactor appears to be steady at 5 g-COD/l. However, the population is not at steady state and is still evolving, with a slow decline in population of slow growing acetoclastic methanogens (XCH<sub>4</sub>s).

In this simulation, filter efficiency of biomass is given as 0.98 and particulate COD as 0.95. The implication of variable filter efficiency needs to be examined in greater depth. Normal filter efficiency is dependent on particle size. The particle size of individual bacteria is obviously smaller than particulate COD in the wastewater. Hence, higher filter efficiency of bacterial biomass retention implies that biomass in the reactor has to undergo structural changes such as formation of flocs and granules leading to enhanced retention. In case 3, the concept population evolution is taken further and the consequences of enhanced retention of slow growing acetoclastic methanogens is examined.

### 7.7.1.3. Case 3. Steady load and start-up. Enhanced retention of methanogenic biomass

It has been observed that the BFBR biomass does undergo selection to floc formation and it shows up a decrease in filter pressure drop as the reactor sludge matures. It is clear that the physical filtration alone is not adequate to develop high activity sludge. The selection pressures imposed by washout in the BFBR, just as in UASB, lead to the formation of high methanogenic activity sludge. In Case 3, the filter efficiency for the retention of slow growing acetoclastic methanogens is increased to 0.99. All other components have the same filter efficiency as in Case 2.

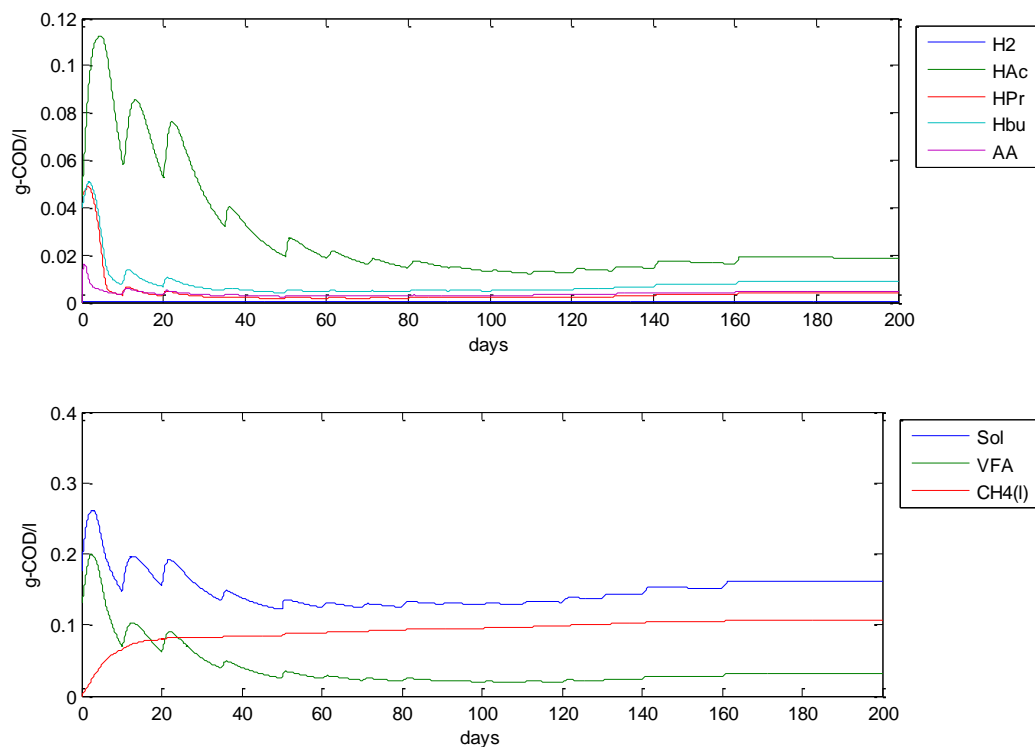


**Figure 33. Case 3. Soluble component concentration in BFBR liquor. Note that dissolved methane is the major component of dissolved COD, followed by acetate, butyrate and propionate.**

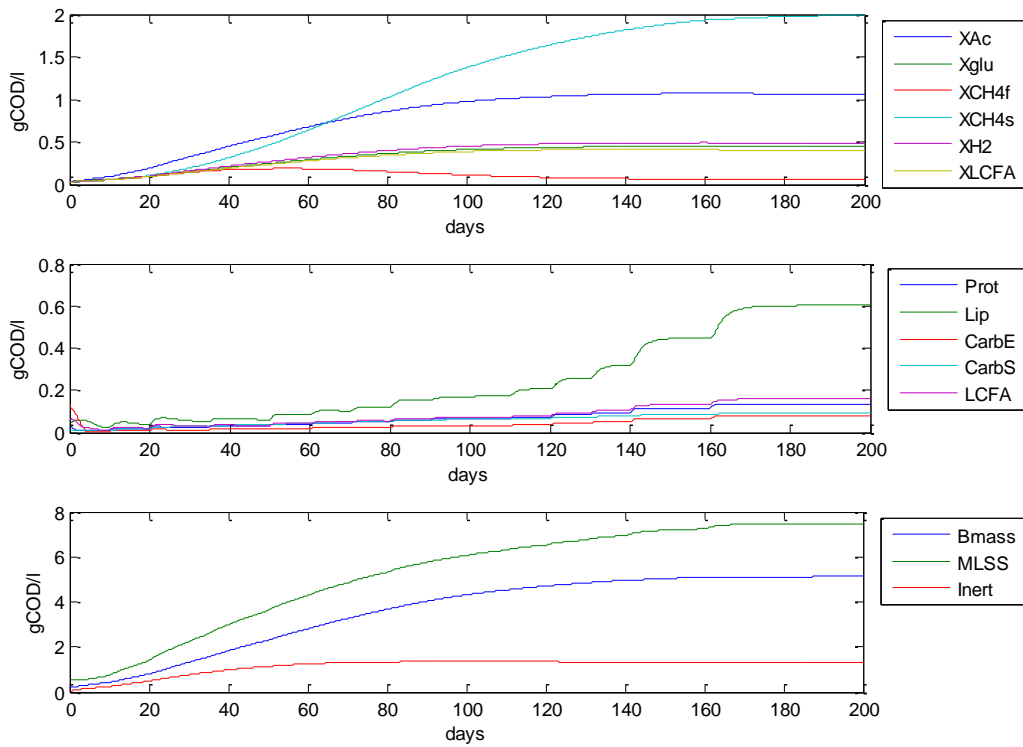


**Figure 34. Case 3. Particulate component concentration in BFBR liquor.**

Figure 34 shows that at filter efficiency 0.99 for slow growing methanogens, there is no increase in VFA even when HRT = 6 h. The solids in the liquor is mainly biomass and inerts and has negligible concentration of particulate COD substrates contained in raw sewage (Figure 34: MLSS – Bmass – Inert). At day 200, the particulate substrate COD in reactor mixed liquor is mainly lipids (0.6 gCOD/I) and LCFA (0.2 gCOD/I). This is at variance from qualitative observations of BFBR, which show that disappearance of scum and greater LCFA formation. Experiments show that lipids are retained very effectively in the reactor as scum. Observations also indicate that efficiency of enzymatic conversion of lipids improves with ageing. The enzymatic conversion rate constants were tweaked in Case 4 for better simulation.

As the load increases, the composition of sludge that evolves in the reactor is highly enriched in slow growing acetoclastic methanogens. Interestingly, the model shows a replacement of fast growth methanogens to slow growth methanogens in a period of 30 to 40 d. This result may be interpreted as the formation of ‘sarcina granules’ usually seen in healthy UASB reactors. The conversion of COD to methane is 65% at HRT 6h.

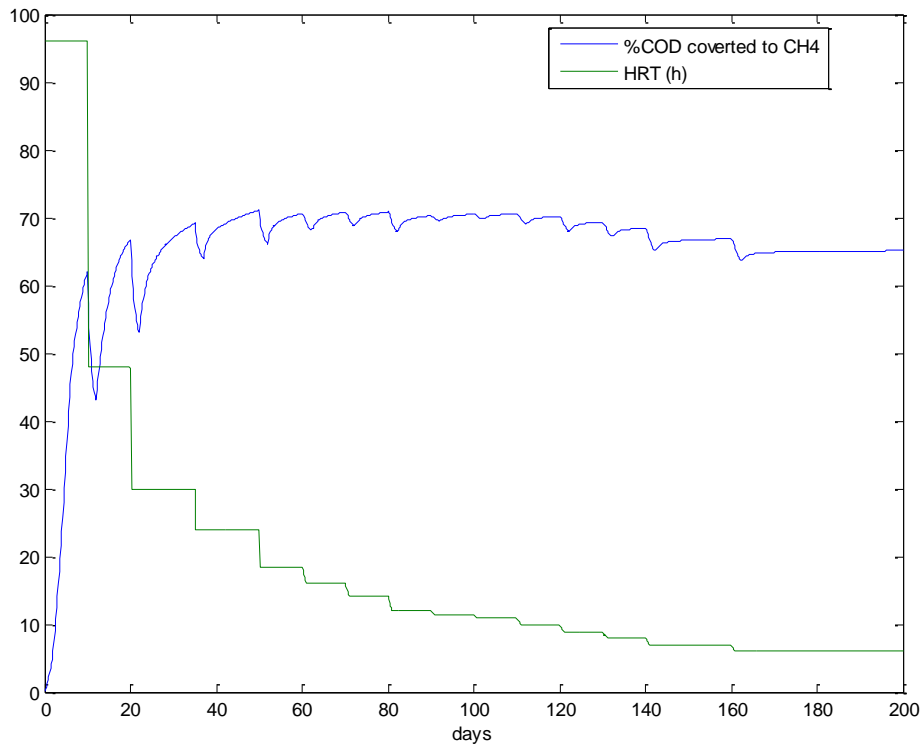


**Figure 35. Case 3: Conversion of sewage COD to methane in BFBR.**

While physical filtration alone cannot retain biomass (it requires the formation of flocs and granules), it plays an important role in retaining suspended solids in the wastewater. Hence, we may conclude that the role of the filter in the BFBR is primarily the retention of suspended solids. The simulation demonstrates the potential of the BFBR to treat low strength sewage. The provision of high efficiency retention system will improve the treatment efficiency by retaining particulate COD, while the formation of flocculant and granular sludge enables conversion to methane at low retention times. At steady and optimum conversion, the particulate substrate COD content in BFBR sludge is very low.

#### 7.7.1.4. Case 4. Steady load with improved fat degradation

The experimental observation of scum degradation as the BFBR ages can be simulated by changing kinetic constants of fat hydrolysis. The maximum rate constant is increased to  $2.5 \text{ d}^{-1}$  from Case 3 value of  $1.5 \text{ d}^{-1}$ . The Contois function inhibition constant remained unchanged at 0.25 ie., when the ratio XLCFA /Lipid  $> 0.25$ , the hydrolysis rate tends to be proportional to lipid concentration and when the ratio is  $< 0.25$ , the hydrolysis rate tends to be proportional to XLCFA

concentration. Hydrolysis of fat is inhibited by LCFA, and the 50% inhibition was increased from 0.1 g COD/l to 0.5 g COD/l.

The resultant reactor mixed liquor concentrations are given in Figure 36. Lipid accumulation (.15 gCOD/l) is much lower than in Case 3 (0.6 gCOD/l). Unlike Case 3, LCFA is greater than sludge lipid content. It matches the experimental observation of changes in nature of scum from hydrophobic to hydrophilic. All other performance parameters do not differ significantly from Case 3.

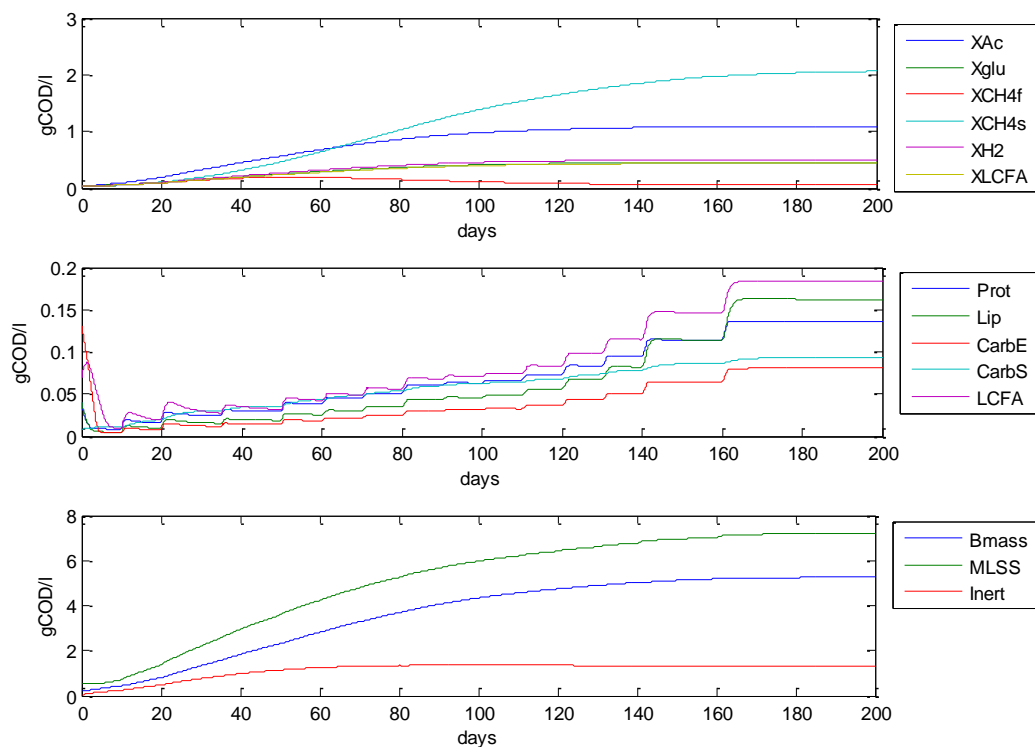


**Figure 36. Case 4: Solid component concentrations in BFBR liquor. The bottom figure gives the biomass and inert solids content in the total MLSS in the reactor. The degradable solids content in the MLSS is seen to be small compared with biomass.**

#### 7.7.1.5. Case 5. Diurnal periodic variable hydraulic loading

Normally sewage flow show diurnal variations with strong peak flow during morning and evening and near zero flow during night. The peaks are accentuated for small sewage treatment units such as for housing colonies. Large capacity flow equalization tanks are required in order to impose constant loads on biological treatment reactors. The equalization tanks need to be agitated in order to prevent settling, it can be source of odour and takes up

valuable land space. If equalization can be avoided, it would be a considerable benefit. The versatility of the model allows determination of the response of the BFBR to strongly fluctuating diurnal flow, as when the BFBR is applied for sewage treatment in housing colony.

Case 5, imposes diurnal variable loads on a BFBR operating as on Day 200 of Case 4, ie., HRT 6h and near steady state. The diurnal hydraulic variation is shown in Figure 37. The peak flow is 3 times the average flow. At peak flow, the HRT is 2hr.

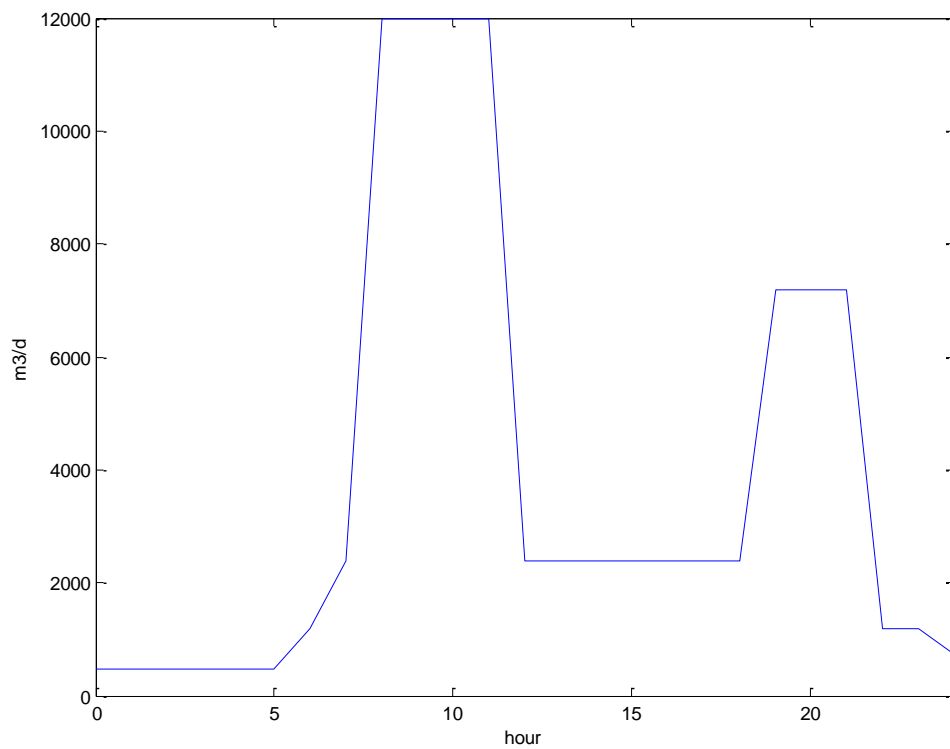


**Figure 37. Case 5: Sewage flow variation within each day (periodic variable hydraulic load).**

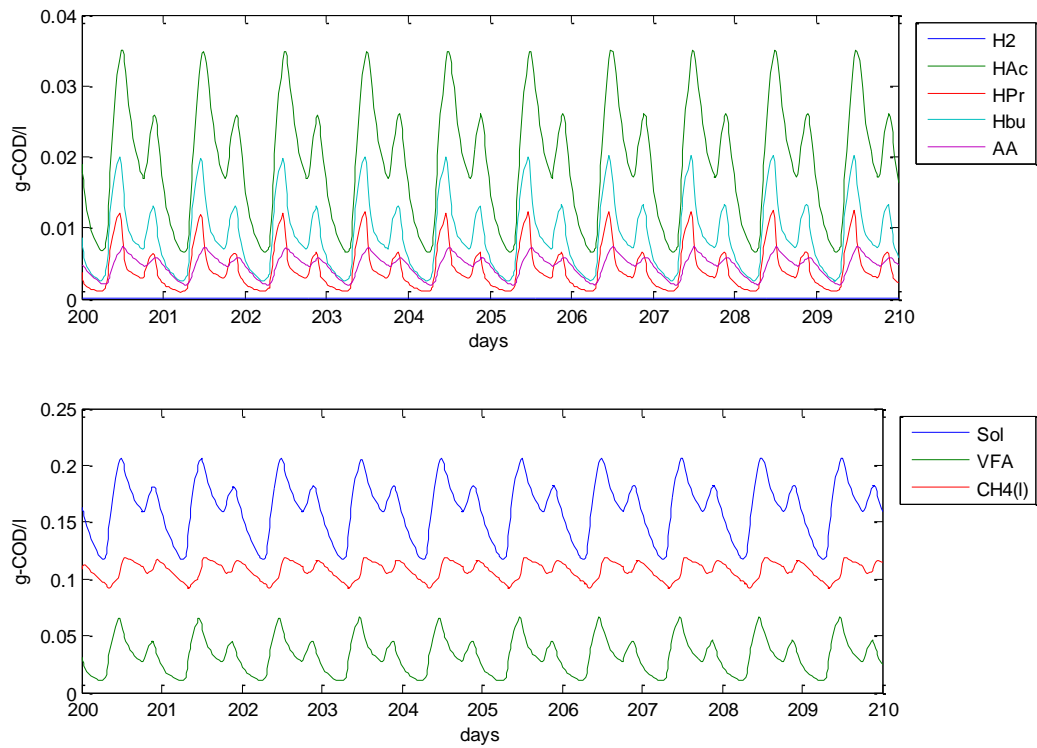


**Figure 38. Case 5. Variation in volatile fatty acids and soluble COD during diurnal periodic hydraulic load variations**

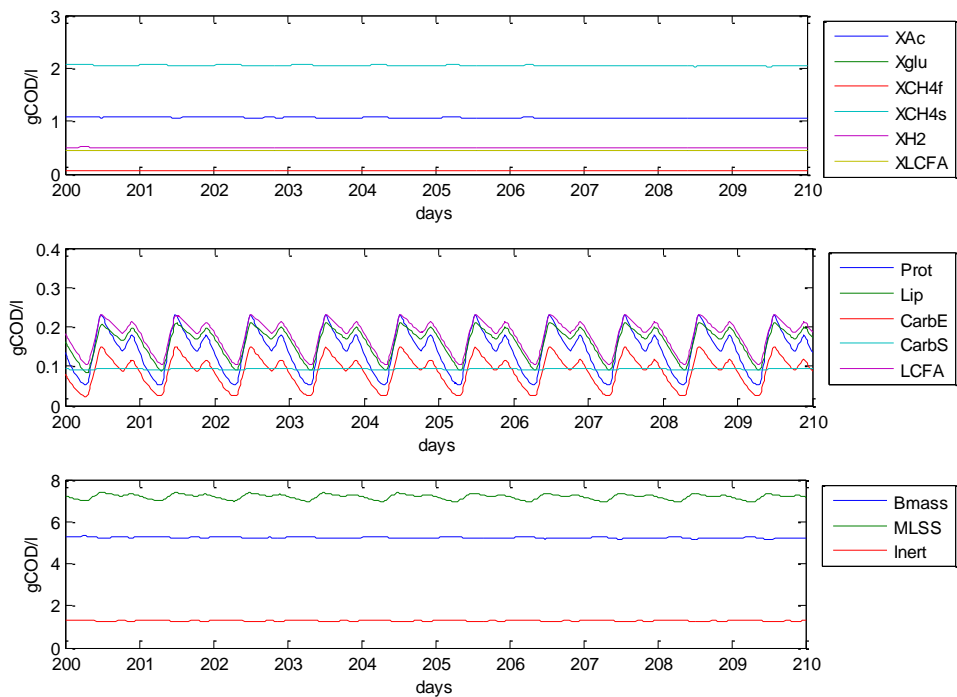


**Figure 39. Case 5. Variation in biomass components and particulate COD components because of periodic hydraulic load variations.**

Figure 38 and Figure 39 shows that the suspended COD in mixed liquor and hence in treated effluent ( $(1-f_e) \times \text{COD}$  in mixed liquor) varies only within narrow band (7 to 7.5 gCOD/l) even when loads fluctuate sharply. The soluble COD changes with load, but even at peak flow, the soluble COD (other than dissolved gas) in effluent does not exceed 60 mg/l.

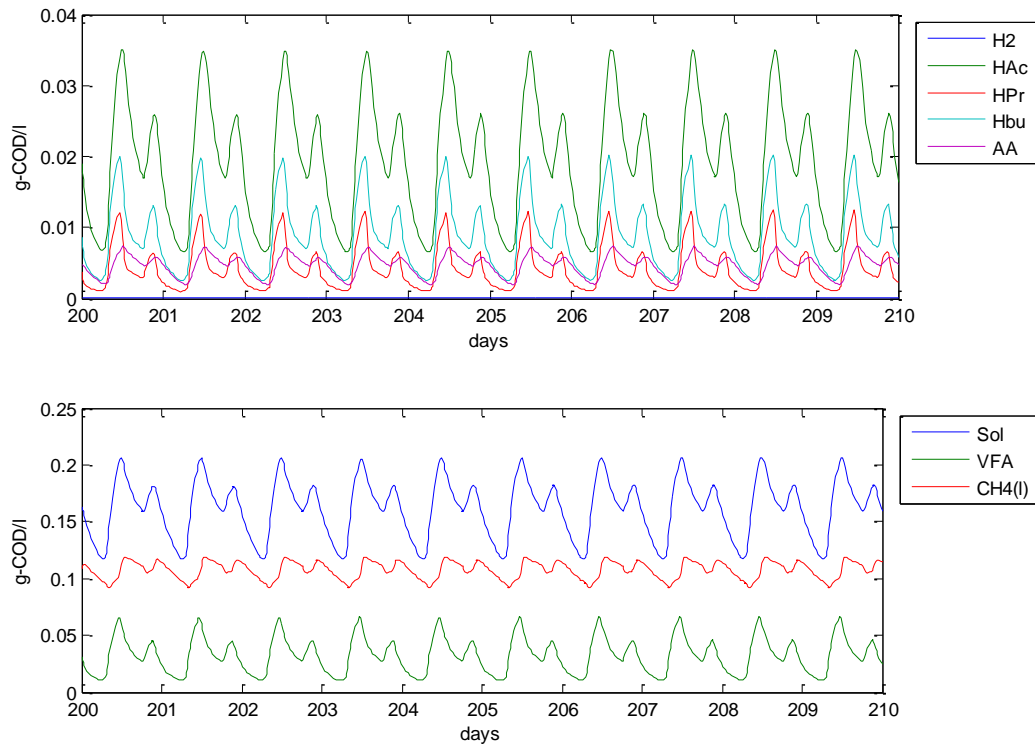


**Figure 38. Case 5. Variation in volatile fatty acids and soluble COD during diurnal periodic hydraulic load variations**

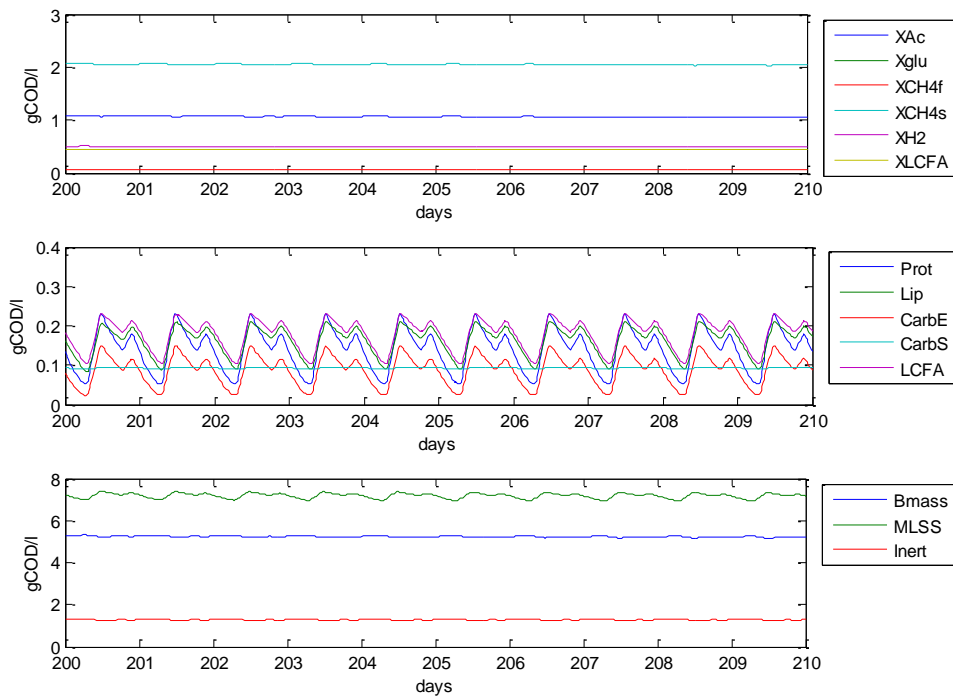


**Figure 39. Case 5. Variation in biomass components and particulate COD components because of periodic hydraulic load variations.**

Time averaged (1 hour) COD and TC balances for 1 day are shown in Figure 40. The difference between COD- in and COD-out is the accumulation of COD in the reactor. The conversion of COD to biogas after a lag period, and hence the peaks of gas production are offset from the flow peak. In fact, gas production is more during the night than during the day. The COD conversion to biogas (daily average) remains unchanged from steady flow.

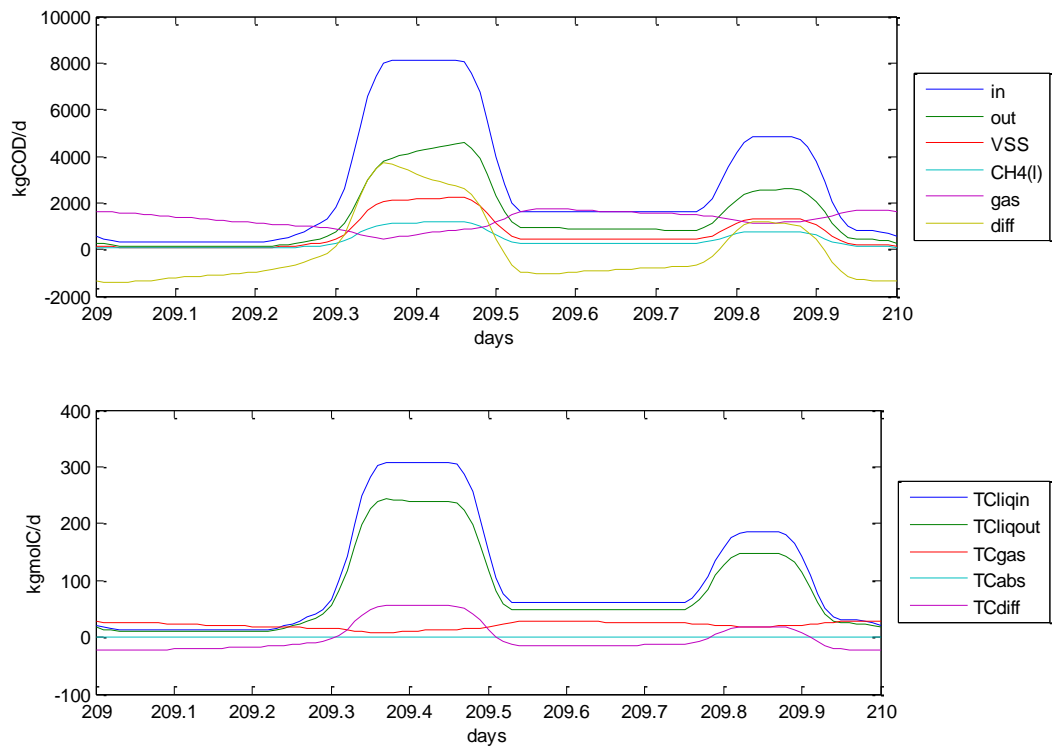


**Figure 40. Case 5, COD and TC balances (1 hour running average). The gas production peaks at night while loads peak during day.**

#### 7.7.1.6. Case 6: Sulphate reduction

In Case 6, sulphate reduction has been added to Case 4. The additional components are SRB biomass, sulphide, sulphate, and hydrogen sulphide in gas. The additional processes are growth and decay of SRB and hydrogen sulphide gas transfer. The main modification is in the Excel data sheet, giving yield coefficients and other data. The MATLAB programme is modified only to the extent of incorporating the rate expression and verifying S balance. Reprogramming and debugging major changes in the model (3 new rate processes, 4 new components, 1 new material balance) requires only minimal effort and demonstrates the versatility of the simulation model.

The feed sewage contains 1 mM sulphate in addition to Case 4 load. SRB growth on hydrogen as energy source alone is modelled. Inhibition of methanogenic bacteria by un-ionised hydrogen sulphide is included in the model.

A subtle aspect in SRB growth is the generation of 2 moles of alkalinity per mol of sulphate reduced. Hence the yield of alkalinity should be corrected

accordingly. Thus alkalinity balance in the previous models (load alkalinity is equal to effluent alkalinity) is not valid in the SRB model.

The mineralization of COD (conversion to CH<sub>4</sub>, sulphide and inert) is 68% (Figure 46) - not significantly different from case without sulphate reduction (Case 4). The best mineralisation efficiency is obtained at 10 h HRT. Further reduction in HRT, decreases the efficiency of treatment. Nearly all of the incoming sulphate is converted to H<sub>2</sub>S and biogas contains 1.17% H<sub>2</sub>S. The composition of feed given in Case 6, has S input only through sulphate. S can enter the system also as organic sulphur. If protein in Case 6, is assumed to have the empirical formula CH<sub>2.03</sub>O<sub>0.6</sub>N<sub>0.3</sub>S<sub>0.05</sub>, the H<sub>2</sub>S content in biogas increases to 1.31%.

The SRB biomass in reactor (Figure 42) is small compared to mass of slow-growth methanogens, but much larger than mass of hydrogenotrophic methanogens. Acetoclastic methanogens are mildly inhibited by 1.17% H<sub>2</sub>S and it explains the larger residual acetate at day 200, 37 mg-COD/l in Case 6 (Figure 41), as compared with 18 mg-COD/l for Case 4 (without sulphate reduction).

The pH shows a very small increase in Case 6 (pH 6.73) with increasing load, as compared with Case 4 (pH 6.64). Figure 44 show a difference of 2 mM between total alkalinity in feed raw effluent and treated effluent. It matches the reduction of 1 mM sulphate in the feed, generating 2 mM alkalinity. It demonstrates the consistency of the model calculations of alkalinity and pH.

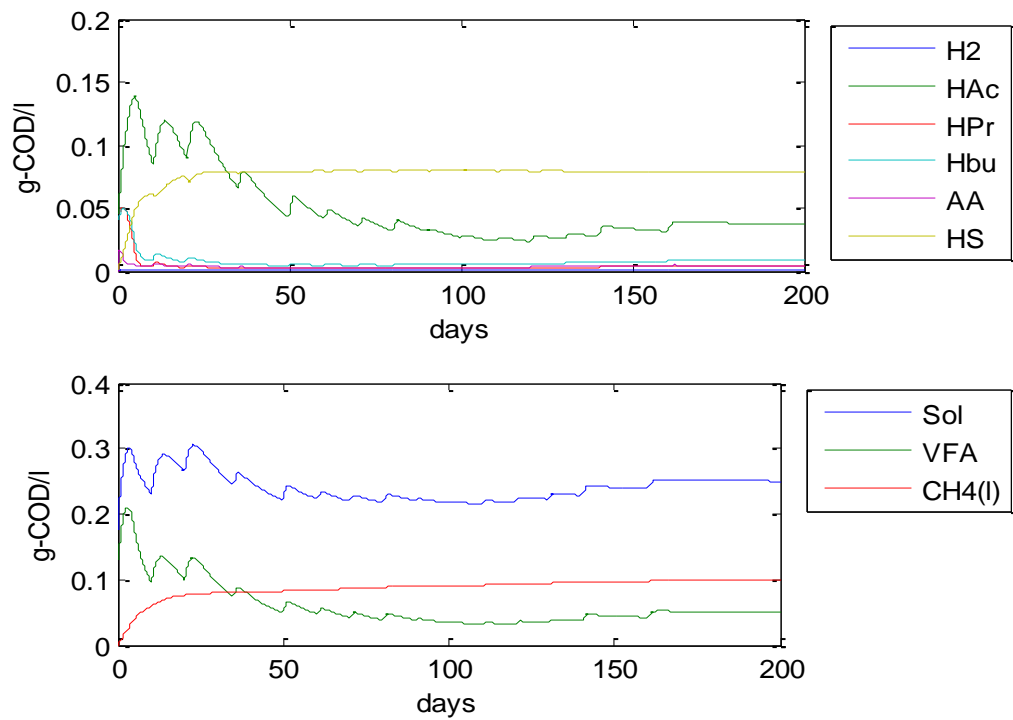


Figure 41. Case 6: soluble COD and soluble component concentrations.

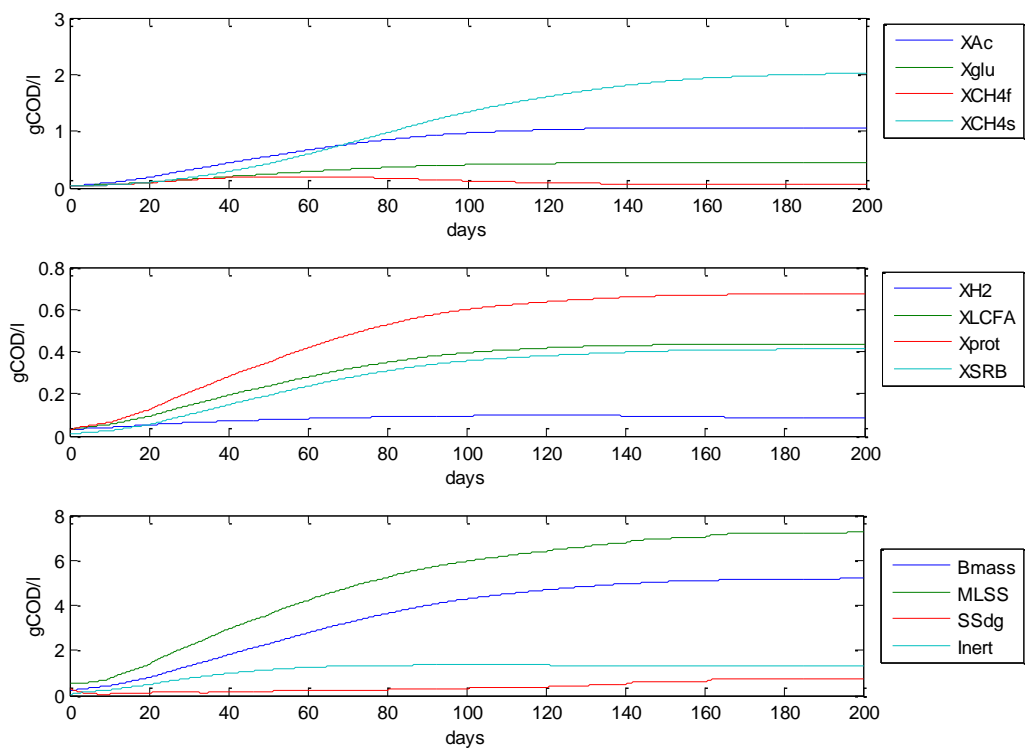


Figure 42. Case 6. Biomass and solids profiles in a BFBF treating sulphate containing sewage.

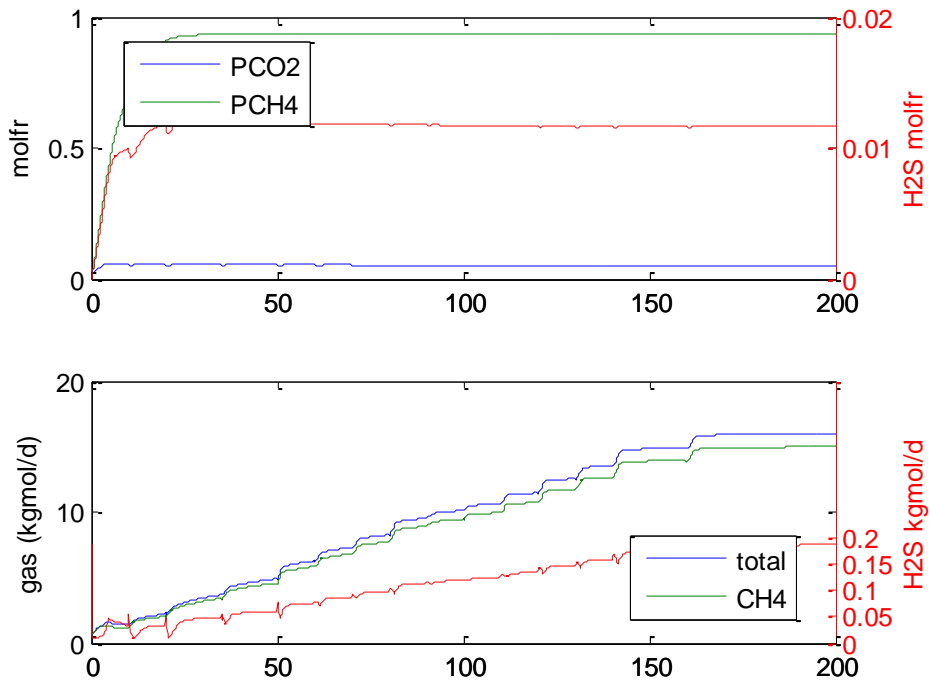


Figure 43. Case 6: Gas composition and gas production rates. H<sub>2</sub>S is plotted on right-hand y-axis.

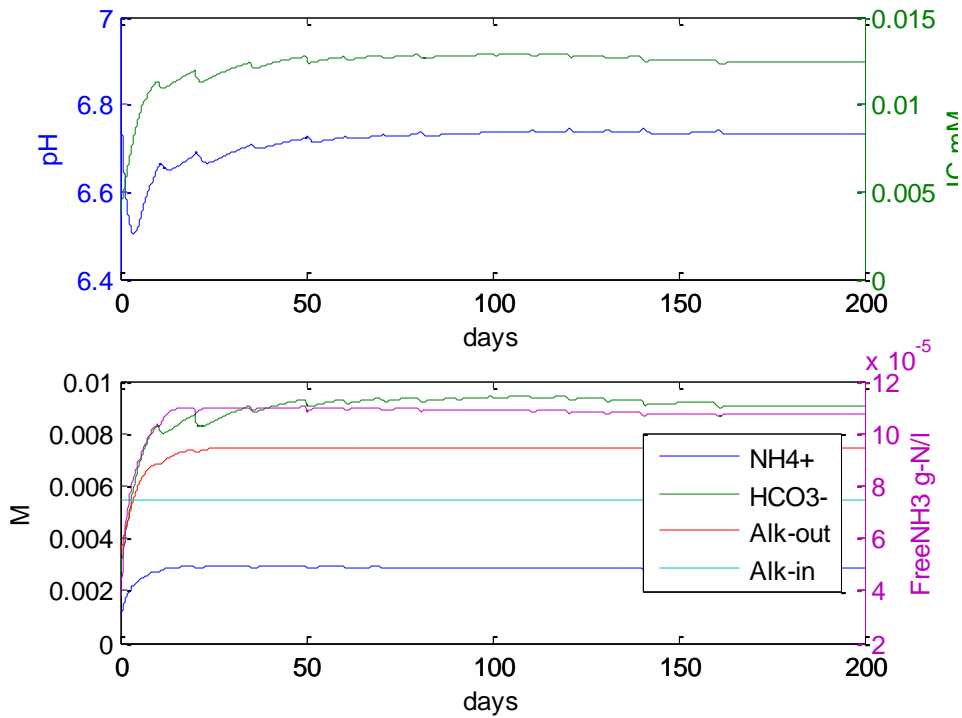


Figure 44. Case 6. pH, total dissolved inorganic carbon evolution is shown (top). The evolution of alkalinity and its bicarbonate and ammonium components.

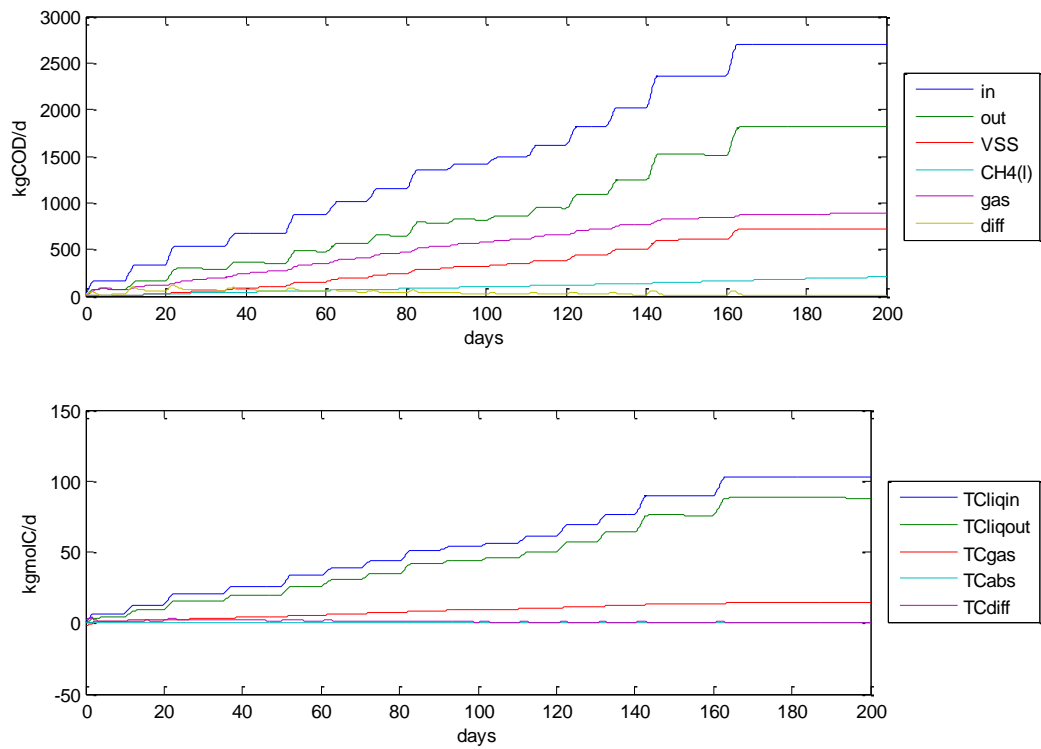


Figure 45. Case 6. COD and carbon balances are shown. CODdiff and TCdiff are the difference between raw effluent and all output products, is near zero, showing steady state operation and also consistency of the calculated concentrations and pH.

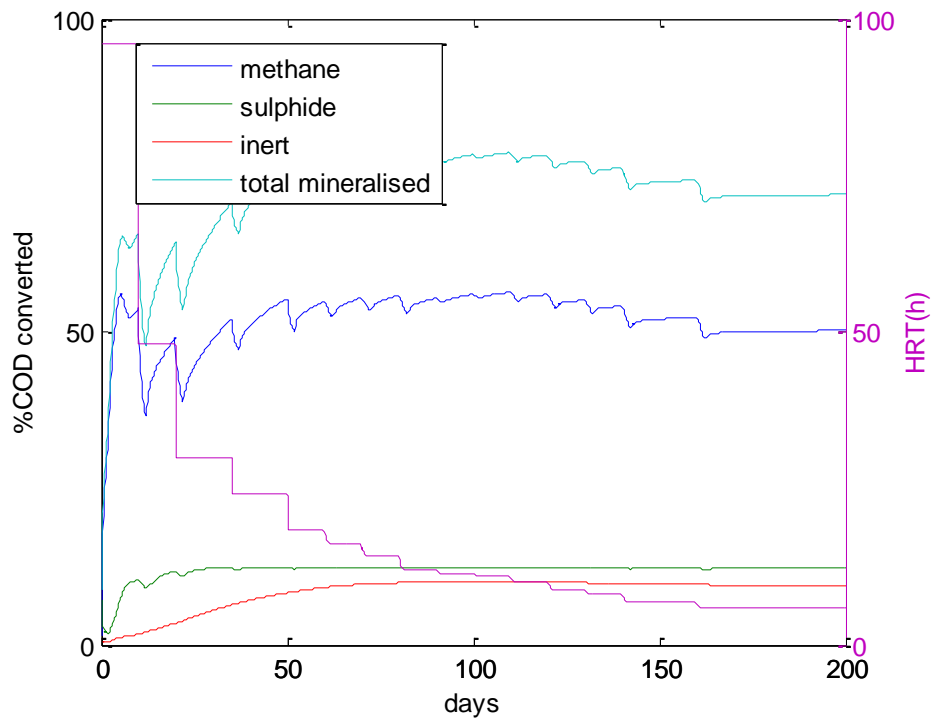


Figure 46. Case 6. COD converted to various mineralized end products. The total mineralised is 68% at day 200 load.

### 7.7.2. Case 7. Simulation of milk effluent treatment in laboratory BFBR

The model was used to determine the performance of BFBR on milk effluent. The active volume of reactor was chosen to match that of the experimental BFBR (lower chamber). The composition of milk effluent is given in Table 1. The effluent COD was 4.475 g/l of which suspended COD was 3 g/l, with fat and LCFA COD of 1.5 g/l. The load was increased by increasing feed rate (Figure 47) . Starting with HRT 30 h, the load was increased in 2 steps to HRT 10 h. The kinetic parameters and biomass retention efficiencies as in Case 4 was retained, except for gas transfer  $K_La$  which was increased to  $80 \text{ d}^{-1}$ , to account for better gas transfer as a result of gas induced agitation. The retention efficiency of solids was increased was to 0.98 from 0.95. The increased retention efficiency represents the tendency for milk solids to coagulate and separate inside the reactor. The results show that treated effluent has very low dissolved COD (Figure 48). The mineralization of incoming COD is 84% (Figure 50). The model clearly simulates lipid scum accumulation. Figure 49 shows lipid concentration peaks during every load increase followed by degradation reaching steady state in a period of 3-4 weeks, as has been observed in the experiments (Sec.6.5.3). There is no accumulation of LCFA in the model results. The model predicts quite well, qualitatively, the dynamic behaviour of the BFBR. The steady performance of the BFBR is accurately predicted, when filter efficiencies are set at 98%.

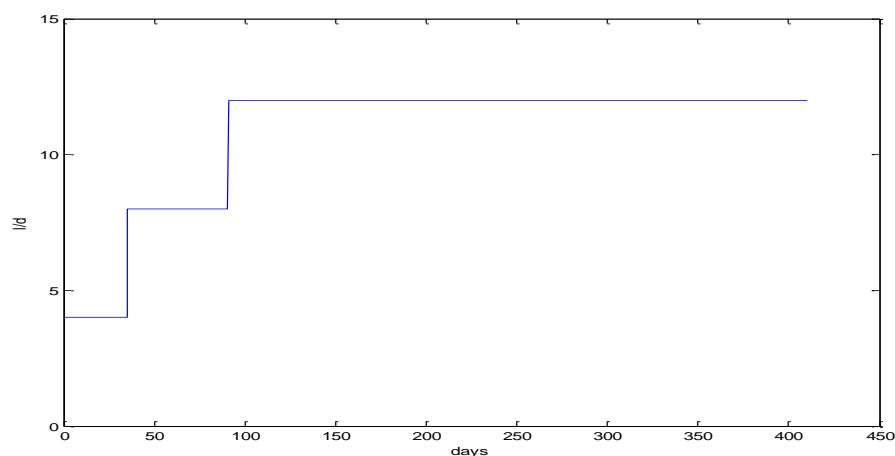


Figure 47. Case 7. Feed flow rate (litres/d) into BFBR. The active volume of reactor is 5 litre.

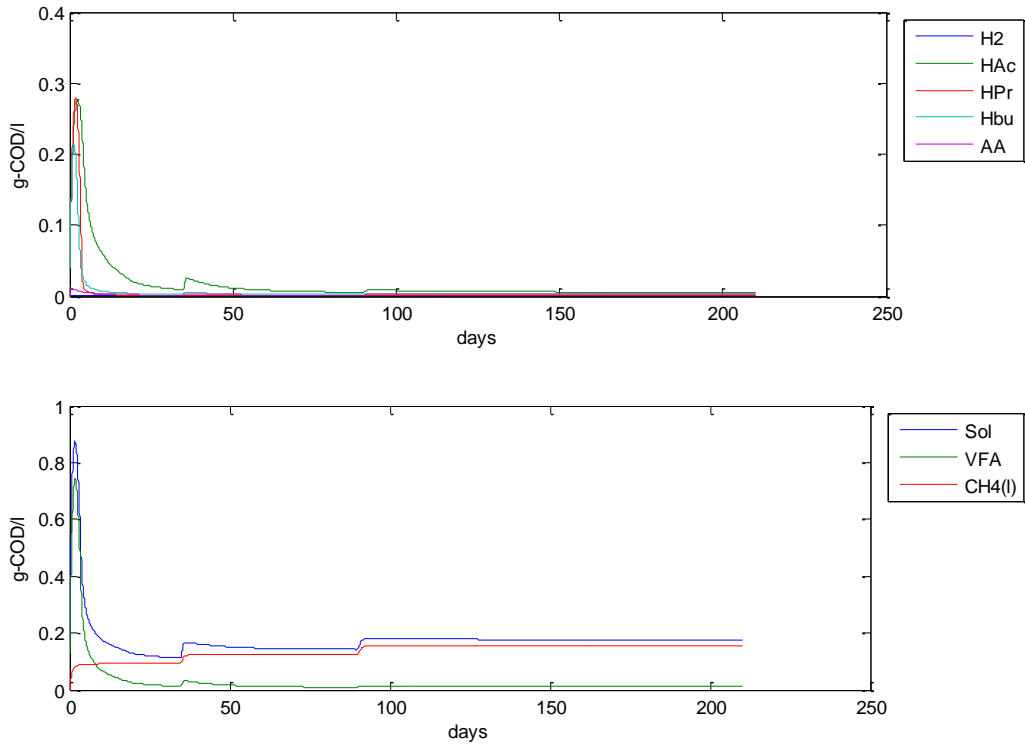


Figure 48. Case 7. Soluble COD and soluble component COD

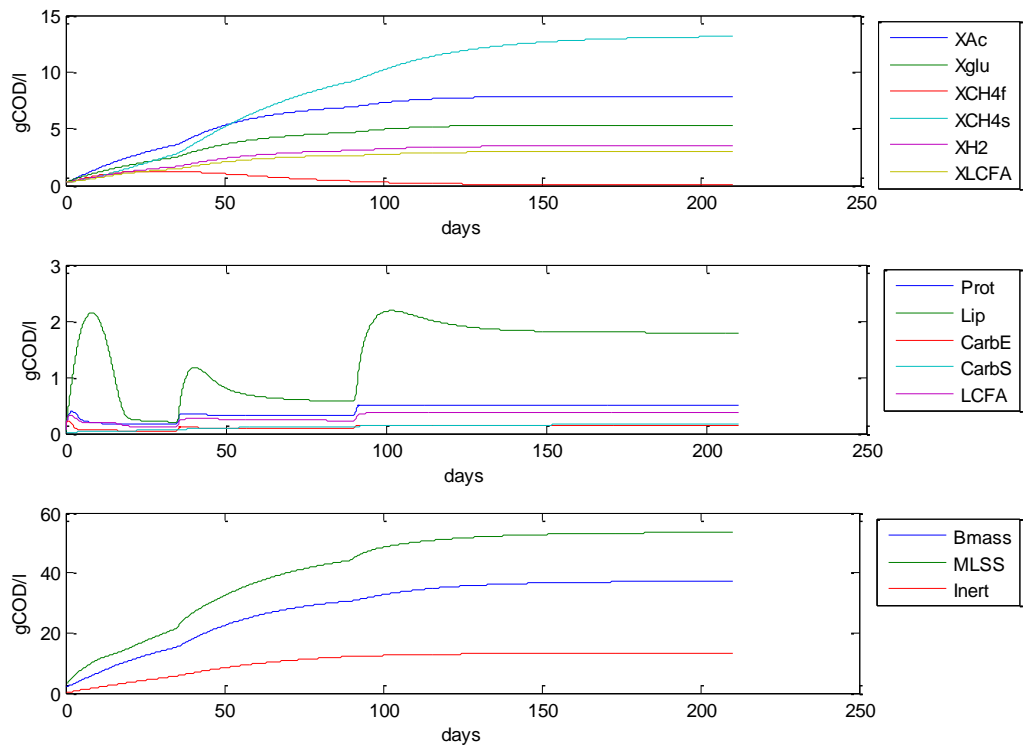
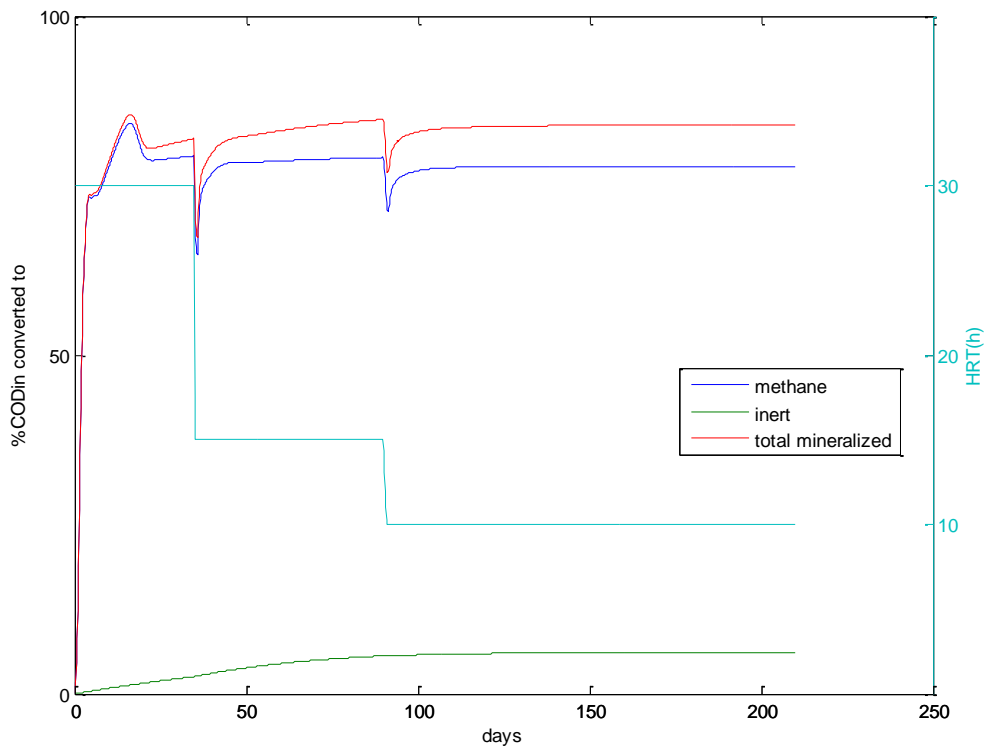


Figure 49. Case 7. Suspended solid COD and particulate component COD in reactor mixed liquor. The bottom figure shows biomass content and inert content in total MLSS in the reactor sludge. The particulate COD content is less than 10% of the total MLSS.



**Figure 50. Case 7: Mineralization of feed COD into methane and inert solids, and total mineralized COD.**

## 7.8. Discussion of BFBR based on simulation results

The model of the BFBR allows insight into some of the difficult to measure processes that occur in the BFBR. The model requires the filter efficiency factor for biomass to be higher than that of particulates in order to reproduce the observed performance. In other words, the retention times for micro-organisms should be higher than that of particulates in order to obtain the desired COD removal efficiency. *Prima facie*, it appears to contradict the hypothesis that hydrolysis of particulates is the rate-limiting process for the degradation of complex wastewater. But the filter efficiency required for micro-organisms is higher than that is filtration efficiency of the buoyant filter as determined with bulking sludge. In other words, BFBR sludge develops filterability, thus generating high biomass retention times. Biological processes like the floc and granule formation aid the separation of biomass from liquid. Hydrodynamic and biological selection pressures are responsible for the formation of flocs. In this respect, the BFBR is similar to the UASB except that selection pressures are

smaller and the BFBR retains flocs of size and settleability of a wider range than possible in the UASB.

On the other hand, the physical filtration mechanism of the buoyant filter is important for the retention of particulate COD. The filter provides the particulate-COD retention times required for COD removal. Flotable solids, in particular, are retained by filtration. Mechanisms such as biosorption of particulates on sludge are not adequate to provide the required particulate retention times. The evolution of the microbial ecology inside the reactor runs counter to the evolution of biosorption or solids retention ability because biosorption lowers the density of a floc and increases its probability of washout. But exocellular enzyme production activity is enhanced as sludge evolves. In steady state operation, the sludge in the BFBR is mainly biomass rather than particulates (see for example Figure 36, Figure 42 and Figure 49). The filter has its main function during the start-up phase, when particulates are retained, biomass slowly evolves and hydrolysis rates increase.

It also explains the experimental observation that, contrary to expectation, BFBR using different efficiency filters had nearly the same COD removal efficiency, (Figure 6. COD removal efficiency in BFBR using different efficiency filters. At steady state, the sludge in the BFBR is mainly biomass while retention and enzymatic hydrolysis is essentially complete and hence there is no difference in COD removal. But the lower efficiency filter is subject to greater instabilities resulting from variations in feed or environment.

Therefore, we conclude that although growth rate of microorganisms such as acetoclastic methanogens is slower than hydrolysis of particulates (see  $\mu_m$  values in Table 9), the microbial substrate uptake rates in a reactor are higher than particulate hydrolysis rates because *organisms accumulate, while particulates get washed out*. Hence active methods of retaining particulates inside the reactor, as in the BFBR, increase the overall reactor COD loading and conversion rate.

The model neglects the role of protozoa in the BFBR. Protozoa can be added as components in the model. A description of the effects of protozoan grazing in BFBR needs classification of particulate substrates, especially bacteria, into floc size fractions. At least two size fractions are required for each species – a grazed

fraction and a non-grazed fraction (floc) for each species. It is obvious that the extension of the model will greatly increase the number of components. Further, it must also be noted that protozoan life cycle is considerably more complex than bacteria and it has implications in reactor performance. Protozoan growth involves cell division as well as spore formation. Simple kinetic expressions do not capture the dynamics of protozoan growth. Sharp changes in protozoan population are observed in the BFBR and these are linked with treatment efficiency. Also, when we have more than one trophic layer in the ecology of the reactor, the mathematical model may have no steady state and could exhibit instability and periodic behaviour.

### 7.9. Source code description

---

The source code *.m* files ( Matlab Ver 7.01) for BFBR Model Ver. 6.9 used in Case 6 simulation, is given in **Appendix**. The code comprises the following:

- main script file *bibr.m* - reads problem data entered through Excel, controls programme execution and displays concentration results.
- function files *mass.m*,
- Function file *rate.m*; function *ratevector* given in file *rate.m* gives the rate expressions for growth of various groups of organisms and the values of various kinetic parameters. Changes in rate expressions or addition of new processes needs modification of this file.
- Function file *pHfinder.m*; required in pH evaluation.
- Function file *chargebal.m* ; required in pH evaluation
- Function file *plotrates.m*. Displays rates of growth, gas production, COD and TC balances.

Data is entered through an Excel file with the following worksheets

1. Soluble: Worksheet is shown in Table 5
2. Particulates: Worksheet is shown in Table 6
3. Soluble inorganic: Worksheet is shown Table 7
4. Gas components: Worksheet is shown in Table 8. Yield coefficients are given in moles gas / gCOD converted.

5. Reactor Worksheet (not shown): Data on reactor volume, gas holdup volume, execution parameters such as time period of simulation, whether periodic flow etc.
6. Flow worksheet (not shown) : Gives the hydraulic load applied
7. Periodic flow worksheet (not shown): Gives the daily periodic flow variation.
8. Clod worksheet (not shown): Gives the composition of raw effluent at varying times. The sheet automatically estimates the alkalinity load, given the pH and partial pressure of carbon dioxide.

## 8. Aspects of scale-up of BFBR

---

The BFBR must be scaled-up for practical application in industrial and municipal sewage treatment. Actual scale-up is not within the scope of the thesis. This chapter briefly discusses the scale-up and engineering issues that need to be confronted in the further development of the BFBR.

The potential applications of the BFBR are in treatment of effluents from

- Papermills using wastepaper
- Dairy
- Food processing
- Sewage treatment
- Slaughterhouses
- Edible oil

### 8.1. Process design specifications

---

The BFBR process design parameters recommendations is culled from the experimental data ( Chapter 6) and given below:

- a. Organic loading rate  
COD loading rate: 6 to 8 kg COD /m<sup>3</sup>/d.
- b. Filter specifications:  
Filter media size: 1 to 1.5 mm  
Filter depth: 10 to 15 cm  
Filtration velocity: 1 to 2 m/h  
Filter pressure drop: < 20 cm w.c.  
Filter backwash velocity: 130 m/h  
Bed expansion: 30%  
Filter backwash interval: 15 to 30 minutes  
Filter backwash volume: ~ 100% of filter volume

The BFBR mathematical model (Chapter 7) can be used to improve the COD loading rate specification if the wastewater can be characterized in detail.

## 8.2. Reactor vessel shape and L/D ratio.

---

The BFBR shape can be either circular or rectangular in cross-section. The cylindrical shape is cost-effective for tall reactors. The trend in advanced high-rate anaerobic reactors is taller reactors (large L/D), reducing the footprint. The L/D ratio for BFBR is limited only by the need to provide sufficient cross-sectional area for arrangement of the filter within the reactor. The filter area required is determined by filter load. Filter hydraulic loading rates are determined by backwash requirement in the treatment of high-strength effluent, whereas, in the treatment of low strength effluent, the hydraulic load generated by effluent as well as backwash are both equally significant.

## 8.3. Mixing system

---

BFBR reactors will generate scum at least during load increases. Scum breaking needs special designed agitators. Reactor design with small liquid-gas interface confines scum accumulation in a small area and makes it easier to design scum disintegrating equipment. Usually mechanical agitators are required for disintegrating scum. It is difficult to provide top entry mechanical mixers in a BFBR because of the filter arranged inside the reactor. It is easier to provide a gas mixer in the BFBR, the mixer having the double function of driving backwash at regular intervals even in the absence of gas generation in the reactor. Gas mixers are not very effective in disintegrating scum. Hence, in the treatment of scum forming complex wastewater (such as dairy effluent), simple gas spargers should be replaced by large bubble mixers (eg. the Infilco-Degremont Cannon mixer<sup>56</sup>). Alternately, the reactor hydrodynamics can be tailored with draft tube and flow deflectors so as to create high velocity suction of scum into the liquor.

## 8.4. Backwash

---

If the strength of the waste is at least 4 g-COD/l, gas production will be sufficient for driving the backwash. Nevertheless, a gas recirculation system is need for backwash during start-up.

The head required for backwash is less than 50 cm. The head requirement need not be confused with liquid head above the filter top. The driving head is

the pressure of gas in the gas accumulation tank. The depth of filtered treated effluent above the filter bed need not be equal to the head required for filter backwash. But the volume of filtered treated effluent should be sufficient for backwash.

### 8.5. Filter arrangement

---

The filter area required is large. The simplest design is inside the reactor vessel. A GLS separator similar to UASB positioned below the filter prevents gas entry into the filter bed and reduces the sludge load on the filter. The filter is retained with mesh on top and the bottom of the filter chamber can be open. The filter has to be partitioned to ensure uniform fluidization and reconstitution of the filter bed. The scale-up of the filter assembly is simple parallel arrangement of several small-size filter chambers.

### 8.6. Filter media manufacture

---

EPS resin is used in the manufacture of moulded polystyrene foam articles. The first step in the manufacture of moulded polystyrene foam articles is expansion of resin into beads by steaming. Hence, it is possible to source the filter material by specifying the resin and time of expansion. The sorting of expanded beads by size and density requires to be carried out specially as these operations are not used in any of the current applications of EPS.

### 8.7. Design of automatic filter backwash control system

---

The backwash control system can be electric or hydraulic.

The electric system requires level or pressure sensors and control valves to trigger the backwash. The outflow of gas from the gas pressure chamber (gas accumulator) has to be completed in less than 10 seconds during which the filter bed expands. Hence large gas exit pipe has to be provided. The valves have open fully and close in this interval. Ordinary full port large size valves cannot open and shut at high speed and special actuators are needed. The level sensor / pressure sensor has to work in a environment where foam and scum are present. It has to be mounted so as to be serviceable without shut-down of the reactor.

The hydraulic gas siphon does not have mechanical and electrical issues, but scale-up is difficult. To recapitulate, the hydraulic gas siphon comprises a downcomer, a riser and a slug catcher. As gas accumulates, the gas-liquid interface in the downcomer is depressed, till gas can exit via the riser. Gas exit should form a slug (Taylor bubble) that pushes out the liquid in the riser to a slug catcher. Thereby the liquid seal is broken and gas collected in the accumulator escapes till liquid enters via the downcomer and the liquid seal reforms. When scaling up to large diameter risers, it is critical to ensure that gas should form a slug and not trickle out through the riser liquid pool. The designer needs to understand the hydrodynamic conditions for slug formation in vertical pipe flow in order to design an automatic hydraulic backwash system.

### 8.8. Start-up and shut down issues

---

BFBR start-up is very similar to UASB reactors. Availability of high activity seed sludge will help start-up the reactor quickly. Even poor quality seed sludge can be used for start-up since washout is less than in other reactors. BFBR reactor with protozoa rich sludge would take time to reach optimal operating efficiency. Further during shutdown, the protozoa population is likely to be wiped out and will take 2 to 3 weeks to re-establish.

### 8.9. Remarks on costs

---

BFBR costs are comparable with that UASB reactors of similar reactor vessel sizes. The BFBR reactor vessels has to fit in gas accumulators and filtered liquid pool. The volumes of filter, gas accumulator and filtered liquid pool are less than 10% of the volume of reactor. In order to have gas pressure of 0.5 to 1m w.c. in the gas accumulator, gas collection GSS baffles must be at least 1 m below the lowest liquid level. The volume above the GSS baffles is considered inactive. In all, as a preliminary estimate, the reactor vessels are about 25% larger than the active volume required for specified loading and conversion efficiency.

## 9. Conclusions

---

The development of high-rate anaerobic reactors in the 1970s and 1980s has led to the widespread adoption of anaerobic wastewater treatment. The state-of-art high-rate anaerobic reactors operate on the principle of retention of methanogenic biomass for contact with wastewater. These reactors are effective in the treatment of wastewaters containing COD in dissolved form. When COD is present as particulates, the high-rate reactor is not effective. A significant fraction of COD in many wastewaters, including sewage, is in the form of degradable particulates – termed ‘complex wastewater’. There has been no major advance in anaerobic technology for complex wastewaters.

The BFBR is a new concept anaerobic reactor designed to enhance the volumetric mineralization rates by increasing the retention times of particulate substrates. It enables the hydrolysis and solubilisation of particulates - slow reactions that are carried out enzymatically outside the bacterial cell.

The BFBR has an integral filter bed that allows the separation and retention of particulate substrates within the reactor. The filter bed is made from floating (buoyant) filter media. The floating filter bed has the advantage of lower solids load and downward backwash which returns filtered solids to the reaction zone. Biogas is accumulated under hydrostatic pressure in the reactor and released periodically to backwash the filter. The release of gas causes the filter bed to fluidize in the downward direction. The filter media was made from polystyrene beads. The bead were prepared by steaming EPS resin. The beads were size sorted to obtain uniform fluidization.

Filtration studies were conducted on the buoyant filter bed to determine filtration efficiency, select filter media size, and determine the backwash parameters.

A laboratory BFBR reactor was operated for 400 days on milk effluent containing fat – a complex wastewater known to cause problems in high-rate anaerobic reactors unless fat is removed by pretreatment. The performance was monitored. The accumulation and degradation of scum in the reactor was studied.

The laboratory BFBR was operated with LCFA (oleate) as sole carbon source to study the microbiological characteristics of reactor sludge.

A dynamic mathematical model for the BFBR comprising a CSTR and a zero volume filter was developed to aid design and to gain insight into the processes inside the reactor.

### 9.1. Key findings

---

- The BFBR is able to treat complex wastewater at high loading rate.
- The buoyant filter arrangement works without choking when backwashed by fluidization at frequent intervals (15 to 20 minutes).
- Beads (1 to 1.5mm diameter) prepared from expandable polystyrene resin is suitable for the filter bed.
- The filter pressure drop has to be limited to 20 cm H<sub>2</sub>O in order clean the filter bed efficiently by fluidized backwash. At higher pressure operation, sludge and filter media bond to form aggregates that are not broken during backwash.
- The fluidization velocity is correctly predicted by the Richardson-Zaki formula
- The automatic gas-driven backwash system works efficiently. It has the advantage of not using high power pumps, sensors and valves.
- The BFBR can treat milk effluent containing fat at loading rate 8 kgCOD/m<sup>3</sup>/d. The COD removal efficiency is greater than 85%. The treated effluent has remarkably low COD (less than 200 mg/l).
- During start-up, fat accumulates in the form of scum, that eventually disappears as hydrolysis rates increase. At steady state, the reactor mixed liquor contains primarily biomass.

- Anaerobic protozoa are present in BFBR sludge. The population of protozoa shows progression from small species (rounds, amoeboids) to large species (flagellates to ciliates). The best quality effluent is obtained when ciliate numbers are high.
- The mathematical model developed can simulate the dynamics of the BFBR under varying hydraulic and organic loads.
- Mathematical model studies show that biomass is retained in the BFBR by the formation of flocs and granules which have good filterability. The BFBR filter is required for retention of particulate-COD, particularly poor settling, floating and non-biosorbing particulates.
- The model is useful for the process design of the BFBR. It can be modified without extensive reprogramme to include new processes and components such as sulphate reduction. The potential of the BFBR for sewage treatment was simulated on the model.
- The BFBR can be scaled-up for practical application. Aspects of scale-up of BFBR are discussed.

The recommended process design parameters for the BFBR are :

- a. COD loading rate: 6 to 8 kg COD /m<sup>3</sup>/d.
- b. Filter specifications:
  - Filter media size: 1 to 1.5 mm
  - Filter depth: 10 to 15 cm
  - Filtration velocity: 1 to 2 m/h
  - Filter pressure drop: < 20 cm w.c.
  - Filter backwash velocity: 130 m/h
  - Bed expansion: 30%
  - Filter backwash interval: 15 to 30 minutes
  - Filter backwash volume: ~ 100% of filter volume

## 9.2. Comparison of BFBR and existing reactors

A summary comparison of the BFBR with various other anaerobic reactors is given in Table 11.

**Table 11.**

Aspect	UASB	Fixed film	Fluidized bed	BFBR
Biomass retention	Depends on settleability	Only biofilm forming microbes are retained	Only biofilm forming microbes are retained	Depends on sludge filterability
Solids retention	Limited capacity of sludge bed to retain solids, lipids lead to sludge washout	Solids can be captured, but leads to bed choking	No capacity to retain solids	High capacity to retain solids, irrespective of its settlability
Mixing of solids and biomass; and gas transfer	Limited by liquid upflow velocity and gas production rate	Poor mixing and very limited gas transfer	Good mixing but not independent of liquid velocity	Any degree of mixing can be provided irrespective of liquid velocity.
Internals	1. Gas solid separation baffles 2. Liquid distributor network	1. Random or structured packing and packing supports 2. Liquid distributor network	1. Only media (sand) dumped inside 2. Distribution network is not required, but hydrodynamic design should enable uniform upflow	1. Filter media holder, and supports 2. Gas solids separation baffles 3. Gas mixing system 4. Liquid distributor not required

## 9.3. Future developments in BFBR technology.

Pressure development in the BFBR filter can be limited by reducing the solids loading to the filter. A gas-solids-separator (GSS) fitted under the filter reduces solids loading to the filter by separating the larger settleable flocs. The GSS can be optimised for the BFBR, with higher efficiency solids separation design. A BFBR GSS does not need steep slopes for solids to slide back by gravity, since intermittent high velocity backflow is available.

The BFBR filter media can be further developed. It is preferable to use materials whose size and density can be better controlled eg. hollow glass beads.

Filter bed design can be improved so as to enhance turbulence during backwash.

Modular filter cartridges can be designed for mass production using plastic moulding technology. The modules will contain filter media with defined characteristics. These modules can be field fitted to any size reactor vessel. It would reduce anaerobic reactor costs, improve performance and make maintenance easy.

#### 9.4. Further study of the science of anaerobic degradation of complex waste

The anaerobic mineralisation of complex waste needs further scientific study. In particular, the mechanism of hydrolysis, the generation of exocellular enzyme activities and its kinetics need to be studied in greater detail. The new findings on protozoa action in anaerobic reactors need to be subjected to wide study. In particular, it is possible that pathogen removals in sewage treatment anaerobic reactors can be enhanced by ciliate-rich anaerobic sludge.

## 10. References

---

- <sup>1</sup> A short history of anaerobic digestion. <http://www.biogas.psu.edu/pdfs/ShortHistoryAD.pdf>. retrieved on 20 Jun 2010.
- <sup>2</sup> [http://en.wikipedia.org/wiki/Anaerobic\\_digestion](http://en.wikipedia.org/wiki/Anaerobic_digestion)
- <sup>3</sup> Stronach S, Rudd T, Lester JN. Anaerobic digestion processes in industrial wastewater treatment. Berlin: Springer Verlag 1986
- <sup>4</sup> J F Malina, FG Pohland. (Editors). Design of Anaerobic Processes for the treatment of industrial and municipal wastes. CRC Press, Boca Raton,1992.
- <sup>5</sup> J Mata-Alvares, Editor. Biomethanation of organic fraction of municipal solid wastes. IWA Publishing, London (2003).
- <sup>6</sup> P. Vandevivere, L. De Baere and W. Verstraete . Types of anaerobic digesters for solid wastes, Chapter in reference 5
- <sup>7</sup> Kaare Hvid Hansen, Irimi Angelidaki, Brigitte K Ahring, 1998. Anaerobic digestion of swine manure: inhibition by ammonia. Wat. Res. 32,1,5-15.
- <sup>8</sup> DM McCartney, JA Oleszkiewicz; Water Environ. Res. (1993),65:655-664
- <sup>9</sup> <http://www.fao.org/docrep/t0541e/T0541E05.htm> Homo-acetogenic bacterial metabolism retrieved on 17 March 2010.
- <sup>10</sup> Rinzema A, Boone M, Knippenberg K, Lettinga G. 1994. Bactericidal effect of long chain fatty acids in anaerobic digestion. Wat Environ. Res. 66 (1): 40-49.
- <sup>11</sup> Hwu CS, Tseng SK, Yuan CY, Kulik Z, Lettinga G. Biosorption of Long chain fatty acids in UASB treatment processes. Wat Res 1998; 32 (5): 1571-1579.
- <sup>12</sup> Sung T O, Martin AD. Thermodynamic equilibrium model in anaerobic digestion process. Biochem. Eng. J. 34 (2007) 256-266.
- <sup>13</sup> Lettinga, G; Hulshoff Pol, Look W. 1991. UASB-process design for various types of wastewaters. Water science and technology;24(8):87-107, 1991.
- <sup>14</sup> Zhang B, Zhang LL, Zhang SC, Shi HZ, Cai WM. 2005. The Influence of pH on Hydrolysis and Acidogenesis of Kitchen Wastes in Two-phase Anaerobic Digestion. Env. Technol, 26, 3, 329 – 340.
- <sup>15</sup> Kim SH, Han SK, Shin HS. 2004. Two-phase anaerobic treatment system for fat-containing wastewater. J Chem Tech Biotechnol. 79, 1, 63-71.
- <sup>16</sup> DO Tas, O Karahan, G Insel, S Ovez, D Orhon, H Spanjers. 2009. Biodegradability and Denitrification Potential of Settleable Chemical Oxygen Demand in Domestic Wastewater. Water Environ. Res., 81, 715-727.
- <sup>17</sup> Gatze Lettinga. Treatment of raw sewage under tropical conditions. In *Design of anaerobic processes for the treatment of industrial and municipal wastes*. Ed. JF Malina, FG Pohland. CRC Press, Boca Raton. 1992

- 
- <sup>18</sup> Y Kalogo and W Vestraete. 1999. Development of anaerobic sludge bed (ASB) reactor technologies for domestic wastewater treatment: motives and perspectives. *World J. Microbiol. Biotechnol.* 15, 523-534.
- <sup>19</sup> Renato Carrha Lietao. 2004. Robustness of UASB treating sewage under tropical conditions. PhD dissertation, Wageningen Agricultural University, Netherlands. <http://library.wur.nl/wda/dissertations/dis3606.pdf>
- <sup>20</sup> Ayoob Torkian. 2004. Performance evaluation of three anaerobic bioreactors: ASBR, HAIS, AND UASB. PhD Thesis. School of Public Health, Isfahan University of Medical Sciences and Health Services, Iran. <http://sharif.edu/torkian/AminPhDThesisFinal.pdf>
- <sup>21</sup> Draaijer H., Maas JAW, Schaapman JE, Khan A. 1992. Performance of the 5 MLD UASB reactor for sewage treatment at Kanpur, India. *Water Science and Technology.* 25, 7, 123-133.
- <sup>22</sup> <http://envfor.nic.in/report/0203/Annex-4.pdf> retrieved on 6 April 2010
- <sup>23</sup> Manual on Sewerage and Sewage Treatment, 2<sup>nd</sup> Edition. 1993. Central Public Health and Environmental Engineering Organisation, Ministry of Urban Development, Government of India.
- <sup>24</sup> Nobuyuki Satoa, Tsutomu Okuboa, Takashi Onodera, Lalit K. Agrawal, Akiyoshi Ohashi, Hideki Harada. 2009. Economic evaluation of sewage treatment processes in India. <http://www.aseanenvironment.info/Abstract/41015575.pdf>
- <sup>25</sup> Nidal Mahmoud, Grietje Zeeman, Huub Gijzen, Gatzke Lettinga. 2003. Solids removal in upflow anaerobic reactors, a review. *Bioresource Technol.* 90, 1–9.
- <sup>26</sup> Metcalf and Eddy Inc. *Wastewater engineering- treatment and reuse – 4<sup>th</sup> Edition.* Tata McGraw-Hill (2003).
- <sup>27</sup> Joseph F Malina. Anaerobic sludge digestion. In *Design of anaerobic processes for the treatment of industrial and municipal wastes.* Ed. JF Malina, FG Pohland. CRC Press, Boca Raton. 1992
- <sup>28</sup> US 6,592,751 dated July 15, 2003. Device for treatment of wastewater. Inventor: Ajit Haridas; Assignee. Council of Scientific and Industrial Research, New Delhi.
- <sup>29</sup> Panicker, S.J., Philipose, M.C., Haridas, A. 2008. Buoyant Filter Bio-Reactor (BFBR)-a novel anaerobic wastewater treatment unit . *Water Science and Technology* 58 (2), pp. 373-377
- <sup>30</sup> Ajit Haridas, S. Suresh, K.R. Chitra, V.B. Manilal. 2005. The Buoyant Filter Bioreactor: a high-rate anaerobic reactor for complex wastewater—process dynamics with dairy effluent. *Water Research* 39 993–1004
- <sup>31</sup> Anderson GK, Yang G. 1992. Determination of Bicarbonate and Total Volatile Acid Concentration in Anaerobic Digesters Using a Simple Titration. *Water Environ. Res.* 64, 53-59
- <sup>32</sup> Weber WJ. *Physicochemical process for water quality control.* 1972. J.Wiley
- <sup>33</sup> Perle M, Kinchie S, Shelef G. 1995. Some biochemical aspects of the anaerobic degradation of dairy wastewater. *Some biochemical aspects of anaerobic degradation of dairy wastewater.* *Water Res.* 29, 1549-1554.
- <sup>34</sup> Priya M, Haridas A, Manilal VB. 2007. Involvement of protozoa in anaerobic wastewater treatment process. *Water Res.* 41,20, 4639-4645.
- <sup>35</sup> Alberto Rozzi and Roberto Passino, 1985. Mathematical models in anaerobic treatment process. in *Mathematical models in biological wastewater treatment.* Edited by Jorgensen, S. E., Gromiee, M. J., Elsevier Science Publishers. 637 – 690.
- <sup>36</sup> Pavlostathis G. Spyros and James M. Gossett, 1986. A kinetic model for anaerobic digestion of biological sludge. *Biotechnol. Bioeng.* 28, 1519 - 1530

- 
- <sup>37</sup> Salman Akhtar Khan, 1994. Modelling of the UASB reactor for an extended pH range. M.Sc. Thesis, IHE DELFT, Netherlands
- <sup>38</sup> Jayaseelan, S., 1997. A simple mathematical model for anaerobic digestion process. *Wat. Sci. Tech.*, 35, 185 - 191
- 39 Batstone, D.J., Keller, J., Newell, R.B., Newland, M., 2000. Modelling anaerobic degradation of complex wastewater. I: model development. *Biores. Tech.* 75, 67 - 74
- 40 D.J. Batstone, J. Keller, I. Angelidaki, S.V. Kalyuzhnyi, S.G. Pavlostathis, A. Rozzi, W.T.M. Sanders, H. Siegrist and V.A. Vavilin. 2002. The IWA Anaerobic Digestion Model No 1 (ADM1). *Water Sci. Technol.* 45, 10, 65-73
- <sup>41</sup> Karin Kovárová-Kovar and Thomas Egli. 1998. Growth Kinetics of Suspended Microbial Cells: From Single-Substrate-Controlled Growth to Mixed-Substrate Kinetics. *Microbiol Mol Biol Rev.* 1998 September; 62(3): 646–666. ( [www.ncbi.nlm.nih.gov/pmc/articles/PMC98929/](http://www.ncbi.nlm.nih.gov/pmc/articles/PMC98929/) retrieved on 21/03/2010)
- <sup>42</sup> Button, D.K. (1985). Kinetics of Nutrient-Limited Transport and Microbial Growth. *Microbio. Rev.* p. 270-297
- <sup>43</sup> Egli T. 1991. On multiple-nutrient-limited growth of microorganisms, with special reference to dual limitation by carbon and nitrogen substrates. *Antonie Van Leeuwenhoek.* Oct-Nov;60(3-4):225-34.
- <sup>44</sup> Christ, O., Wilderer, P. A., Angerhofer, R., Faulstich, M., 2000. Mathematical modeling of the hydrolysis of anaerobic processes. *Wat. Sci. Tech.*, 41, No. 3, 61 - 65
- <sup>45</sup> Vavilin, V. A., Rytov, S. V., Lokshina, L. Ya., 1996. A description of hydrolysis kinetics in anaerobic degradation of particulate organic matter. *Biores. Tech.*, 56, 229 - 237.
- <sup>46</sup> Vavilin, V. A., Schelkanov, M. Yu., Lokshina, L. Ya., Rytov, S.V., Jokela, J., Salminen, E., 2002. A comparative analysis of a balance between the rates of polymer hydrolysis and acetoclastic methanogenesis during anaerobic digestion of solid waste. *Wat. Sci. Tech*, 45, No. 10, 249 - 254.
- <sup>47</sup> Merkel, W., and Krauth, K., 1999. Mass transfer of carbon dioxide and methane in anaerobic reactors under dynamic substrate loading conditions. *Wat. Res.* 33, No. 9, 2011 - 2020
- 48 R E Treybal. "Mass transfer operations". McGraw Hill
- <sup>49</sup> Angelidaki, I., Ellegaard, L., Ahring, B.K., 1993. A mathematical model for dynamic simulation of anaerobic digestion of complex substrates: focusing on ammonia inhibition. *Biotechnol. Bioeng.* 42, 159 - 166
- <sup>50</sup> C. Rosen, D. Vrecko, K.V. Gernaey, M.N. Pons and U. Jeppsson. 2006. Implementing ADM1 for plant-wide benchmark simulations in Matlab/Simulink. *Water Sci. Technol.* 54,4,11-19.
- <sup>51</sup> EPA van Langerak, MMH Beekmans, JJ Beun, HVM Hamelers , G Lettinga. 2000. Influence of phosphate and iron on the extent of calcium carbonate precipitation during anaerobic digestion. *J Chem Technol Biotechnol .* 74, 1030-1036.
- <sup>52</sup> Heijnen, J.J., van Loosdrecht, M.C.M., Tjihuis, L., 1992. A black-box mathematical model to calculate auto- and heterotrophic biomass yield based on Gibbs energy dissipation. *Biotechnol. Bioeng.* 40, 1139–1154.
- <sup>53</sup> von Stockar U, Maskow T, Liu J, Marison IW, Pati R. 2006. Thermodynamics of microbial growth and metabolism: An analysis of the current situation. *J Biotechnol.* 121, 517–533.
- <sup>54</sup> Moller HB, Sommer SG, Ahring B. 2004. Methane productivity of manure, straw and solid fractions of manure. *Biomass and Bioenergy* 26,485 – 495.
- <sup>55</sup> Siegrist H, Vogt D, Garcia-Heras JL, Gujer W. 2002. Mathematical model for meso- and thermophilic anaerobic sewage sludge digestion. *Environ. Sci. Technol.* 36, 1113-1123.
- <sup>56</sup> [http://www.infilcodegremont.com/images/pdf/cannon\\_mixer.pdf](http://www.infilcodegremont.com/images/pdf/cannon_mixer.pdf). Retrieved on 24 May 2010.

## Appendix: Source code (Case 6).

---

The source code *.m* files ( Matlab Ver 7.01) for BFBR Model Ver. 6.9 used in Case 6 simulation, is given below.

```
% BFBR Anaerobic reactor process model
% Author: Ajit Haridas, NIIST, Thiruvananthapuram 695019 India
%       ajitharidas@niist.res.in
% Version 6.9 BFBR with sulphate reduction
%       13 May 2010       PhD Thesis Case 6 simulation; Alk production added
%                       by modifying yield coefficient;
%
%
%       global Hion told ugas pHprofile
%
%read active vol of reactor, filter efficiency, recycle ratio
[reactordata] = xlsread('data4','reactor');
V = reactordata(1);
recycle = reactordata(3);
pf = reactordata(4);
delay = reactordata(5);
Qgascir = reactordata(6);
tend = reactordata(7);
Temp = reactordata(8);
RST = reactordata(9); % 12 April 2008
Mgas = reactordata(10); % 21 Aug 2008

if pf == 0
    Q = xlsread('data4','flow'); % Q(:,2) = Q(:,2).*recycle;
else
    Q = xlsread('data4','periodicflow');
% periodic flow rates convert from l/h to l/d.
    Q = [Q(:,1)/24 Q(:,2)*24];
end
% read daily flow Qdaily
Qdaily = xlsread('data4','flow');
% read periodic flow variation in a day
Qvar = xlsread('data4','periodicflow');
% effluent discharge rate; sludge wasting rate
Qw = Q;
pHinitial = 7.0; % feed pH
LowpH = 7.0; HighpH = 7.1; % pH low and high set points
% Hion proportional set point function
pHset = [0 1; LowpH 1; HighpH 0; 14 0]; pHset(:,1)=10.^-pHset(:,1);
% Qgascir = .5%gas circulation rate through absorber mol/d per reactor vol.
[YS YSname] = xlsread('data4','soluble');
[YX YXname] = xlsread('data4','insoluble');
[YIS YISname] = xlsread('data4','solubleinorganic');
[YG YGname] = xlsread('data4','gas');
nS = size(YS,2); % number of soluble components
nX = size(YX,2); % number of insoluble components
```

```

nIS = size(YIS,2); % number of inorganic components
nG = size(YG,2); % number of gas components
nC = nS+nX+nIS+nG; % total number of components
nP = size(YS,1); % total number of processes
% load variation with time
Load = xlsread('data4','load'); %Load(:,2:end) = Load(:,2:end)./recycle;
Load = Load(:,1:nC+1);
%
data = [YS YX YIS YG];
name = [YSname(1,2:end) YXname(1,1:end) YISname(1,1:end) YGname(1,1:end)];
% [data text] = xlsread('data','yield');
% name = (text(1,2:end));
CHON = data(1:5,:);
molwt = [CHON * [12;1;16;14;32]]';
% Ver 6.9, COD of SO4 is taken as zero; hence S = 64 gCOD/mol
CODpermol = [CHON * [32;8;-16;-24;64]]';
CODperg = CODpermol./molwt;
COD2C = (CHON(:,1)./(CODpermol'+ (CODpermol'==0)))';
COD2C(end-nG+2) =1; % conversion factor for PCH4 is 1
NmolpergCOD = CHON(1:nS+nX,4)./CODpermol(1:nS+nX)';
SmolpergCOD = CHON(1:nS+nX,5)./CODpermol(1:nS+nX)';
%
% yield coefficients
Y = data(6:end-5,:);
charge = data(end-4,:);
plus = data(end-3,:);
K = data(end-2,:);
fe = data(end-1,:);
if (RST == 1); % 12 April 2008
'RESTART MODE .... continue?'
pause;
tstart = t(end)
Cinitial = C(end,:)'
else
Cinitial = data(end,:); tstart = 0;
end
%
% initial condition array for ODE having initial values of C and V
CVinitial = [Cinitial;V];
%
% check stoichiometry
% sum of each row gives COD conservation of each process
CODcheck = sum(Y(:,1:nS+nX),2)
% sum over rows (converted to Cmol yield) gives TC conservation
TCcheck = Y*COD2C';
% Recalculating stoichiometry CO2 yield
Y(1:end-4,nS+nX+2) = Y(1:end-4,nS+nX+2)-TCcheck(1:end-4);
TCcheck = Y*COD2C' % recheck TC balance
%
% calculate ammonia from N balance; ammonia is in mol/l units
Ncheck = Y(:,1:nS+nX)*NmolpergCOD + Y(:,nS+nX+1);
Y(:,nS+nX+1) = Y(:,nS+nX+1) - Ncheck;
% recheck nitrogen balance
Ncheck = Y(:,1:nS+nX)*NmolpergCOD + Y(:,nS+nX+1)
%
% calculate SO4 from S balance; SO4 (gmol/l); H2S (gCOD/l);
Scheck = Y(:,1:nS+nX)*SmolpergCOD + Y(:,nS+nX+4);
Y(:,nS+nX+4) = Y(:,nS+nX+4) - Scheck;
Scheck = Y(:,1:nS+nX)*SmolpergCOD + Y(:,nS+nX+4)
% 15 May 2010; Alk yield = -2*sulphate yield
Y(:,nS+nX+3) = -2*Y(:,nS+nX+4);
% solving the ODEs
% display feed flow, feed conc and set graph for online intergration display
% time and flow are interpolated for plotting only, but mass.m takes Q
time = tstart:tend/500:tend;
inflow = interp1(Q(:,1),Q(:,2),(time - pf*round(time-0.5)),'linear');
% delay = 0.0; % outflow takes place after this time delay
outflow = ...

```

```

        interp1(Qw(:,1),Qw(:,2),...
        (time+pf*(delay - round(time+delay-.5))), 'linear');
    flow = [inflow' outflow'];
% plot inflow and outflow
    figure(1);
    subplot(3,1,1);
    if (pf==0)
        plot(time,flow);legend('in','out');
        axis([tstart tend 0 1.25*max(inflow)]);
        ylabel('m3/d'); % plot load flow rate
    else
        plot([24*Q(:,1) Q(:,2)]);
        ylabel('m3/d'); xlabel('hour');
    end
%
    inconc = interp1(Cload(:,1),Cload(:,2:end),time,'linear');
    Hguess = 10^-7.0;
% plot soluble and insoluble load concentrations
    figure(1);subplot(3,1,2);i=[1 nS+nX-5:nX+nS]; ...
    plot(time,inconc(:,i)); ...
    legend(name(i),-1); ylabel('gCOD/l'); % xlabel('days');
% plot flow and loads separately for thesis
    figure(20);
%
    subplot(3,1,1);
    plot(24*Q(:,1), Q(:,2)); %legend('in','out','Location','EO');
    xlim([0 24]);
    ylabel('m3/d'); xlabel('hour');
%
% solve ODE
    figure(1);subplot(3,1,3); % online graph
    options = odeset('RelTol',1e-2,'MaxStep',0.1,...
    'OutputFcn',@odeplot,'OutputSel',[1:nS]);
    legend(name(1:nS),-1); ylabel('gCOD/l');
[t CV] = ode23s(@mass,[tstart
tend],CVinitial,options,Cload,V,Q,pf,Y,Qw,fe,nS,nX,nIS,nG,nC,Mgas,charge,Hguess
,K,plus,Qgascir,pHset,delay,recycle,Temp);
%
% separate concentration change and volume change
    C = CV(:,1:end-1); V=CV(:,end);
    S = sum(C(:,1:nS),2);
    VFA = sum(C(:,4:6),2);
    CH4_l= C(:,2);
    Biomass = sum(C(:,nS+1:nS+8),2);
    MLVSS = sum(C(:,nS+1:nS+nX),2);
    SS = sum(C(:,nS+9:nS+nX-1),2);
    Inert = C(:,nS+nX);
    IC = C(:,nS+nX+2);
    Alk = C(:, nS+nX+3);
% plot results
    figure(2);subplot(2,1,1);
    plot(t,C(:,3:nS));
    legend(name(3:nS),-1); ylabel('g-COD/l'); xlabel('days');
    figure(2); subplot(2,1,2); plot(t,[S,VFA,CH4_l]);
    legend('Sol','VFA','CH4(l)',-1);
    ylabel('g-COD/l'); xlabel('days');
    figure(3);subplot(3,1,1);
    plot(t,C(:,(nS+1):(nS+4)));
    legend(name(nS+1:nS+4),-1);ylabel('gCOD/l'); xlabel('days');
    figure(3);subplot(3,1,2);
    plot(t,C(:,(nS+5):(nS+8)));
    legend(name(nS+5:nS+8),-1);ylabel('gCOD/l'); xlabel('days');
    figure(3); subplot(3,1,3); plot(t,[Biomass,MLVSS,SS,Inert]);
    legend('Bmass','MLSS','SSdeg','Inert',...
    'Location','EO');
    ylabel('gCOD/l'); xlabel('days');
    figure(4);subplot(2,1,1);
    [AX H1 H2] = plotyy(pHprofile(:,1),-log10(pHprofile(:,2)),t,IC);
    ylabel ('pH'); xlabel('days');

```

```

        set(get(Ax(2), 'Ylabel'), 'String', 'IC mM');
% plot reactor volume and gas composition
figure(5);
subplot(2,1,1);
[AX,H1,H2]=plotyy(t,C(:,end-nG+1:end-1),t,C(:,end));
legend(name(end-nG+1:end-1), 'Location', 'best');
ylabel('molfr');
ylabel(AX(2), 'H2S molfr');
% display rates, COD balance and pH variation (these are again recalculated)
plotrates1(t,C,Cload,Hguess,Q,pf,Qw,fe,V,nS,nX,nIS,nG,charge,K,...
    plus,COD2C,Qgascir,pHset,recycle,delay,Y,CODperg,Temp);

```

### Material balance function mass.

```

function dCdt = mass(t,CV,Cloadvar,V,flow,pf,Y,wasteflow,...
    fe,nS,nX,nIS,nG,nC,Mgas,charge,Hguess,K,plus,...
    Qgascir,pHset,delay,recycle,Temp)
    global Hion told ugas pHprofile;
% interpolate flow to get Q
Q = interp1(flow(:,1),flow(:,2),(t - pf*round(t-0.5)), 'linear');
Qw = interp1(wasteflow(:,1),wasteflow(:,2),(t+pf*(delay - round(t+delay-
    0.5))), 'linear');
V = CV(end); C = CV(1:end-1);
%
%
    Cout = C.*(1-fe)'; % 14/4/2008 variable fe for each component
    Cload = interp1(Cloadvar(:,1),Cloadvar(:,2:end),t, 'linear');
% determine hrt at particular time
    hrt = V/Q;
% is this the first time pHfinder is being called?
    if t < 1e-3
        Hion = Hguess; told = 1e-3; Qgas = 0;
        pHprofile = [t Hion];
    else
        if t > told + 1e-3
            Hion = pHfinder(C,Hion,charge,K,plus);
        end
    end
    ratevector = rate(C,Hion,Qgascir,pHset,ugas,Temp);
    Qgas = ratevector(end);
    ugas = Qgas*V*1e-3/0.01;
% CO2 stripping from recycle liq.
% IC index nS+nX+2; 21/4/08 bug in freeCO2 fixed
    eff_strip = 0.9; % stripping efficiency
    freeCO2 = [ ones(nS+nX+1,1); (1-
        eff_strip*Hion/(K(nS+nX+2)+Hion)); ones(nC-(nS+nX+2),1) ];
    Crecycle = Cout.*freeCO2;
% Qw and recycle have Cout concentration
    r = ratevector(1:end-1);
% matl. balance for liq phase
    dCdt = (Cload'+recycle*Crecycle)/hrt - ...
        ((Qw+recycle*Q)/V)*Cout + Y'*r - C*(Q-Qw)/V;
% matl balance of gas phase
    for i = (nS+nX+nIS+1) : (nS+nX+nIS+nG)
        dCdt(i) = (Y(:,i))*r - Qgas*C(i))*V/Mgas;
    end
% dV/dt = Q- Qw, rate of change of volume = inflow - outflow
    dCdt(nS+nX+nIS+nG+1) = Q - Qw;
    told = t;
    format short, [t C']
    format short e, [t Hion ]
    pHprofile = [pHprofile; t Hion];

```

### Function ratevector

```

function ratevector = rate(C,Hion,Qgascir,Hionset,ugas,Temp)
% decay yield of inert carbon increased to 20%; causes accumulation of HAC

```

```

    pH = -log10(Hion);
% various pH inhibition functions for use in rate expressions
fpH1 = [0 0; 6 0; 6.5 1; 7.2 1; 9.0 0; 14 0];
pHinhib1 = interp1(fpH1(:,1),fpH1(:,2),pH,'linear');
fpH2 = [0 0; 5 0; 6.5 1; 7.2 1; 9.0 0; 14 0];
pHinhib2 = interp1(fpH2(:,1),fpH2(:,2),pH,'linear');
fpH3 = [0 0; 5 0; 6.5 1; 7.2 1; 8.0 0; 14 0];
pHinhib3 = interp1(fpH2(:,1),fpH2(:,2),pH,'linear');

%
% Various Temperature dependence coefficients
theta = [ .024 .035 .055 .063 .069 .08 .1];
fT = exp(theta*(Temp - 35));

% Variable names; enter manually every time a new component is added
Glu = C(1); CH4 = C(2); H2 = C(3); HAC=C(4);
HPr=C(5); HBU = C(6); AA= C(7); H2S=C(8);
XAc = C(9); XGlu = C(10); XCH4f = C(11); XCH4s = C(12); XH2 = C(13);
XLCFA = C(14);XProt = C(15); XSRB = C(16);
Prot = C(17); Lip = C(18); CarbE = C(19);
CarbS=C(20); LCFA = C(21); Inert = C(22);
NH3=C(23); IC=C(24); Alkst=C(25); SO4=C(26);
PCO2=C(27); PCH4 = C(28); PH2S = C(29);

%
freeNH3 = NH3 / (1 + Hion/5e-10);
% Monod growth function on total NH3; inhibition due to free NH3
fNH3 = ( NH3/(.05/17 + NH3) ) ;

%
% calculate free H2S (inhibits XCH4, XH2);
freeH2S = H2S/(1+ 10^-6.9/Hion);

%
kd = 0.02*fT(5); % first order decay coeff for all biomass
P = 1; % total gas pressure atm

% rate equations
% CO2 stripping
% KLa = 9.69*ugas^0.83;
% Overall vol.gas tr coeff (1/d) units for evolved gas
KLa = 40;
KH = 40; % atm / (mol/l) (Note KH =1/Khgas data from Excel not used)
aCO2 = 1 - 1.585e-6/(1.585e-6 + Hion); % IC fraction as dissolved CO2
rstrCO2 = KLa * (aCO2*IC - PCO2*P/KH);

% CH4 stripping
KLa = 40; % Overall vol.gas tr coeff (1/d) units
KH = 800; % atm / (mol/l)
rstrCH4 = KLa * (CH4/64 - PCH4*P/KH);

% H2S stripping
KLa = 40;
KH = 20;
rstrH2S = KLa * (freeH2S/80 - PH2S*P/KH);

% Proteolysis by AA utilizer XProt; inhibited by AA;
% Contois function of Prot and XProt
k = 4*fT(1) ; Ks = 0.5 ; Ki2 = .1;
rhyProt = k * (Prot / (Ks*XProt + Prot)) * ...
XProt * (Ki2/(Ki2 + AA)) * pHinhib2;

% lipolysis by LCFA utilizer XLCFA: inhibited by LCFA and H2
% Contois function is proportional to biomass at ...
% high solids/biomass ratio and proportional to solids at low solids/biomass
k = 2.5*fT(1) ; Ks = .25 ; Ki2 = 0.5; Ki3 = .01;
% 10 May 2010; error corrected *XLCFA instead of * XAc
rhyLip = k * Lip * (XLCFA / (Ks*XLCFA + Lip))*...
(Ki2/(Ki2 + LCFA))* Ki3/(Ki3+H2) * pHinhib2;

% hydrolysis of carbohydrate easy degrading fraction by glucose utilizer
k = 3*fT(1) ; Ks = 0.25 ; Ki2 = .1;
% put k=2 to match Siegrist 2004 fig 4 test
rhyCarbE = k * (CarbE / (Ks*XGlu + CarbE)) * XGlu * ...
(Ki2/(Ki2 + Glu)) * pHinhib2; % this is a Contois function

% Contois function is proportional to biomass at...
% high solids/biomass ratio and proportional to solids at low solids/biomass
% hydrolysis of carbohydrate slow degrading fraction

```

```

k = 0.2*fT(1) ; Ks = 0.5 ; Ki2 = .1;
rhyCarbS = k * (CarbS / (Ks*XGlu + CarbS)) * XGlu * ...
(Ki2/(Ki2 + Glu)) * pHinhib2; % this is a Contois function
% Contois function is proportional to biomass at...
% high solids/biomass ratio and proportional to solids at low solids/biomass
% growth of XProt amino acid degraders
mu = 5.0*fT(5); Ks = .128*fT(5);
rgXProt = mu * XProt * (AA/(Ks + AA))* fNH3* pHinhib1;
% decay of amino acid degraders
rdXProt = kd*XProt;

% growth of acetoclastic methanogens fast;
% inhibited by free Ammonia Ki=25mg/l
% inhibited by PH2S Ki = 0.04 molfr.
mu = .7*fT(5); Ks = .3*fT(7);
Ki=25e-3*fT(6); % 4/4/2008 freeNH3 =25e-3 unit debugged
KiPH2S = 0.04;
rgXCH4f = mu * XCH4f * (HAc/(Ks + HAc))*...
fNH3 * pHinhib3 / (1 + freeNH3*14/Ki) / (1+(PH2S/KiPH2S));
% decay of acetoclastic methanogens fast
rdXCH4f = kd*XCH4f;

%
% 4/4/2008 growth of acetoclastic methanogens slow;
% inhibited by free Ammonia Ki=25mg/l
mu = .35*fT(5); Ks = .04*fT(7);
Ki=25e-3*fT(6); % freeNH3 Ki =25e-3 g/L
rgXCH4s = mu * XCH4s * (HAc/(Ks + HAc))* fNH3 *...
pHinhib3 / (1 + freeNH3*14/Ki) / (1+(PH2S/KiPH2S));
% decay of acetoclastic methanogens slow
rdXCH4s = kd*XCH4s;

%
% growth of acetogens on butyrate; inhibited by HAc
mu = 0.68*fT(5); Ks = 0.05*fT(5); Ki = 1.5*fT(5);
% 6/4/2008 Ks reduced to 0.05 from .18
rgXAcBu = mu * XAc * (HBu/(Ks + HBu))*(Ki/(Ki + HAc))* fNH3 * pHinhib1;

%
% growth of acetogens on propionate (inhibited by HBu,HAc,H2)
mu = 0.54*fT(5); Ks = 0.02*fT(7);
Ki = 2*fT(5); Ki2 = 1.5*fT(5);
Ki3 = 16e-4*fT(6); % 4/4/2008 Ks reduced to 0.04 from 0.125
rgXAcPr = mu * XAc * (HPr/(Ks + HPr))*(Ki/(Ki + HBu))*...
(Ki2/(Ki2+HAc))* fNH3* pHinhib1 * Ki3/(Ki3 + H2);
% decay of acetogens
rdXAc = kd*XAc;

%
% growth of Butyrate producers on glucose
mu = 5.0*fT(5); Ks = 0.5*fT(5); Ki = .8*fT(5);
% 0.05 Ks as per Siegrist
rgXGlu = (mu * Glu*XGlu)/(Ks + Glu) * fNH3 * pHinhib2 ;
% decay of butyrate producers
rdXGlu = kd*XGlu;

%
% growth of LCFA degraders
mu = 0.6*fT(5); Ks = 0.5*fT(2);
Ki = 1.5*fT(5); Ki2 = 16e-3*fT(6);
% mu, Ki, Ki2 from Siegrist EST 2002
rgXLCFA = mu * (LCFA / (Ks*XLCFA + LCFA))*...
(Ki/(Ki + HAc))* XLCFA * fNH3 * pHinhib1 * Ki2/(Ki2 + H2);
% decay of LCFA organisms
rdXLCFA = kd * XLCFA; % 5/4/2008 error corrected

% growth of XH2
mu = 2.0*fT(5); Ks = 0.001*fT(6); % 2,.001 as per Siegrist
rgXH2 = mu * H2 * XH2 / (Ks + H2) / (1+(PH2S/KiPH2S));
% decay of XH2
rdXH2 = kd * XH2;

% growth of SRB
mu = 3.0*fT(5); Ks1 = 0.0005*fT(6);
Ks2 = 1e-5; % Ks2 = 1e-5M SO4

```

```

        rgXSRB = mu * H2 * XSRB / (Ks1 + H2) * SO4 / (Ks2 + SO4);
% decay of SRB
        rdXSRB = kd * XSRB;
% absorption of carbon dioxide per unit reactor volume
% Qgascir rate of gas circulation mole/d per unit reactor volume
        if pH < 6.8
            rCO2abs = Qgascir*PCO2
        else
            if pH < 7.5
                rCO2abs = Qgascir*(PCO2)*interp1(Hionset(:,1), Hionset(:,2),
                    Hion,'linear')
            else
                rCO2abs = 0
            end
        end
end
% total gas production per unit liquor volume
        Qgas = rstrCH4 + rstrCO2 + rstrH2S - rCO2abs;
%
ratevector = [ rhyProt rhyLip rhyCarbE rhyCarbS rgXProt rdXProt...
        rgXCH4f rdXCH4f rgXCH4s rdXCH4s rgXAcBu rdXAc ...
        rgXGlu rdXGlu rgXAcPr rgXLCFA rdXLCFA rgXH2 rdXH2 rgXSRB rdXSRB...
        rstrCH4 rstrCO2 rstrH2S rCO2abs Qgas]';

```

### Function pHfinder

```

function Hion = pHfinder(C, Hguess, charge, K, plus)
y = chargebal(Hguess, C, charge, K, plus);
if y < 0
    for j = 2:100000;
        y = chargebal(Hguess*j, C, charge, K, plus);
        if y > 0
            Hionrange = [(j-1) j]*Hguess; break
        else
            end
        end
        multiply = j
    else
        for j = 2:100000
            y = chargebal(Hguess/j, C, charge, K, plus); y
            if y < 0
                Hionrange = [1/j 1/(j-1)]*Hguess ;
                break
            else
                end
            end
            divide = j
        end
        % options = optimset('disp','iter');
        options = optimset;
        Hion = fzero(@chargebal, Hionrange, options, C, charge, K, plus);

```

### Function chargebalance

```

function y = chargebal(x, C, charge, K, plus)
% in moles of electrons
        alpha1 = plus - (K ./ (K + x));
        Weakion = (alpha1.*charge)*C ;
% if pH > 9, do correction for CO3(2-) species
        if x < 1e-9
            Weakion = Weakion - 2*10^-16.6*C(end-3)/(x^2 + 10^-6.3*x + 10^-16.6);
        end
        y = x + Weakion - (10^-14)/x;

```

### Function plotrates1

```

function plotrates1(tdata,Cdata,Cloadvar,Hion,flow,pf,wasteflow,fe,Vol,
    nS,nX,nIS,nG,charge,K,plus,COD2C,Qgascir,pHset,
    recycle,delay,Y,CODperg,Temp)
%read ratenames from data1.xls
    [dummy ratename] = xlsread('data4','ratename');
%strip out leading blank rows in data1.xls ratename sheet (in Matlab 6)
    % ratename = ratename(7:end,1);
% restrict data to nt points
    tstart = 1e-3+tdata(1); tlast=tdata(end);
    nt = 1000; deltat = (tlast - tstart)/nt;
    t = tstart:deltat:tlast;
% interpolate data
    Q = interp1(flow(:,1),flow(:,2),(t-pf*round(t-.5)),'linear');
    Qw = interp1(wasteflow(:,1),wasteflow(:,2),(t+pf*(delay - round(t+delay-
        0.5))), 'linear');
    V = interp1(tdata,Vol,t,'nearest');
    Cload = interp1(Cloadvar(:,1),Cloadvar(:,2:end),t,'linear');
    C = interp1(tdata,Cdata,t,'nearest');
    HRT = 24*V./Q;
% time average CODliqin
    CODliqin = deltat*cumtrapz(sum(Cload(:,1:nS+nX),2).*Q') ./t'; % CODliqout
    = deltat*cumtrapz(C(:,1:nS+nX)*[ones(nS,1);(1-fe)*ones(nX,1)].*Qw') ./t'; %
    time average CODliqout
    CODsliqout = deltat*cumtrapz(C(:,1:nS)*[1-fe(1:nS)].*Qw') ./t'; %14/4/2008
with variable filter eff.
    CODxliqout = deltat*cumtrapz(C(:,1+nS:nS+nX)*[1-fe(1+nS:nS+nX)].*Qw') ./t';
% 23/12/2008 soluble and insol COD calc separately
%
% 6 May 2010 time average over a running interval trunning (days)
    trunning = 2;
% window size = number of values in tmovavg;
% using the running average function filter
    windowSize = round(trunning/deltat);
    CODliqindata = sum(Cload(:,1:nS+nX),2).*Q';
    CODliqin = filter(ones(1,windowSize)/windowSize,1,CODliqindata);
    CODsliqoutdata = C(:,1:nS)*[1-fe(1:nS)].*Qw';
    CODxliqoutdata = C(:,nS+1:nS+nX)*(1-fe(nS+1:nS+nX)).*Qw';
    CODsliqout = filter(ones(1,windowSize)/windowSize,1,CODsliqoutdata);
    CODxliqout = filter(ones(1,windowSize)/windowSize,1,CODxliqoutdata);
    CODliqout = CODxliqout + CODsliqout;
%
    TCload = Cload(:,1:nS+nX+nIS)*COD2C(1:nS+nX+nIS)';
    TCconc = C(:,1:nS+nX+nIS)*((1-
        fe(:,1:nS+nX+nIS)).*COD2C(:,1:nS+nX+nIS)');
% TCliqin = deltat*cumtrapz(TCload.*Q') ./t';
% TCliqout = deltat*cumtrapz(TCconc.*Qw') ./t';
% 7 May 2010 running averages
    TCliqin = filter(ones(1,windowSize)/windowSize,1,TCload.*Q');
    TCliqout = filter(ones(1,windowSize)/windowSize,1,TCconc.*Qw');
%
%
for n = 1:nt+1
    Hion = pHfinder(C(n,:),'Hion,charge,K,plus);
    pH(n) = -log10(Hion);
    ugas = 0.0; % gas velocity, a dummy variable for later use in Kla est.
    ratevector(n,:) = rate(C(n,:),'Hion,Qgascir,pHset,ugas,Temp)';
end
% gas flow in mol/d
    Gasflow = ratevector(:,end-4:end).* repmat(V',1,5);
    QCH4 = Gasflow(:,1);
    QCO2 = Gasflow(:,2);
    QH2S = Gasflow(:,3);
    Qabs = Gasflow(:,4);
    Qgas = Gasflow(:,5);
% plot cummulative gas production for batch reactors
% volumetric gas yield
%     gasvolyield = deltat*cumtrapz(gasrates) ./ repmat(V',1,3);

```

```

% Theoretical gas yield for batch load
% ThCH4pergVS = (1/.04043)*(sum(C(1,1:nS+nX))/64)/
%               ((C(1,1:nS+nX))* (1./CODperg(1:nS+nX)))
% CH4pergVS= (1/0.04043)*gasvolyield(:,3) /
%            ((C(1,1:nS+nX))* (1./CODperg(1:nS+nX)));
% CH4 0.04043 mol/l at 298K; methane yield litre at 25C per g VSS initial load
% figure(10);
% plot(t,gasvolyield,t,CH4pergVS*10);
% ylabel('Gas prod gmol/l-reactor, CH4 10*1/gVSS');
% legend('tot', 'CO2', 'CH4', '10*CH4 l/gVSS'); title('Batch reactor');
% plot gas production
figure(5);
subplot(2,1,2);
[AX,H1,H2]=plotyy(t,[Qgas QCH4],t,QH2S);
ylim(AX(1),[0 20]);
ylim(AX(2),[0 0.5]);
ylabel('gas (kgmol/d)');
legend('total','CH4','Location','best');
set(get(AX(2),'YLabel'),'String','H2S kgmol/d')
% plot pH, HCO3 and Alk for sulphate reduction case
HCO3 = C(:,nS+nX+2).*10^-6.3/(Hion+10^-6.3);
Alk_out = C(:,nS+nX+3); Alk_in = Cload(:,nS+nX+3);
NH4 = C(:,nS+nX+1).*Hion/(Hion + 10^-9.3);
figure(12);
[AX,H1,H2] = plotyy(t,[HCO3 C(:,nS+nX+3)],...
t,pH);
ylabel(AX(2),'pH'); xlabel('days');
ylabel(AX(1), 'meq');
legend('bicarbonate','total alk','Location','best');
% plotting ratevariables. This has to be multiplied by corresponding Yield
coeff. to get actual rate of reaction.
figure(6);
subplot(4,1,2);
i = [5:8]; plot(t,ratevector(:,i));
ylabel('gCOD/l/d');
legend(ratename(i,:), -1);
subplot(4,1,1);
i = [1:4]; plot(t,ratevector(:,i));
ylabel('gCOD/l/d');
legend(ratename(i,:), -1);
subplot(4,1,3);
i = [9:12]; plot(t,ratevector(:,i));
ylabel('gCOD/l/d');
legend(ratename(i,:), -1);
subplot(4,1,4);
i = [13:16]; plot(t,ratevector(:,i));
ylabel('gCOD/l d');
legend(ratename(i,:), -1);
% plot total ammonia and free ammonia on 2nd y axis
figure(4);
subplot(2,1,2);
[AX,H1,H2]= plotyy(t,[NH4,HCO3,Alk_out,Alk_in],...
t,14*C(:,nS+nX+1)./(1+Hion/5e-10));
xlabel('days');
ylabel(AX(1), 'M');
legend('NH4+', 'HCO3-', 'Alk-out', 'Alk-in', 'Location', 'best');
ylabel(AX(2), 'FreeNH3 g-N/l');
% integral averages; use in periodic flow
CODgas = deltat*cumtrapz(64*QCH4+ 80*QH2S)./t';
CODCH4dis = deltat*cumtrapz(C(:,2).*Qw')./t';
% 7 May 2010 running averages
CODCH4_g = filter(ones(1,windowSize)/windowSize,1,64*QCH4);
CODCH4_l = filter(ones(1,windowSize)/windowSize,1,C(:,2).*Qw');
CODCH4 = CODCH4_l + CODCH4_g;
CODH2S_g = filter(ones(1,windowSize)/windowSize,1,64*QH2S);
CODHS_l = filter(ones(1,windowSize)/windowSize,1,C(:,nS).*Qw');
CODHS = CODH2S_g + CODHS_l;
CODgas = CODCH4_g + CODH2S_g;

```

```

        CODinert = filter(ones(1,windowSize)/windowSize,1,...
            C(:,nS+nX).*(1-fe(nS+nX)).*Qw');
        CODmin = CODCH4 + CODHS + CODinert;
        CODconv = 100*[CODCH4 CODHS CODinert CODmin]./repmat(CODliqin,1,4);
% plot percentage of COD gassified and HRT
figure(11);
[AX,H1,H2]=plotyy(t,CODconv,t,HRT);...
% make Yaxis1 (handle AX(1)) limits 0 to 100
ylim(AX(1),[0 100]);
xlabel('days'); ylabel('%COD converted');
legend('methane','sulphide','inert','total mineralised', 'Location',
'best')
set(get(AX(2),'Ylabel'),'String','HRT(h)');
% COD balance test
CODdiff = [CODliqin - CODsliqout - CODxliqout - CODgas];
format('short');
COD = [CODliqin CODsliqout CODxliqout CODgas CODCH4dis CODdiff]
% plot COD in and out
figure(9); subplot(2,1,1);...
plot(t,[CODliqin, CODliqout,CODxliqout, ...
CODCH4dis, CODgas, CODdiff]);
%
xlim([209 210]);
ylabel('kgCOD/d'); xlabel('days');
legend('in','out','VSS','CH4(l)','gas','diff', ...
'Location','EO');
% axis([tstart,tlast,-20,max(CODliqin)]);
%
% Carbon balance check
% TCgas = deltat*cumtrapz(QCH4+QCO2))./t';
TCabs = deltat*cumtrapz(Qabs)./t';
% TCabs = V*Qgascir*C(:,end-1); %BUG not valid for variable pH control
% 7 May 2010 running average TC
TCgas = filter(ones(1,windowSize)/windowSize,1,QCH4+QCO2);
TCabs = filter(ones(1,windowSize)/windowSize,1,Qabs);
TCdiff = TClmqin - TClmqout - TCgas - TCabs;
TC = [TClmqin TClmqout TCgas TCabs TCdiff]
% plot TC balance
figure(9);
subplot(2,1,2); plot(t,TC);
%
xlim([209 210]);
ylabel('kgmolC/d'); xlabel('days');
legend('TClmqin','TClmqout','TCgas','TCabs','TCdiff',...
'Location','EO');

```